

**UCSF**

**UC San Francisco Electronic Theses and Dissertations**

**Title**

Genetic Cooperation in BRAF(V600E)-induced Non-Small Cell Lung Cancer Using Genetically Engineered Mouse Models of Cancer

**Permalink**

<https://escholarship.org/uc/item/6q94m9w8>

**Author**

Juan, Joseph

**Publication Date**

2015

Peer reviewed|Thesis/dissertation



Genetic Cooperation in BRAF(V600E)-induced Non-Small Cell  
Lung Cancer Using Genetically Engineered Mouse Models of Cancer

by

Joseph Juan

DISSERTATION

Submitted in partial satisfaction of the requirements for the degree of

DOCTOR OF PHILOSOPHY

in

Cell Biology

in the



## ACKNOWLEDGMENTS

I would not be in the position I am in today if it weren't for the tremendous help I've received from mentors, colleagues, friends and family. I owe much of my success to these individuals and am pleased to acknowledge all those that have helped me obtain my doctoral degree.

First and foremost, I would like to thank my advisor, Dr. Martin McMahon for his support, wisdom, expertise, and patience. I am extremely grateful for the opportunity to be a member of your laboratory and for the insights, knowledge, and direction you've given me over the years. Your passion and commitment to both science and mentorship has been evident throughout my time in the lab and has served as both a source of great motivation for myself as well as something to aspire to. Your mentorship has been instrumental in shaping my personal and scientific development, and it has been a true honor and wonderful experience growing as a scientist under you.

I would also like to thank the members of my thesis committee, Dr. Frank McCormick, Dr. Allan Balmain, and Dr. William Weiss. Thank you for your mentorship, advice, and insightful critiques in my research projects and dissertation. You have all played a large role in my success as a graduate student and I cannot thank you enough for helping me reach all of my goals.

I am thankful for the members of the McMahon laboratory, both past and present, with whom I've had the privilege of working with and who have all helped shape my graduate career. To Roch-Philippe Charles, Anny Shai, Victoria Durban, and Eric Collisson, thank you for the technical expertise, advice, and perspectives you've provided me with during the early years of my tenure in the lab. To Ed van Veen and Paddy O'Leary, thank you for your generosity in

sharing your time, expertise, and advice with me. Our conversations, brainstorming sessions, and collaborations have been instrumental in my progress and growth in the lab, and I could not ask for better individuals to work with. To Jillian Silva and Daphne Pringle, thank you for all of our interactions, conversations, and advice.

To my fellow graduate students, thank you for the camaraderie we've built as we've taken this journey through graduate school together. To Christy Trejo, thank you for setting an example to follow and leading the way for the rest of us. To Shon Green, Evan Markegard, Marian Deuker, and Rachel O'Keefe, thank you for the great conversations we've had regarding our research, careers, and life in general. To all my classmates, especially Kevin Mark and Kari Morrissey, thank you for the advice, motivation, and focus you've provided throughout the years and the friendships we've built both in and outside of work.

Each one of you has made UCSF a pleasant and wonderful place to work, and I would like to thank you all for contributing to my growth both as a scientist and as an individual, and for being voices of insight and reason through what can sometimes be a daunting odyssey.

I am especially grateful to my family for always being there for me. To my Mom and Dad, Minerva and Gilberto, thank you for your unwavering love and unconditional support. You've given me everything I could ever ask for from a parent and so much more. I would not be where I am today without the values and work ethic you instilled in me growing up and without the strong foundation you've built for me and our family. To my brother and sister, James and Karen, thank you for being such wonderful siblings and for the laughs and experiences we've had together. To my best friend, Robby, you've always been like a brother to me and I thank you for your unwavering support, friendship, and the sense of pride you've given me in all my accomplishments, both big and small. To my future parent-in-laws, Abegail and Charles, and

future brother- and sister-in-laws, Laurence, Mikael, and Kristine, thank you for providing me with a home away from home and for always making me feel welcome in your household and treating me as one of the family. And to our dogs, both Sophie and Wollybear, thank you for your unconditional loyalty and love, and for your company on the late nights of reading and writing.

Most importantly, to my fiancée and future wife, Frances, thank you for your love and support through this entire journey. You've pushed me to settle for nothing less than my best and have encouraged me at each and every step through this process. Thank you for inspiring me in everything I do and for sharing with me all the ups, downs, and celebrations that come with graduate school. I am truly blessed to share all of this with you and I can't wait to see where the next chapter of our lives takes us next.

## ABSTRACT

### GENETIC COOPERATION IN BRAF(V600E)-INDUCED NON-SMALL CELL LUNG CANCER USING GENETICALLY ENGINEERED MOUSE MODELS OF CANCER

Joseph Juan

Lung cancer is the most common cause of death due to cancer in the world and the most recent statistics from the CDC reveal that in 2011 in the United States alone, lung cancer accounted for 207,339 patient diagnoses and 156,953 deaths. The largest type of lung cancer, non-small cell lung cancer (NSCLC), accounts for nearly 90% of this disease. Data from both humans and preclinical models have revealed that this disease is driven by sustained activation of the RAS/RAF/MEK/ERK MAPK pathway. However, while a strong initiator of tumorigenesis, BRAF<sup>V600E</sup> expression on its own is not sufficient to drive lung cancer formation. This is due to the need for cells to acquire the prerequisite “Hallmarks of Cancer” required for tumorigenesis, which oftentimes necessitates the activation of separate, cooperating pathways. Use of genetically engineered mouse models (GEMM) of cancer has provided us valuable insight into these mechanisms of cooperation driving cancer progression. In particular, use of the *Braf*<sup>CA</sup> GEMM of cancer has given us a better molecular understanding of the initiation, progression, and therapy of tumors driven by the MAPK pathway in multiple tissues including skin and lung.

Using the *Braf*<sup>CA</sup> GEM model of lung cancer and taking a candidate-based approach, I have identified a central role for Wnt/ $\beta$ -catenin signaling in the initiation and progression of lung cancer. Specifically, my results indicate that Wnt/ $\beta$ -catenin signaling is both necessary for and

sufficient to bypass the proliferative arrest observed in BRAF<sup>V600E</sup>-driven lung tumors through its ability to regulate c-MYC expression. However, my results also show that the ability of this pathway to drive progression to adenocarcinoma is through downstream effectors independent of c-MYC. Taking an unbiased approach using Sleeping Beauty transposon-mediated mutagenesis I have also identified a number of novel candidate cancer genes in pathways playing a role in driving BRAF<sup>V600E</sup>-initiated lung cancer progression. Some notable candidates currently being validated and pursued include a number of genes highly mutated in human cancers including *Fat1*, *Stag2*, and *Arid2*, and pathways with potential ties to cancer including axonal guidance.

These studies demonstrate the molecular complexity involved in the initiation and progression of BRAF<sup>V600E</sup>-driven NSCLC, as well as the potential efficacy of targeting these cooperating pathways to combat this disease.

## TABLE OF CONTENTS

Acknowledgments.....	iii
Abstract.....	vi
List of Tables.....	x
List of Figures.....	xi
<b>Chapter 1. Introduction.....</b>	<b>1</b>
Non-small cell lung cancer.....	1
BRAF <sup>V600E</sup> signaling and genetic cooperation in progression to Non-small cell lung cancer.....	2
.....	2
RAS/RAF/MEK/ERK signaling.....	4
Canonical Wnt/ $\beta$ -catenin signaling.....	6
Use of genetically engineered mouse models to study human cancer.....	8
Sleeping Beauty Mutagenesis.....	9
<b>Chapter 2. Role of Wnt/<math>\beta</math>-catenin/c-MYC Signaling in Lung Tumorigenesis.....</b>	<b>12</b>
Abstract.....	12
Introduction.....	13
Results.....	15
Discussion.....	30
Materials and Methods.....	34



<b>Chapter 3. <i>In vivo</i> Sleeping Beauty Screen to Identify Potential Tumor Suppressor Genes and Oncogenes Important for Lung Cancer Progression.....</b>	<b>78</b>
Abstract.....	78
Introduction.....	78
Results.....	79
Discussion.....	82
Materials and Methods.....	83
<b>Chapter 4. Conclusions and Future Perspectives.....</b>	<b>94</b>
<b>References.....</b>	<b>98</b>

## LIST OF TABLES

<b>Chapter 3. <i>In vivo</i> Sleeping Beauty Screen to Identify Potential Tumor Suppressor Genes and Oncogenes Important for Lung Cancer Progression.....</b>	<b>78</b>
Table 1. Genes involved in lung adenocarcinoma progression of BRAF <sup>V600E</sup> -initiated tumors (GKC).....	91
Table 2. Genes involved in lung adenocarcinoma progression of BRAF <sup>V600E</sup> -initiated tumors (gCIS).....	92
Table 3. Trunk driver genes involved in lung adenocarcinoma progression of BRAF <sup>V600E</sup> -initiated tumors.....	93

## LIST OF FIGURES

<b>Chapter 2. Role of Wnt/<math>\beta</math>-catenin/c-MYC Signaling in Lung Tumorigenesis.....</b>	<b>12</b>
Figure 2-1. $\beta$ -catenin is required for BRAF <sup>V600E</sup> -induced lung tumorigenesis.....	38
Figure 2-2. BRAF <sup>V600E</sup> cooperates with gain-of-function CTNNB1* to promote lung tumorigenesis .....	42
Figure 2-3. BRAF <sup>V600E</sup> and CTNNB1* cooperate to promote malignant lung carcinogenesis. ....	45
Figure 2-4. Dual regulation of c-MYC expression by CTNNB1* and BRAF <sup>V600E</sup> .....	49
Figure 2-5. Sustained c-MYC expression promoted BRAF <sup>V600E</sup> -induced lung tumorigenesis but fails to promote malignant lung cancer progression.....	51
Figure 2-6. c-MYC fails to promote malignant cancer progression of BRAF <sup>V600E</sup> -initiated lung tumors.....	56
Figure 2-7. Overexpression of c-MYC bypasses growth arrest of BRAF <sup>V600E</sup> -induced lung adenomas, in a two switch model of lung tumorigenesis.....	60
Figure 2-8. BRAF <sup>V600E</sup> -induced lung tumorigenesis is WNT ligand dependent .....	65
Figure 2-9. KRAS <sup>G12D</sup> cooperates with CTNNB1* to promote lethal lung tumorigenesis.....	71
Figure 2-10. Grading scheme used to classify BRAF <sup>V600E</sup> -initiated lung lesions.....	72
Figure 2-11. Schematic of <i>Braf</i> <sup>CA</sup> , <i>BAT-GAL</i> , <i>Ctnnb1</i> , <i>R26</i> <sup>MYC</sup> , and <i>s</i> alleles.....	74
Figure 2-12. Cooperation of BRAF <sup>V600E</sup> and Wnt/ $\beta$ -catenin signaling bypasses the growth arrest of BRAF <sup>V600E</sup> -induced lung adenomas and drives progression to lung adenocarcinoma.....	76

**Chapter 3. *In vivo* Sleeping Beauty Screen to Identify Potential Tumor Suppressor Genes and Oncogenes Important for Lung Cancer Progression.....78**

Figure 3-1. Experimental set-up for SB screen in BRAF<sup>V600E</sup>-initiated lung tumors.....87

Figure 3-2. Detection of SB transposase expression.....88

Figure 3-3. Mouse survival times were shortened and tumor progression was induced by SB-mediated mutagenesis.....89

# CHAPTER 1

## INTRODUCTION

### *Non-small cell lung cancer*

Lung cancer is the most common cause of death due to cancer in the world and the most recent statistics from the CDC reveal that in 2011 in the United States alone, lung cancer accounted for 207,339 patient diagnoses and 156,953 deaths. Lung cancer can be divided into two major types: small cell lung cancer (SCLC) (10-15% of all lung cancer cases) and non-small cell lung cancer (NSCLC) (85-90%). Three main subtypes of NSCLC: large cell carcinoma (10-15%), squamous cell carcinoma (25-30%), and adenocarcinoma (40%). In regards to adenocarcinoma, the most common subtype of NSCLC, patients with this disease have a fairly poor prognosis (1). The 5-year survival rate from 1995 to 2001 for patients with lung cancer was 15.7%, but varies depending on stage of disease at time of diagnosis. Patients harboring either stage IA, IIA, IIIA, or IV disease displaying a 49%, 30%, 14%, and 1% survival rate, respectively. Such poor prognosis reflects a need to better understand the molecular mechanisms underlying lung tumor progression and maintenance in order to develop successful therapies.

Currently, the standard of care for this disease includes radiation, chemotherapy (typically a combination of two of the following: Cisplatin, Carboplatin, Paclitaxel, or Pemetrexed), and/or surgery. However, advances in the past decade on both the genetics and signaling of cancer as well as the interaction of tumor cells with the microenvironment and immune system have led to tremendous advances in both immunotherapies and targeted therapies in combating this disease.

Comprehensive molecular profiling of non-small cell lung tumors has revealed that lung cancer can be sub-divided into genetically relevant sub-classes of driver mutations. And of these driver mutations, the majority falls into the Ras-Raf-MEK-ERK signaling pathway, with upregulation and mutations in this pathway being detected in approximately 76% of all lung cancer cases in a recent study by The Cancer Genome Atlas Research Network (2). This strong selective pressure to activate the MAPK pathway during NSCLC formation led to an attractive hypothesis: that the frequent mutation of this pathway may be a sign of its importance in the process of lung tumor formation and that a successful strategy against this disease may involve therapeutic interventions aimed at blocking this signaling pathway. This has paved the way for the use of targeted therapies against nodes of this pathway for lung cancer patients in the clinic, most notably EGFR tyrosine kinase inhibitors that have demonstrated survival benefits for a subset of NSCLC patients (3).

***BRAF<sup>V600E</sup> signaling and genetic cooperation in progression to Non-small cell lung cancer***

With this strong association between NSCLC formation and activation of the RAF/MEK/ERK MAPK signaling pathway our lab felt there was a need to understand the contribution of this pathway, and specifically the BRAF<sup>V600E</sup> oncogene to the initiation, progression, and response to therapeutics in NSCLC. However, despite its frequent activation in NSCLC patients, what our lab demonstrated was that activation of the BRAF<sup>V600E</sup> oncogene in the murine lung epithelium failed to form cancers, and instead led to the formation of benign lesions that underwent a senescence-like proliferative arrest following approximately 15-20 population doublings (4). This mirrored previous findings demonstrating that activation of the RAF/MEK/ERK MAPK pathway on its own fails to drive tumorigenesis in other settings. For

example, in skin the activation of the BRAF<sup>V600E</sup> oncogene specifically in melanocytes results in the formation of benign, senescent nevi (5). In both the lung and skin, cancer formation only occurs when sustained, oncogenic MAPK activation is combined with additional genetic events such as the loss of the *Tp53* or *Cdkn2a* tumor suppressor genes.

It was realized early on that cancers do not arise from a single mutation, but instead progression to malignant tumors requires multiple, sequential genetic alterations which allow cells to acquire the requisite traits to form a cancer, traits which Robert Weinberg and Douglas Hanahan would coin as “The Hallmarks of Cancer” (6). These traits include the ability to sustain proliferative signaling, evading growth suppressors, resisting cell death, enabling replicative immortality, inducing angiogenesis, and activating invasion and metastasis. That no single mutation or activated pathway is capable of driving all these hallmarks on its own has led to the concept of cooperation in which multiple mutations must act in concert to allow a cell to not only increase its rate of growth beyond the extrinsic cues dictated by its local environment, but also to escape the intrinsic anti-tumor mechanisms in place to limit such unrestrained growth. Studies using acute transforming retroviruses provide the earliest evidence of cooperation. The avian virus MH2 and the murine virus J2, which induce carcinomas in chickens and lymphomas in mice, respectively, both harbor the *v-myc* and *v-raf* oncogenes. It was discovered that the ability of J2 and MH2 to promote tumorigenesis both depend on the cooperation of *v-raf* with *v-myc*. However, despite the powerful selection for these two oncogenes acting in concert during cancer formation, the molecular basis underlying the cooperation of *v-raf* with *v-myc* was never extensively explored. Progress in the field of cancer research using *in vitro* transformation assays, *in vivo* mouse models of cancer, and genome-wide sequencing analyses, has led to the

identification of a vast number of protooncogenes and tumor suppressors whose combined activations and losses, respectively, contribute to tumorigenesis.

Yet we still do not fully understand the mechanistic details concerning how such mutations affect diverse cellular signaling networks to drive tumor formation. Determining how oncogenes and tumor suppressors cooperate to influence cellular programs to both drive proliferation as well as suppress ensuing intrinsic anti-tumor programs will help us identify potential therapeutic targets through an understanding of the dependencies of tumors on specific oncogenic signals. Such insights will allow us to not only better understand the molecular mechanisms involved in intrinsic anti-tumor responses but also allow us to better comprehend and predict the response of tumors to therapeutic interventions, providing us with a basis for designing effective therapeutic strategies in the future.

### ***RAS/RAF/MEK/ERK signaling***

Normal activation of the RAS/RAF/MEK/ERK mitogen-activated protein kinase (MAPK) pathway begins with extracellular mitogens binding to membrane receptor tyrosine kinases (RTKs). This leads to the association of the G-protein Ras with GTP, followed by the activation of Raf, which phosphorylates and activates MEK, which in turn phosphorylates and activates ERK, which ultimately leads to the regulation of various cellular processes including the activation of transcription factors involved in proliferation, differentiation, and survival. Mutations in this pathway therefore serve to keep this pathway permanently on, driving many of the hallmarks of cancer required for tumor formation.

It is therefore not surprising that the RTK/RAS/RAF signaling pathways is frequently deregulated in NSCLC, with recent studies detecting putative somatic driver mutations and/or



copy number alterations in 76% of lung adenocarcinoma patients (2). Of these oncogenes KRAS, EGFR, and BRAF were found at high frequency with driver events found in 32%, 11%, and 7% of patients, respectively.

The importance of this pathway in tumorigenesis is reflected in the strong antitumor responses elicited in patients when targeted therapies against this pathway are utilized. Two RTK inhibitors, erlotinib and gefitinib are currently used in the clinic to treat NSCLC. With erlotinib specifically, in a randomized, multicenter open-label trial, erlotinib improved progression-free and overall survival rates by a significant margin over platinum-based chemotherapy and was approved in May of 2013 as a first-line treatment for NSCLC (7). To further iterate the importance of this pathway in maintaining NSCLC, with the success of inhibitors against the BRAF<sup>V600E</sup> oncogene in melanoma there are numerous clinical trials underway to assess the efficacy of these therapies in NSCLC patients.

Despite this important role for the RAS/RAF/MEK/ERK MAPK pathway in driving tumorigenesis, taking a deeper look at the clinical data suggests that inhibiting this pathway may not be sufficient to elicit an antitumor response in all NSCLC patients. For example, in multiple clinical trials using either the EGFR TKIs erlotinib or gefitinib in EGFR mutation-positive NSCLC patients, including the Iressa Pan-Asia Study (IPASS), First-Signal, and EURTAC trials, objective response as defined by the Response Evaluation Criteria in Solid Tumors (RECIST) failed to be seen in anywhere between 15.4-42% of patients evaluated (8). Perhaps this can be explained by the dependence of tumors on multiple cooperating pathways regulating the requisite hallmarks of cancer, and therefore in order to elicit tumor regression in some patients we must also target these cooperating pathways. This reasoning is evident in the recent increase of clinical trials assessing the efficacy of combination therapies versus single agent therapies in treating

cancer. However, before we can target these pathways to successfully combat cancer, we must first identify which of these pathways play key roles in tumorigenesis and understand at the molecular level how these pathways complement with one another to influence the initiation, growth, progression, and response to therapies of these tumors.

### ***Canonical Wnt/ $\beta$ -catenin signaling***

In its most simplified view, when the canonical Wnt/ $\beta$ -catenin signaling pathway is inactivate, either through the absence of Wnt ligands in the microenvironment or due to the presence of pathway antagonists, beta-catenin is recruited to the APC destruction complex, where the kinases casein kinase 1 $\alpha$  (CKI $\alpha$ ) and GSK3 $\beta$  phosphorylate  $\beta$ -catenin at key residues in exon 3, marking it for proteasomal degradation. Upon activation of the Wnt/ $\beta$ -catenin signaling pathway, typically through the binding of secreted Wnt ligands to their cognate receptors, the APC complex is inactivated, allowing for  $\beta$ -catenin stabilization, accumulation, and subsequent translocation into the nucleus where it binds to TCF/LEF-1 proteins and transcriptional co-activators to regulate the expression of key genes, including c-MYC, and drive key biological processes including proliferation and differentiation.

With its ability to drive biological processes that also serve as hallmarks of cancer, it has been demonstrated that aberrant activation of this pathway can drive tumorigenesis in the same tissues in which this pathway normally plays a critical role in the embryonic development of that tissue as well as where it maintains adult stem and progenitor cells. The most notable example of this is in the intestine: the Wnt/ $\beta$ -catenin pathway is essential for the development of this tissue and regulates adult tissue homeostasis via stem cell renewal in the intestinal crypts, and its deregulation leads to the formation of colorectal cancer (9). In the lung previous studies in

various mouse models had shown that  $\beta$ -catenin activity both coincides with and is necessary for the development of the distal lung which, perhaps not coincidentally, is the same region of the lung from which NSCLC forms (10). Additionally, in the adult lung,  $\beta$ -catenin activity also coincides with and is necessary for proper regeneration of the lung following injury (11).

Despite the fact that mutations in  $\beta$ -catenin and APC are relatively rare in NSCLC, reports in the past few years indicate that the Wnt/ $\beta$ -catenin pathway may be upregulated in a majority of human NSCLC cell lines and tissue samples. For example, in resected NSCLCs a majority of tissues were found to stain positively for either Wnt1 or aberrant  $\beta$ -catenin expression (12). Clinically, evidence for Wnt/ $\beta$ -catenin pathway activation corresponded with poor prognosis. Several studies have detected both Wnt upregulation and amplification leading to autocrine Wnt signaling in human NSCLC lines, and more importantly that the growth of these cells are dependent on the presence of these Wnt ligands. For instance, in A549 cells expression of a dominant negative Wnt2 construct reduced the growth of these cells both in vitro and in a xenograft mouse model (13). Finally, TCGA data reveals that a large number of Wnt ligands display either copy number alterations and/or aberrant expression in NSCLC patients. These include: Wnt1, 2, 3a and 7b, which have been demonstrated to play a role in both lung development and repair in adult tissues, and also positively correlated with lung tumorigenesis, Wnt5a, an activator of non-canonical Wnt signaling, whose upregulation has been correlated with lung tumor metastasis, and Wnt7a, which has actually been demonstrated to be lost in NSCLC through promoter hypermethylation, suggesting a tumor suppressive role for this Wnt ligand in lung tumorigenesis (14). Due to this strong evidence pointing to the importance of the Wnt/ $\beta$ -catenin pathway in NSCLC formation, we explored the role of the Wnt/ $\beta$ -catenin in the

process of lung tumorigenesis as well as its potential as a therapeutic target both *in vitro* and *in vivo*.

### ***Use of genetically engineered mouse models to study human cancer***

Genetically engineered mouse models (GEMMs) of human cancer have played an integral role in our understanding of the molecular basis of this disease. Use of transgenic mice have allowed us to validate putative oncogenes and tumor suppressor genes, dissect the function and downstream signaling of these genes during tumorigenesis, as well as test the necessity and sufficiency of these cancer genes in tumor formation, maintenance, and progression (15).

Despite the utility of the original GEMMs in modeling tumorigenesis, enforced expression of oncogenes or loss of tumor suppressor genes in entire tissues throughout the lifetime of an animal led to the formation of cancers that did not always faithfully recapitulate the human disease. More faithful modeling of the sporadic nature of somatic human cancers therefore required an ability to mimic the stochasticity of oncogene activation and/or tumor suppressor gene deletion in one or a few number of cells. This has led to the creation of conditional mouse models in which oncogenes are expressed from their endogenous locus only after Cre-mediated recombination of the appropriate loxP-flanked chromosomal DNA elements (*Braf*<sup>CA</sup> and *Kras*<sup>LSL</sup> mice) or Flp-mediated recombination of the appropriate frt-flanked chromosomal DNA elements (*Braf*<sup>FA</sup> mice), overexpressed from exogenous loci following the excision of loxP or frt-flanked STOP cassettes upstream of exogenous promoters (*RFS-Myc* and *RCL::Sleeping Beauty* mice), or in which tumor suppressor genes are deleted upon excision of loxP- or frt-flanked exons by Cre or Flp recombinases, respectively (16). The creation of these conditional mouse models has therefore given researchers remarkable spatiotemporal control

over the expression of oncogenes and tumor suppressors via the use of tissue-specific and inducible Cre/Flp recombinases.

In studying lung cancer formation, oncogene activation or tumor suppressor deletion is restricted to the lung through use of Cre and/or Flp recombinase-regulated alleles along with intranasal delivery of Cre or Flp recombinase-expressing adenoviruses or lentiviruses. Furthermore, while activation or deletion of genes was once forced to occur simultaneously in any given animal, combination of mutant alleles controlled by either the Cre/lox or Flp/frt recombinase systems now grants us sequential and spatial regulation of these different genes.

### ***Sleeping Beauty Mutagenesis***

There have typically been two approaches in studying the roles of cancer genes in the mouse: (1) generating engineered alleles and testing their role in tumorigenesis in a candidate-based approach and (2) use of retroviral insertional mutagenesis for forward genetics screens. While the candidate-based approach using transgenic and knock-in mice is the gold standard in validating and defining the oncogenicity of candidate cancer genes, this system has extreme limits in regards to discovery of novel oncogenes and tumor suppressors. This system requires expensive, complex, and time-consuming breeding schemes and because of this is typically limited to the validation rather than discovery of cancer genes. For decades researchers have utilized insertional mutagenesis to gain insights into numerous cellular and development processes in lower organisms, most notably in *Drosophila*. However, prior to the development of the Sleeping Beauty (SB) mutagenesis system, insertional mutagenesis in mammals was extremely limited. While retroviruses are capable of activating or inactivating genes via their integration into the host genome as a provirus, the retroviral system is limited in its ability to

only form mammary and hematopoietic tumors. It was just a decade ago that the development of a new insertional mutagenesis system known as Sleeping Beauty (SB) mutagenesis finally gave researchers tools capable of inducing cancer in solid tumors (17). This system was the first cut-and-paste transposon system to have activity in mammals and was aptly named Sleeping Beauty as this system utilizes transgenes that are reconstructions of consensus sequences identified in an ancient Tc1/mariner transposable element which allowed researchers to revert the mutations inactivating its transposition, reawakening these once mobile DNA elements (18). The use of the SB system in combination with numerous GEMMs of cancer in the past decade has transformed our understanding of the molecular basis for this disease.

The Sleeping Beauty transposon-mediated somatic mutagenesis system contains two major components (1) a transposable element and (2) a transposase mediating the transposition of these elements. Improvement on the SB system led to the construction of the T2/Onc and T2/Onc2 transposons specifically for mutagenesis. They are engineered to maximize transposon “hopping” throughout the genome and have the ability to both activate genes via the presence of a retroviral LTR and splice donor, as well as inactivate genes via the presence of splice acceptor sites on both DNA strands and a bidirectional polyA sequence; this allows the T2/Onc and T2/Onc2 transposons to induce expression of truncated proteins. These transposable elements were used to create transgenic mice with transposon donor arrays of either moderate or high transposon copy number. A knock-in mouse was created to regulate transposase expression through the knock-in of a CAGGS-SB11 allele regulated by a Cre-dependent STOP cassette into the mouse *Rosa26* locus. Thus, similar to the activation and inactivation of genes in other conditional GEMMs of cancer, SB activation and transposition of the transposable elements is spatially and temporally restricted by the regulation of Cre expression; each transposon flanked

by inverted repeats recognized by the transposase allowing these elements to be cut out of its current site in the genome via double-stranded breaks and inserted into any TA dinucleotide in the genome. In regards to cancer gene discovery with this system, it was reasoned that if a transposon (or transposons) landed in a site that transformed that cell or conferred that cell with a growth advantage, then there would be a strong selective pressure to maintain the transposon(s) at that site.

Indeed, this system has demonstrated great success in inducing and accelerating tumorigenesis in multiple mouse tissues, including both hematopoietic and solid tumors. These include previous SB screens in squamous cell carcinoma, B-cell lymphoma, chronic lymphoblastic leukemia, pancreatic cancer, hepatocellular carcinoma, and colorectal cancer and have facilitated the identification and subsequent validation of numerous candidate cancer genes and pathways including a previously unknown role for axon guidance molecules in driving pancreatic cancer (19).

It is for these reasons that we chose to take advantage of the SB mutagenesis system to search for novel genes and pathways capable of bypassing the barriers to BRAF<sup>V600E</sup>-mediated lung cancer formation. To do this we combined our *Braf*<sup>CA</sup> allele with a Cre-activatable CAGGS-SB10 allele knocked-in to the *Rosa26* locus (*Rosa26-CAGGS-LSL (RCL)::SB*) into the aforementioned high copy number T2/Onc2 transposon donor mouse. The purpose of our SB screen was therefore to take an unbiased approach to identify additional genes and pathways capable of cooperating with oncogenic BRAF<sup>V600E</sup> to drive progression to adenocarcinoma, which would provide insight into the evolutionary forces influencing NSCLC formation, and allow us to separate driver mutations from passenger mutations in human cancers.

## CHAPTER 2

### ROLE OF WNT/ $\beta$ -CATENIN/C-MYC SIGNALING IN LUNG TUMORIGENESIS\*

#### ABSTRACT

Oncogene-induced senescence (20) is proposed as a cellular defense mechanism that restrains malignant progression of oncogene expressing, initiated tumor cells. Consistent with this, expression of BRAF<sup>V600E</sup> in the mouse lung epithelium elicits benign tumors that fail to progress to cancer due to an apparent senescence-like proliferative arrest. Here we demonstrate that nuclear  $\beta$ -catenin $\rightarrow$ c-MYC signaling is essential for early-stage proliferation of BRAF<sup>V600E</sup>-induced lung tumors and is inactivated in the subsequent senescence-like state. Furthermore, either  $\beta$ -catenin silencing or pharmacological blockade of Porcupine, an acyl-transferase essential for WNT ligand secretion and activity, significantly inhibited BRAF<sup>V600E</sup>-initiated lung tumorigenesis. Conversely, sustained activity of  $\beta$ -catenin or c-MYC significantly enhanced BRAF<sup>V600E</sup>-induced lung tumorigenesis and rescued the anti-tumor effects of Porcupine blockade. These data indicate that early-stage BRAF<sup>V600E</sup>-induced lung tumors are WNT dependent and suggest that inactivation of WNT $\rightarrow$  $\beta$ -catenin $\rightarrow$ c-MYC signaling is a trigger for the senescence-like proliferative arrest that constrains the expansion and malignant progression of BRAF<sup>V600E</sup>-initiated lung tumors. Moreover, these data further suggest that the trigger for OIS in initiated BRAF<sup>V600E</sup> expressing lung tumor cells is not simply a surfeit of signals from oncogenic BRAF, but an insufficiency of WNT $\rightarrow$  $\beta$ -catenin $\rightarrow$ c-MYC signaling. These data have

---

\* This chapter has been published: Juan J, Muraguchi T, Iezza G, Sears RC, McMahon M. Diminished WNT $\rightarrow$  $\beta$ -catenin $\rightarrow$ c-MYC signaling is a barrier for malignant progression of BRAF<sup>V600E</sup>-induced lung tumors. *Genes Dev* 2014;**28**:561-75.



implications for understanding how genetic abnormalities cooperate to initiate and promote lung carcinogenesis.

## INTRODUCTION

Non-small cell lung cancer (NSCLC) is a leading cause of cancer mortality with adenocarcinoma its most common subtype (1). Driver mutations in proto-oncogenes have been identified in NSCLC, providing a rational strategy for the successful clinical deployment of pathway-targeted therapies targeting oncoproteins such as EGF receptor, ROS1 or AML4-ALK in genetically-defined subsets of lung cancer patients (7, 21-23).

Mutationally activated KRAS is the most common driver oncoprotein in NSCLC ( $\geq 25\%$ ) but also the most pharmacologically intractable (23). However, certain KRAS effectors are directly implicated as *bona fide* NSCLC oncogenes such as *BRAF* that is mutated in  $\sim 8\%$  of NSCLC, with one quarter of such mutations encoding the constitutively active  $BRAF^{V600E}$  oncoprotein (23, 24). While agents that specifically inhibit  $BRAF^{V600E}$  have been developed, *BRAF* mutation has proven an unreliable prognostic marker for the clinical effectiveness of such agents. Indeed, whereas vemurafenib is successful in treating *BRAF* mutated melanoma, it displays limited efficacy against *BRAF* mutated colorectal or thyroid cancer (25-28). Although *BRAF* mutated NSCLC cell lines are MEK inhibitor sensitive *in vitro*, it remains to be seen whether patients with *BRAF* mutated lung cancer will be clinically responsive to agents that target  $BRAF^{V600E} \rightarrow MEK \rightarrow ERK$  signaling (29, 30).

To explore mechanisms of lung carcinogenesis in detail, we generated mice (*Braf*<sup>fCA</sup>) carrying a conditional allele of *BRAF* in which expression of normal BRAF is converted to BRAF<sup>V600E</sup> following the action of Cre recombinase (Fig. 2-11a) (4, 5, 31, 32). Expression of BRAF<sup>V600E</sup> in the lung epithelium elicits multifocal, MEK-dependent lung tumors with short latency and 100% penetrance (4, 29, 33). However, these tumors remain benign and rarely progress to NSCLC unless combined with additional genetic events (4, 33).

Key unresolved questions in this model are: 1. What promotes an initiated BRAF<sup>V600E</sup> expressing lung epithelial cell to become a benign lung tumor; 2. What triggers the senescence-like proliferative arrest of BRAF<sup>V600E</sup>-induced benign tumors and; 3. Does bypass of senescence inevitably result in malignant progression to NSCLC? To address these questions we explored the potential importance of WNT signaling, a pathway implicated in lung development, homeostasis and cancer, in BRAF<sup>V600E</sup>-induced lung tumorigenesis (10, 11, 34-37). Our results indicate that WNT→β-catenin→c-MYC signaling is essential for BRAF<sup>V600E</sup>-induced lung tumorigenesis. Moreover, they indicate a striking linearity of the role of this pathway in sustaining BRAF<sup>V600E</sup> driven lung tumor growth. However, whereas co-expression of BRAF<sup>V600E</sup> with mutated β-catenin led to malignant NSCLC, co-expression of BRAF<sup>V600E</sup> with c-MYC did not. Taken together, these data emphasize the key role of cooperating signaling pathways in the initiation of lung tumorigenesis, the maintenance of tumor cell proliferation and the acquisition of malignant characteristics.

## RESULTS

### ***β-Catenin activity correlates with proliferation of BRAF<sup>V600E</sup>-initiated lung tumors***

To test for a role for WNT signaling in BRAF<sup>V600E</sup>-induced lung tumorigenesis, we generated mice carrying a Cre-activated *BRaf<sup>CA</sup>* allele and a transgenic reporter for nuclear β-catenin/TCF activity (*BAT-GAL*, Fig. 2-11b) (10). BRAF<sup>V600E</sup> expression was initiated in the lung epithelium of compound *BRaf<sup>CA</sup>; BAT-GAL* mice using Adenovirus-Cre (Ad-Cre, 10<sup>7</sup> pfu), with mice euthanized for analysis at 6 or 12 weeks post-initiation (p.i.). Six weeks p.i. BRAF<sup>V600E</sup>-induced lung tumors expressed BAT-GAL activity (Fig. 2-1a) and remained proliferative as assessed by Ki67 expression in Surfactant Protein C expressing (SPC+) tumor cells (Figs. 2-1a & 2-1b) or by BrdU incorporation (not shown). By contrast, 12 weeks p.i., BAT-GAL activity and proliferation in BRAF<sup>V600E</sup>-induced lung tumor cells were greatly diminished (Fig. 2-1b) consistent with the onset of senescence-like proliferative arrest. As a control, we assessed BAT-GAL activity in BRAF<sup>V600E</sup>/TP53<sup>Null</sup> lung tumors emerging in similarly initiated *BRaf<sup>CA</sup>; Trp53<sup>ff</sup>; BAT-GAL* mice. These tumors sustain their proliferation, do not undergo cell cycle arrest and also retained BAT-GAL activity providing evidence of ongoing β-catenin signaling (Figs. 2-1a & 2-1b). These data indicate that BAT-GAL activity correlates with the proliferation status of BRAF<sup>V600E</sup>-induced lung tumor cells.

### ***β-catenin is required for BRAF<sup>V600E</sup>-initiated lung tumorigenesis***

To determine if β-catenin is required for lung tumorigenesis, BRAF<sup>V600E</sup> expression was initiated in the lungs of *BRaf<sup>CA</sup>* mice that were either heterozygous or homozygous for a conditional null allele of β-catenin (*Ctnnb1<sup>f</sup>*, Fig. 2-11c) with tumorigenesis assessed 12 weeks p.i. (4, 29, 38). The lungs of *BRaf<sup>CA</sup>; Ctnnb1<sup>f/+</sup>* mice exhibited tumorigenesis similar to that

observed in control *BRaf<sup>CA</sup>* mice (Fig. 2-1c). By contrast, *BRaf<sup>CA</sup>; Ctnnb1<sup>flf</sup>* mice displayed a significant reduction in tumor burden (29% vs. 4%, Figs. 2-1c & 2-1d,  $p < 0.001$ ). Moreover, immunofluorescence analysis of lung tumors that formed in *BRaf<sup>CA</sup>; Ctnnb1<sup>flf</sup>* mice revealed them to retain  $\beta$ -catenin expression, most likely due to the failure of Cre recombinase to silence both copies of *Ctnnb1<sup>f</sup>* (Fig. 2-1c). This striking reduction of lung tumorigenesis combined with the retention of  $\beta$ -catenin expression in those tumors that formed in *BRaf<sup>CA</sup>; Ctnnb1<sup>flf</sup>* mice, provides compelling evidence for its importance in early-stage BRAF<sup>V600E</sup>-induced lung tumorigenesis.

### ***Stabilized $\beta$ -catenin expression cooperates to promote BRAF<sup>V600E</sup>-induced lung carcinogenesis***

We next tested whether a stabilized form of  $\beta$ -catenin would cooperate with BRAF<sup>V600E</sup> to sustain tumor growth and promote malignant progression to NSCLC. To do so we employed a Cre-activated  $\beta$ -catenin allele (*Ctnnb1<sup>ex3(f)</sup>*, Fig. 2-11d) in which exon 3 of *Ctnnb1* is flanked by loxP sites such that Cre recombinase excises sequences required for APC-mediated  $\beta$ -catenin destruction leading to expression of a stabilized form of  $\beta$ -catenin (CTNNB1\*) (39). Consistent with previous data, CTNNB1\* expression in mouse lung failed to elicit any overt lung pathology at any time point analyzed (36) (Data not shown). However, BRAF<sup>V600E</sup> and CTNNB1\* co-expression led to a dramatic increase in lung tumor burden whether measured at 4 or 10-12 weeks p.i. (Fig. 2-2a). This increased tumor burden led to a striking reduction in mouse survival with 100% of *BRaf<sup>CA</sup>; Ctnnb1<sup>ex3(f)/+</sup>* mice reaching end-stage by 13 weeks p.i. By contrast, 100% of the control *BRaf<sup>CA</sup>* or *Ctnnb1<sup>ex3(f)/+</sup>* mice remained alive 16 weeks p.i. As reported previously, we also observed cooperation between oncogenic KRAS<sup>G12D</sup> and CTNNB1\* in lung tumorigenesis (Fig. 2-9) (36). Ki67 staining revealed that BRAF<sup>V600E</sup>/CTNNB1\* co-expressing

tumors displayed an elevated proliferative index compared to tumors expressing BRAF<sup>V600E</sup> alone at either early (4 weeks) or late (12 weeks) time points p.i. (Figs. 2-2c & 2-2d). Most notably, CTNNB1\* co-expression prevented the decrease in cell proliferation observed in lung tumors 12 weeks after BRAF<sup>V600E</sup> expression. Immunofluorescence staining revealed that BRAF<sup>V600E</sup>/CTNNB1\* co-expressing tumors sustained c-MYC expression, a known  $\beta$ -catenin/TCF target gene, by comparison to tumors with BRAF<sup>V600E</sup> expression alone (Fig. 2-2c) (40). However, despite the fact that Cyclin D1 is co-regulated by  $\beta$ -catenin and ERK1/2 MAP kinase signaling in colorectal cancer cells (41), there was no difference in Cyclin D1 between the two groups of tumors, similar to previous reports (Figs. 2-2c & 2-2d) (42). These results suggest that, although it elicits no lung pathology on its own, activated  $\beta$ -catenin is a potent promoter of the proliferation of BRAF<sup>V600E</sup>-induced lung tumors.

Given the ability of CTNNB1\* expression to promote BRAF<sup>V600E</sup>-induced lung tumorigenesis, we assessed whether BRAF<sup>V600E</sup>/CTNNB1\* co-expressing tumors displayed malignant progression using previously established grading criteria (43). Oncogene expression was initiated in either *BRAF<sup>CA</sup>* or *BRAF<sup>CA</sup>; Ctnnb1<sup>ex3(f)/+</sup>* mice with tumor grade assessed at 10-12 weeks p.i. (Fig. 2-3b & Fig. 2-10e). BRAF<sup>V600E</sup>-induced lung lesions were comprised almost exclusively of hyperplasias (15.31%) and Grade I benign adenomas (83.37%) and only rarely (<2%) did we detect larger Grade II benign adenomas (Fig. 2-3b). Indeed, even 16-24 weeks p.i., BRAF<sup>V600E</sup>-induced lung tumors remained low grade and benign (Fig. 2-6a) (4, 29, 33). By contrast, BRAF<sup>V600E</sup>/CTNNB1\* co-expressing tumors displayed clear evidence of malignant progression as early as 10 weeks p.i. at which time 34% of tumors were Grade III advanced adenomas and 7% were Grade IV lung adenocarcinomas (Fig. 2-3b). Indeed, this degree of

cancer progression is similar to that observed in BRAF<sup>V600E</sup>/TP53<sup>Null</sup> lung tumors at the same time point (4). These data indicate that sustained activity of  $\beta$ -catenin, a genetic lesion that has no effect alone on lung epithelial cells, drives progression of BRAF<sup>V600E</sup>-initiated benign adenomas towards adenocarcinoma.

To determine if co-expression of CTNNB1\* would influence tumor cell differentiation, tissue sections of BRAF<sup>V600E</sup> or BRAF<sup>V600E</sup>/CTNNB1\* expressing lung tumors, at either early (4-8 weeks) or late (12 weeks) times p.i., were analyzed by immunostaining (Figs. 2-3c & 2-3d). As observed previously, BRAF<sup>V600E</sup>-induced benign lung tumors expressed the NKX2.1 transcription factor, SPC and Aquaporin 5 (AQP5) but failed to express Clara Cell antigen (CC10) (29). To our surprise, BRAF<sup>V600E</sup>/CTNNB1\* expressing lung tumors displayed the same pattern of marker expression at both early and late time points. We noted that occasional late-stage BRAF<sup>V600E</sup>/CTNNB1\* expressing lung tumors displayed reduced NKX2.1 and SPC expression with evidence of elevated N-cadherin and  $\alpha$ -smooth muscle actin expression (Fig. 2-3d, bottom panel as indicated and data not shown), but the significance of this remains unclear. Consequently, despite its ability to promote malignant progression, expression of CTNNB1\* did not appear to have a major influence on the differentiation status of the majority of BRAF<sup>V600E</sup>-induced lung tumor cells.

***Tumor cell proliferation is under the dual control of both BRAF<sup>V600E</sup> and CTNNB1\* signaling through effects on c-MYC***

Nuclear  $\beta$ -catenin regulates expression of RNAs involved in processes central to the aberrant behavior of cancer cells (44). Two well characterized target genes are Cyclin D1 and c-

MYC (40, 41). As reported previously, we noted that c-MYC, but not Cyclin D1, expression correlated with diminished  $\beta$ -catenin activity in BRAF<sup>V600E</sup>-induced benign lung tumors (Fig. 2-2d) (42). To further explore this, we generated BRAF<sup>V600E</sup>/CTNNB1\*/TP53<sup>Null</sup> (BCT) lung cancer derived cells from an end-stage *BRaf<sup>cA</sup>; Ctnnb1<sup>ex3(f)/+</sup>; Trp53<sup>flf</sup>* mouse (Figs. 2-4a & 2-4b & Experimental Procedures). Untreated BCT cells display detectable phospho (p)-ERK1/2, express normal and activated CTNNB1\* (upper and lower bands respectively) as well as c-MYC, Cyclin D1 and CDK4 (Fig. 2-4a). Treatment of BCT cells with either of two different siRNAs against CTNNB1 (si $\beta$ -cat1/2) extinguished expression of both normal and mutationally activated CTNNB1, inhibited c-MYC expression (>50%) but had no effect on either Cyclin D1 or CDK4 expression (Fig. 2-4a). Interestingly, inhibition of either CTNNB1\* expression or pharmacological inhibition of BRAF<sup>V600E</sup>→MEK→ERK signaling (PD325901) each had inhibitory effects on c-MYC mRNA and protein abundance, but combined inhibition of both pathways largely extinguished c-MYC expression (Figs. 2-4b & 2-4c) (45). These data suggest that c-MYC expression is under dual control of both  $\beta$ -catenin and BRAF<sup>V600E</sup> and is consistent with previous data indicating an important role for these pathways in the regulation of c-MYC in various settings including lung tumorigenesis (40, 46, 47).

Treatment with either sib-Cat1 or PD325901 led to a striking reduction in the percentage of BCT cells in S phase with a concomitant increase of cells in G1 indicating that coordinate BRAF<sup>V600E</sup> and  $\beta$ -catenin signaling is required for BCT cell cycle progression (Fig. 2-4d). In separate experiments, we showed that the anti-proliferative effects of MEK1/2 inhibition in BRAF<sup>V600E</sup>/TP53<sup>Null</sup> lung cancer cells could be overcome by c-MYC:ER activation (Not shown) (48, 49). To test if the effects of  $\beta$ -catenin silencing could also be overcome by sustained c-

MYC activity, BCT cells were engineered to express c-MYC:ER. As expected, treatment of BCT cells with sib-Cat1 suppressed their proliferation by ~50% (Fig. 2-4e). Although activation of c-MYC:ER (with 4-HT) had no effect on the baseline proliferation of BCT cells, it was able to substantially restore the proliferation of cells treated with sib-Cat1 (Fig. 2-4e). Importantly, expression/activation of c-MYC:ER had no effect on BRAF<sup>V600E</sup>→MEK→ERK activity in BCT cells (Fig. 2-4f). Hence, the growth inhibitory effects of β-catenin silencing can be substantially overcome by ectopic c-MYC activity.

### ***Sustained c-MYC expression promotes BRAF<sup>V600E</sup>-induced benign lung tumorigenesis***

Given the importance of c-MYC in the cooperation of BRAF<sup>V600E</sup> and CTNNB1\* for lung tumorigenesis we tested the ability of sustained c-MYC expression to promote BRAF<sup>V600E</sup>-induced benign lung tumorigenesis using mouse strains (*RFS<sup>MYC</sup>*) in which cDNAs encoding either wild-type (WT) or a phospho-site mutant (T58A) of c-MYC were recombined into the Rosa26 locus downstream of a floxed-STOP element (Fig. 2-11e) (16, 50, 51). Hence, Ad-Cre treatment of *BRaf<sup>CA</sup>; RFS<sup>MYC</sup>* mice leads to co-expression of both BRAF<sup>V600E</sup> and either WT or T58A c-MYC in the lung epithelium.

Lung tumorigenesis was initiated in five cohorts of mice: 1. *BRaf<sup>CA</sup>*; 2. *BRaf<sup>CA</sup>; RFS<sup>MYC(WT)/+</sup>*; 3. *BRaf<sup>CA</sup>; RFS<sup>MYC(WT)/(WT)</sup>*; 4. *BRaf<sup>CA</sup>; RFS<sup>MYC(T58A)/+</sup>* and; 5. *BRaf<sup>CA</sup>; RFS<sup>MYC(T58A)/(T58A)</sup>* with mice euthanized for analysis at 4-8 or >16 weeks p.i. As expected, expression of endogenous c-MYC was detected by immunofluorescence in BRAF<sup>V600E</sup>-induced lung tumors at the early but not at the later time point (Fig. 2-5a). By contrast, c-MYC was readily detected in tumors derived from all of the other genotypes at both early and late time points, indicating co-activation of the



*BRAF*<sup>CA</sup> and *RFS*<sup>MYC</sup> alleles in lung tumors (Fig. 2-5a), a result confirmed by immunoblotting of tumor-derived lysates from *BRAF*<sup>CA</sup> (lanes 1 & 2), *BRAF*<sup>CA</sup>; *RFS*<sup>MYC(WT or T58A)/+</sup> (lanes 3-6) or *BRAF*<sup>CA</sup>; *RFS*<sup>MYC(WT)/(WT)</sup> (lanes 7-11) mice (Fig. 2-5b).

Kaplan-Meier analysis indicated that expression c-MYC (WT or T58A) in the lung had no effect on mouse survival (Data not shown). By contrast, *BRAF*<sup>CA</sup> mice, either heterozygous or homozygous for the WT or T58A *RFS*<sup>MYC</sup> alleles, displayed significantly reduced survival compared to *BRAF*<sup>CA</sup> controls (Fig. 2-5c, p<0.001 vs. *RFS*<sup>MYC/+</sup> and p<0.0001 vs. *RFS*<sup>MYC/MYC</sup>). Moreover, there appeared to be an activity and gene dosage effect such that *BRAF*<sup>CA</sup> mice heterozygous for *RFS*<sup>MYC(T58A)</sup> reached end-stage more rapidly than *BRAF*<sup>CA</sup> mice heterozygous for *RFS*<sup>MYC(WT)</sup> (p<0.001). In addition, *BRAF*<sup>CA</sup> mice homozygous for either *RFS*<sup>MYC</sup> allele succumbed to end-stage disease more rapidly than their heterozygous littermates (p<0.0001). In this case there was no statistically significant difference between the c-MYC alleles used (Fig. 2-5d).

Consistent with previous reports, expression of c-MYC alone failed to elicit any overt pathology in the lung even at 24 weeks p.i. (52). However, expression of a single *RFS*<sup>MYC</sup> allele with BRAF<sup>V600E</sup> led to a significant increase in tumor size and burden (Figs. 2-5d & 2-5e). Consistent with their further diminished survival, *BRAF*<sup>CA</sup> mice homozygous for either *RFS*<sup>MYC</sup> allele displayed a significant increase in tumor burden compared to relevant controls (Fig. 2-5e). Hence, like CTNNB1\*, c-MYC significantly enhanced BRAF<sup>V600E</sup>-induced lung tumorigenesis without having an overt pathological effect itself on the mouse lung epithelium.

To assess the effects of c-MYC on the proliferation of BRAF<sup>V600E</sup>-induced tumors, oncogene expression was initiated in a second group of mice at lower dose Ad-Cre (10<sup>6</sup> pfu) to induce fewer tumors and allow the mice to live longer. Using Ki67 expression as an indicator, BRAF<sup>V600E</sup>/c-MYC co-expressing tumors displayed both elevated and sustained proliferation (Figs. 2-5f & 2-5g) at both early (8 weeks p.i., 35% vs. 20%) and late time points (17.5 weeks p.i., 20% vs. 5%) (Fig. 2-5f) compared to control BRAF<sup>V600E</sup>-induced lung tumors. Furthermore, when transit through S phase was assessed by long-term BrdU labeling (7 days), greater than 50% of SPC+ BRAF<sup>V600E</sup>/c-MYC<sup>T58A</sup> expressing tumor cells incorporated BrdU whereas less than 10% of BRAF<sup>V600E</sup> expressing tumor cells were BrdU positive (Fig. 2-5g). These results support the hypothesis that an insufficiency of β-catenin→c-MYC signaling is responsible for the proliferative arrest of late-stage BRAF<sup>V600E</sup>-initiated lung tumor cells.

***c-MYC expression fails to promote malignant progression of BRAF<sup>V600E</sup>-induced lung tumors***

c-MYC's ability to promote BRAF<sup>V600E</sup>-induced lung tumorigenesis prompted us to test whether BRAF<sup>V600E</sup>/c-MYC co-expression would promote lung carcinogenesis. To that end tumorigenesis was initiated with a low dose (10<sup>6</sup> pfu) of Ad-Cre in each of the *BRAF<sup>CA</sup>*; *RFS<sup>MYC</sup>* cohorts described above with mice euthanized at 4-8, 10-14 or 16+ weeks p.i. to assess lung tumor grade (Fig. 2-6 & 2-10) (43). As before, BRAF<sup>V600E</sup>-induced lung lesions were largely hyperplasias or benign Grade I adenomas no matter the time of analysis (Fig. 2-6a). Although >70% of BRAF<sup>V600E</sup>/c-MYC induced tumors displayed progression to Grade II large benign adenomas, none of these lesions were Grade III high-grade adenomas or Grade IV adenocarcinomas (Fig. 2-6a). This was true for all combinations of BRAF<sup>V600E</sup> and c-MYC (WT or T58A) and regardless of the time point analyzed (not shown). Hence, despite c-MYC's ability

to promote early-stages BRAF<sup>V600E</sup>-induced tumorigenesis, it was unable to cooperate with BRAF<sup>V600E</sup> for malignant transformation of cells, in contrast to other genetic alterations such as CTNNB1\*, PIK3CA<sup>H1047R</sup> or silencing of TP53 or INK4A/ARF (4, 33, 53). These data are consistent with those of others using a similar system to analyze the effects of sustained MYC activity on BRAF<sup>V600E</sup>-induced lung tumorigenesis (54). Finally, BRAF<sup>V600E</sup>/c-MYC<sup>T58A</sup> co-expressing tumors expressed NKX2.1, SPC and AQP5 at all time points indicating that c-MYC had not altered the differentiation status of BRAF<sup>V600E</sup>-initiated lung tumor cells (Figs. 2-6c & 2-6d).

***c-MYC rescues the inhibitory effects of  $\beta$ -catenin silencing on BRAF<sup>V600E</sup>-induced lung tumorigenesis***

Although c-MYC is regarded as a potentially important  $\beta$ -catenin effector, there are numerous targets of  $\beta$ -catenin that may play an important role in BRAF<sup>V600E</sup>-induced lung tumorigenesis (42, 44, 53). Since  $\beta$ -catenin silencing inhibited BRAF<sup>V600E</sup>-induced lung tumorigenesis, we tested the ability of c-MYC to rescue that effect. To do so, lung tumorigenesis was initiated in *BRaf<sup>CA</sup>* mice, either heterozygous or homozygous for *Ctnnb1<sup>ff</sup>* and either with or without one *RFS<sup>MYC(T58A)</sup>* allele with mice euthanized for analysis 12 weeks p.i. (Fig. 2-6e). As before,  $\beta$ -catenin silencing inhibited BRAF<sup>V600E</sup>-induced lung tumorigenesis (Figs. 2-2, 2-6e & 2-6f). However, when c-MYC<sup>T58A</sup> was co-expressed with BRAF<sup>V600E</sup> we observed substantial rescue of lung tumorigenesis in *BRaf<sup>CA</sup>* mice homozygous for the *Ctnnb1<sup>ff</sup>* allele (Figs. 6e&f). These data suggest that c-MYC expression rescued the proliferation of BRAF<sup>V600E</sup>/CTNNB1<sup>Null</sup> initiated lung tumor cells.

Immunofluorescence analysis of  $\beta$ -catenin expression revealed that  $\sim 100\%$  of tumors that formed in either  $BRaf^{CA}$  or  $BRaf^{CA}; Ctnnb1^{flf}$  mice expressed  $\beta$ -catenin (Fig. 2-6e). By contrast,  $>75\%$  tumors forming in  $BRaf^{CA}; Ctnnb1^{flf}; RFS^{MYC(T58A)}$  mice were either completely negative for CTNNB1 expression or displayed a mixture of CTNNB1-positive and negative tumor cells (Figs. 2-6f). Hence, the ability of c-MYC to rescue the anti-tumor effects observed in  $BRAF^{V600E}/CTNNB1^{Null}$  cells strongly suggests that c-MYC expression is a crucial target downstream of  $\beta$ -catenin required for  $BRAF^{V600E}$ -induced benign lung tumor cell proliferation.

***Overexpression of c-MYC reactivates tumor proliferation in already growth arrested  $BRAF^{V600E}$ -initiated tumors***

We next asked whether the senescence-like proliferative arrest associated with loss of c-MYC expression in  $BRAF^{V600E}$ -initiated adenomas was irreversible, or whether reactivation of c-MYC expression could bring these tumor cells back into cell cycle. We were able to temporally dissociate the activation of  $BRAF^{V600E}$  expression from its endogenous locus from transgene overexpression of c-MYC by generating  $Braf^{FA/+}; RFS^{Myc(T58A)}; SpC-Cre:ER$  compound mice. The  $Braf^{FA}$  allele relied on Flp recombinase activity to initiate oncogenic  $BRAF^{V600E}$  expression, which was delivered to the lung epithelium by low titer Adenovirus-Cre. In contrast, c-Myc transgene expression was regulated by Cre recombinase, whose expression itself was targeted to tumor cells through use of the SpC promoter and whose activity was regulated by the presence of tamoxifen (delivered by intraperitoneal (IP) injection of tamoxifen into these animals).

$Braf^{FA/+}; RFS^{Myc(T58A)}; SpC-Cre:ER$  compound mice were infected with  $10^6$  p.f.u. of Flp expressing adenovirus (Adenovirus-Flp) to induce benign tumorigenesis (Fig. 2-7a). At 12 weeks

p.i., when BRAF<sup>V600E</sup>-initiated tumors are growth arrested, mice were injected with either vehicle or tamoxifen to induce expression of c-MYC<sup>T58A</sup> in SpC-positive tumor cells. Lung tumor burden, size, and number were assessed 4 and 8 weeks later. Tamoxifen-injected mice displayed an increase in tumor burden and size (145410  $\mu\text{m}^2$ ) over vehicle-injected mice (59442  $\mu\text{m}^2$ ) (Fig. 2-7b & 2-7c). This increase in tumor burden and size was accompanied by a greater proliferative index within these BRAF<sup>V600E</sup>-initiated tumors (Figs. 7e-7f). Tamoxifen-treated mice had a significantly higher percentage of BrdU+ tumor cells (23.3%) compared to vehicle-treated mice (13.9%) following one week of labeling. These results demonstrated that the growth arrest observed in BRAF<sup>V600E</sup>-driven benign adenomas is not senescence, but instead a strong proliferative arrest caused by insufficient c-MYC expression.

These experiments also allowed us to discern whether cooperation of c-MYC with BRAF<sup>V600E</sup> is the result of the initiation of tumorigenesis in a lung cell subpopulation different from that transformed by BRAF<sup>V600E</sup> alone (and perhaps fated to bypass the proliferative arrest observed in other cell types with BRAF<sup>V600E</sup> expression) or whether c-MYC overexpression results in accelerated and prolonged proliferation in the same population of cells. Despite an increase in tumor burden, size, and proliferative index, our results demonstrated that there was not a statistically significant increase in tumor number in compound mice with activated BRAF<sup>V600E</sup> and overexpressed c-MYC compared to BRAF<sup>V600E</sup> only mice, consistent with the latter model.

***BRAF<sup>V600E</sup>-induced lung tumorigenesis is dependent on WNT $\rightarrow$  $\beta$ -catenin $\rightarrow$ c-MYC signaling***

$\beta$ -catenin plays an important role in the assembly and function of adherens junctions as well as a downstream mediator of canonical WNT signaling (44). Hence, we tested whether the initiator of nuclear  $\beta$ -catenin signaling required for BRAF<sup>V600E</sup>-induced lung tumorigenesis might be WNT ligands in the microenvironment of incipient BRAF<sup>V600E</sup>-initiated tumor cells. Mice and humans express 19 WNT ligands such that conventional knockout experiments are logistically challenging. However, WNT acylation, which is essential for secretion and activity, is critically dependent upon a palmitoyl transferase known as Porcupine (PORCN) against which pharmacological inhibitors have been developed (55-57). One such agent, LGK974, shows specificity and selectivity for PORCN over other similar enzymes (55, 58).

To test the WNT dependency of BRAF<sup>V600E</sup>-induced tumorigenesis, lung tumors were initiated in *BRaf*<sup>CA</sup> mice that were then treated with either vehicle or LGK974 (5mg/kg, qd, 5 days/week) starting 1 week p.i. with mice euthanized for analysis 5 weeks later. Similar to  $\beta$ -catenin silencing, LGK974 inhibited BRAF<sup>V600E</sup>-induced tumorigenesis by >75% (Figs. 2-8a & 2-8b). Moreover, analysis of tumor cell proliferation (Ki67) revealed that the small tumors that formed in LGK974 treated mice displayed diminished proliferation (Fig. 2-8c). To test the specificity of the anti-tumor effects of LGK974 we initiated tumorigenesis in *BRaf*<sup>CA</sup> mice heterozygous for either the Cre-activated *Ctnnb1*<sup>ex3f/+</sup> or *RFS*<sup>MYC(T58A)</sup> alleles to determine if tumor cell autonomous maintenance of  $\beta$ -catenin $\rightarrow$ c-MYC signaling would rescue the inhibitory effects of LGK974 on lung tumorigenesis. Remarkably, expression of either CTNNB1\* or c-MYC<sup>T58A</sup> completely rescued the inhibitory effects of LGK974 on BRAF<sup>V600E</sup>-induced tumorigenesis (Fig. 2-8a) whether assessed by overall tumor number, size or total burden (Fig. 2-8b). These data confirm the key inhibitory specificity of LGK974 for the WNT $\rightarrow$   $\beta$ -catenin $\rightarrow$ c-

MYC signaling pathway in this model system. Moreover, notwithstanding important differences in lung cancer progression, these data demonstrate the critical dependency of BRAF<sup>V600E</sup>-induced lung tumorigenesis on the WNT→ $\beta$ -catenin→c-MYC signaling axis.

Previous literature has also suggested that Wnt ligands can have both pro- and anti-tumorigenic effects and that this occurs in a context-dependent fashion. While our LGK974 experiments demonstrate a key role for Wnt ligand secretion in lung tumor initiation, because use of the Porcupine inhibitor indiscriminately blocks the secretion of all Wnt ligands, the role of the individual contributions of each Wnt ligand to this process remained uncertain. Because of this, we also wanted to characterize the effects of the overexpression of each individual Wnt ligand on lung tumorigenesis in a systematic fashion. We felt that this was an important question to address because it not only gives us greater insight into the role of individual Wnt ligands in tumorigenesis, but also potentially provides both prognostic biomarkers for this disease as well as rational targets for new therapeutic strategies looking to block Wnt signaling in NSCLC.

When looking at the genetic alterations found in human lung adenocarcinoma samples, the typical mutations known to activate Wnt/ $\beta$ -catenin activity in other cancers such as gain of function mutations in  $\beta$ -catenin or loss of APC or AXIN are relatively rare. This is in contrast to numerous reports such as that from Stuart Aaronson's lab suggesting that activated Wnt/ $\beta$ -catenin is detected in a majority of primary tissues and cell lines from NSCLC patients.

The Wnt/beta-catenin pathway is a complex and highly regulated system, and therefore there are multiple nodes in which mutations, deletions, and amplifications can lead to aberrant Wnt/beta-catenin pathway activation and lung cancer formation. Based on literature on patient samples, we asked whether Wnt secretion could explain some of the upregulated  $\beta$ -catenin

signaling in lung cancer patients. Indeed, when looking at TCGA data for alterations in all 19 Wnts (data not shown), we see that a number of them are found to be upregulated and/or amplified in NSCLC patients, suggesting that this is a potential mechanism of Wnt/ $\beta$ -catenin activation for these tumors. Beyond this, another interesting observation is typically only one or a few Wnt ligands seem to be upregulated and/or amplified in any one tumor sample, and indeed when looking across all 19 Wnt ligands there was a tendency for mutations or expression changes in any one Wnt gene to be mutually exclusive of the other Wnts.

Because evidence from human NSCLC suggests that these tumors typically will only upregulate or amplify one or two specific Wnt ligands, we wanted to first test whether any single Wnt ligands would be sufficient to drive tumorigenesis, and if so which ones. To accomplish this *Braf<sup>CA</sup>* mice were infected with lentiviruses containing constructs expressing both Cre-recombinase (used to initiate BRAF<sup>V600E</sup> expression in the lung epithelium), and a single V5-epitope tagged Wnt ligand (Fig. 2-8d). While we chose to test all 19 Wnts we had a subset that we predicted should have an impact on lung tumorigenesis. These include: Wnt1, 2, 3a and 7b which have been demonstrated to play a role in both lung development and repair in adult tissues, and also positively correlated with lung tumorigenesis; Wnt5a, an activator of non-canonical Wnt signaling, whose upregulation has been correlated with lung tumor metastasis; and Wnt7a, which has actually been demonstrated to be lost in NSCLC through promoter hypermethylation, suggesting a tumor suppressive role for this Wnt ligand in lung tumorigenesis.

While still preliminary, results from this experiment have so far demonstrated that overexpression of either Wnt1 or Wnt3a in conjunction with BRAF<sup>V600E</sup> activation has a negative impact on mouse survival through an acceleration of tumor growth (data not shown). All of the mice infected with either Wnt1 or Wnt3a succumbed to lung tumorigenesis within 12 weeks post



infection. In contrast, all of the mice infected with the other 17 Wnts were still alive and healthy at this same time point.

Histological analysis also reveals that  $Braf^{CA/+}$  mice infected with Wnt1 or Wnt3a harbor advanced adenomas and adenocarcinomas whereas GFP-infected control mice only had benign adenomas (Fig. 2-8e & Fig. 2-8g). To emphasize the differential response of these tumors to different Wnt ligands, overexpression of Wnt7a seems to elicit an opposite response and instead suppressed tumor formation in our  $Braf^{CA}$  mice (Fig. 2-8f).

Staining for the V5 epitope tagged onto the C-terminus of each Wnt confirms Wnt expression from the lentiviral construct (Fig. 2-8h). Immunofluorescence analysis also reveals that V5-tagged Wnt ligands are associated with the membranes of these tumors, consistent with the hypothesis that Wnt ligands act directly on tumor cells to enhance lung tumor proliferation and progression. Our results indicate that while overexpression of specific Wnt ligands are indeed sufficient to sustain tumor proliferation and drive tumor progression, our results also demonstrate that Wnt ligands can play differential roles in regards to lung tumorigenesis. While still preliminary, it seems that either Wnt1 or Wnt3a overexpression is sufficient to accelerate  $BRAF^{V600E}$ -driven tumorigenesis and facilitate tumor progression, whereas expression of Wnt7a seems to suppress lung tumorigenesis.

These results also suggest that in regards to human NSCLC, amplification and overexpression of specific Wnt ligands may be an important mechanism of tumor maintenance and progression. Indeed, several studies have detected both Wnt upregulation and amplification leading to autocrine Wnt signaling in human NSCLC lines, and more importantly that the growth of these cells are dependent on the presence of these Wnt ligands. For instance, in A549 cells

expression of a dominant negative Wnt2 construct reduced the growth of these cells both in vitro and in a xenograft mouse model.

## DISCUSSION

*BRAF* is mutated in 6-8% of human lung cancers but in GEM models expression of *BRAF*<sup>V600E</sup> in the lung epithelium results only in benign lung tumors that rarely progress to cancer due to a senescence-like proliferative arrest with some similarity to OIS (4, 24, 59). In cultured cells, sustained RAF→MEK→ERK signaling elicits an immediate proliferative arrest followed by OIS without any initial phase of cell proliferation (60, 61). By contrast, expression of *BRAF*<sup>V600E</sup> in lung epithelial cells elicits clonally-derived tumors that undergo ~15-20 population doublings prior to the onset of senescence-like growth arrest (4, 33). Here we demonstrate that WNT→β-catenin signaling, a pathway essential for normal lung development and homeostasis, is critically required for early-stage *BRAF*<sup>V600E</sup>-induced lung tumorigenesis. Furthermore, the senescence-like growth arrest observed in late-stage *BRAF*<sup>V600E</sup> expressing tumors appears due to an insufficiency of β-catenin activity leading to reduced c-MYC expression. While it remains unclear by what mechanism(s) WNT ligand signaling becomes limiting in this situation, one possibility is that *BRAF*<sup>V600E</sup> expressing tumor cells are responding to a stromal source of WNT ligand(s), for example from macrophages, such that as the tumors reach a certain size, there is insufficient exposure to WNT thereby triggering cell cycle arrest through diminished β-catenin→c-MYC signaling (62). An alternative would be that sustained *BRAF*<sup>V600E</sup>→MEK→ERK activity generates a negative feedback circuit to WNT receptors or other components of WNT signaling that restricts the cells ability to respond to WNT ligands in the tumor microenvironment as suggested in OIS triggering in other circumstances (20). An

obvious question is whether a requirement for  $\beta$ -catenin signaling is unique to BRAF<sup>V600E</sup>-initiated lung tumorigenesis or whether this is a general requirement for lung cancers driven by other oncogenes (1, 23). In this regard, we and others have demonstrated that expression of CTNNB1\* accelerated KRAS<sup>G12D</sup>-induced lung carcinogenesis in GEM models, suggesting that a more general dependency on WNT signaling for lung carcinogenesis (Fig. 9) (36, 37). Finally, the role of  $\beta$ -catenin in BRAF<sup>V600E</sup>-induced neoplasia is not restricted to lung tumorigenesis as both primary tumor growth and subsequent metastatic dissemination of BRAF<sup>V600E</sup>/PTEN<sup>Null</sup> melanomas is diminished in the absence of  $\beta$ -catenin (63).

As indicated by analysis of cultured BCT cells, expression of c-MYC appears under the dual control of both oncogenic BRAF<sup>V600E</sup> and WNT $\rightarrow$   $\beta$ -catenin signaling such that loss of either signal has potent anti-tumor effects through effects on c-MYC (40, 46, 47). This bears similarity to the situation in *KRAS* mutated colorectal cancer (CRC) cells where Cyclin D1 is under the dual control of the same two pathways (41). However, in CRC both pathways are mutationally altered through *KRAS* mutation in combination with either APC silencing or mutation of  $\beta$ -catenin (64). However during early-stage lung tumorigenesis, the signal for  $\beta$ -catenin $\rightarrow$ c-MYC signaling does not require mutational activation but instead relies on the presence of WNT ligands, most likely from the tumor microenvironment. The importance of c-MYC as a downstream effector of oncogenic KRAS<sup>G12D</sup> or BRAF<sup>V600E</sup> is emphasized by the anti-tumor effects of an inhibitor of c-MYC (Omo-MYC) that suppresses KRAS<sup>G12D</sup>-induced lung tumorigenesis (47, 65). Moreover, BRAF<sup>V600E</sup> cooperates with other deregulated signaling pathways such as the PI3'-kinase pathway to sustain c-MYC expression in either lung or prostate tumorigenesis (33, 66). However, the fact that expression/activation of c-MYC failed to elicit

any pathology in the lung emphasizes that c-MYC is necessary but not sufficient to initiate lung tumorigenesis (Fig. 2-5 & Fig. 2-12) (52). Finally, in contrast to previous reports, we obtained no evidence that c-MYC promoted invasion or metastasis of BRAF<sup>V600E</sup>-induced lung tumors (67).

Although *CTNNB1* is mutated in ~5% of human NSCLC, there is insufficient evidence regarding coincident mutation with either *KRAS* or *BRAF* (23). Importantly, WNT→ $\beta$ -catenin signaling is reported to be active in NSCLC derived cell lines through a multiplicity of mechanisms including autocrine production of WNT ligands, diminished secretion of WNT antagonists such as Dickkopf (DKK1-4) or WNT Inhibitory Factor 1 (WIF1) (37, 47, 68-70). The observation that BRAF<sup>V600E</sup>/TP53<sup>Null</sup> lung tumors retained BAT-GAL activity even at late time points is consistent with reports linking TP53 silencing to  $\beta$ -catenin through effects on miR34 expression (71). Consequently, the frequency of *CTNNB1* mutation may underestimate the importance of WNT→ $\beta$ -catenin signaling in NSCLC (37). Given that there are now reliable target genes and reporters for nuclear  $\beta$ -catenin activity and inhibitors of WNT signaling it should be possible to parse out the importance of this pathway in different cancer types leading to prognostic marker guided clinical trials of agents that target this pathway.

Silencing of TP53, INK4A/ARF or expression of PIK3CA<sup>H1047R</sup> can promote bypass of the senescence-like growth arrest in BRAF<sup>V600E</sup>-induced benign lung tumors thereby promoting malignant lung cancer progression (4, 33). This begged the question as to whether bypass of senescence is synonymous with malignant progression. Our results indicated that, whereas CTNNB1\* promoted malignant progression of BRAF<sup>V600E</sup>-induced lung tumors, c-MYC did not

(Fig. 2-12). These data suggest that malignant progression requires more than simple bypass of the senescence-like proliferative arrest displayed by BRAF<sup>V600E</sup>-induced lung tumors and is consistent with previous data indicating that c-MYC does not fully rescue the effects of loss of  $\beta$ -catenin function in the gastrointestinal tract (53). Although  $\beta$ -catenin→c-MYC signaling is critically required for sustained proliferation of BRAF<sup>V600E</sup> expressing lung tumors, there must be branch points downstream or CTNNB1\*, independent of c-MYC, that influence malignant progression. Experiments to address this question using a forward genetics screen in our *Braf*<sup>CA</sup> mouse model will be described in subsequent chapters.

GEM models of KRAS- or BRAF-initiated lung tumorigenesis have revealed the remarkable complexity of biochemistry and cell biology that occurs even in the earliest stages of transformation. Such tumors are regulated by both instructive (initiated by the oncogene) and permissive (regulated by the tumor microenvironment) signals required for tumor initiation and clonal expansion. Previous studies have emphasized the importance of tumor cell autonomous pathways instructed by oncogenic KRAS or BRAF such as the ERK MAP kinase, PI3'-kinase→AKT, Rac1→NF-kB, NKX2.1 signaling and others (4, 29, 33, 72-75). However, these data indicate the potential importance of growth factor signaling in providing a permissive tumor microenvironment that renders lung epithelial cells responsive to mutational activation of oncogenes. Moreover it remains likely, as observed in other circumstances, that factors present in the tumor microenvironment will play an important role in the response of *BRAF* mutated cancer cells to pathway-targeted therapy (76, 77).

## MATERIALS AND METHODS

### *Mice and Adenovirus delivery*

All animal experiments were conducted in accordance with protocols approved by the UCSF Institutional Animal Care and Use Committee (IACUC). *BRaf<sup>CA</sup>* (*BRaf<sup>tm1Mmcm</sup>*), *LSL-KRas<sup>G12D</sup>* (*Kras<sup>tm4Tyj</sup>*), *RFS<sup>MYC(WT) or (T58A)</sup>* (*Gt(ROSA)26Sor<sup>tm1(myc)Rcse</sup>*, *Gt(ROSA)26Sor<sup>tm1(myc\*T58A)Rcse</sup>*), *BAT-GAL* (*B6.Cg-Tg(BAT-lacZ)3Picc/J*), *Ctnnb1<sup>ex3(f)</sup>* (*Ctnnb1<sup>tm1Mmt</sup>*) and *Ctnnb1<sup>f</sup>* (*Ctnnb1<sup>tm2Kem</sup>*) mice were bred and genotyped as previously described (4, 10, 38, 39, 50, 78). Stocks of Adenovirus encoding Cre recombinase (Ad-CMV-Cre) were purchased from Viraquest (North Liberty, IA) and instilled into the lungs of adult mice as previously described (4, 79).

### *Histology and quantification of lung tumor burden*

Lungs were processed for analysis as described previously (33). Hematoxylin and Eosin (H&E) stained slides were scanned with an Aperio ScanScope scanner with quantification performed using Aperio Spectrum ImageScope software. Tumor number and size were measured per lobe and overall tumor burden was calculated as (area of lung lobe occupied by tumor)/(total area of lobe) in  $\mu\text{m}^2$  (33).

### *Treatment of mice with pathway-targeted therapeutics*

For treatment of mice, NVP-LGK974-AE (LGK974, Novartis) was formulated in 0.5%(w/v) methylcellulose (Fluka Analytical)/0.5%(v/v) Tween-80 (Sigma Aldrich) and administered by oral gavage (po) at 5 mg/kg per mouse once per day (q.d) for 5 days/week.

### ***Immunostaining of mouse lung tissue, LacZ detection and immunoblotting***

Mouse lungs were fixed in zinc-buffered formalin, processed and embedded in paraffin, cut into 5 $\mu$ m sections and mounted on glass slides. Citrate-mediated antigen retrieval was performed and then the following antibodies were used for detection: anti- $\beta$ -catenin (Cell Signaling Technology), anti-AQP5 (Calbiochem), anti-Ki67, (Abcam), anti-BrdU, anti-CC10, anti-Cyclin D1, anti-SPC, anti-NKX2.1 (aka TTF-1) (Santa Cruz Biotechnology), c-MYC (Epitomics), and V5 (Life Technologies).

$\beta$ -galactosidase activity driven by the BAT-GAL transgene was assessed in paraformaldehyde fixed sections incubated with 5-bromo-4-chloro-3-indolyl- $\beta$ -d-galactoside (X-Gal) for 16 hours as described previously (10).

50 $\mu$ g aliquots of cell proteins were probed with antisera against c-MYC (Epitomics), Cyclin D1, phospho-ERK1/2 (pT202/PY204), total ERK1/2 (Cell Signaling technology), and anti-b-actin (Sigma). Immunoblots were visualized using the Odyssey Classic or Odyssey Fc, with data analyzed using either the Odyssey application software v3.0.30 or Image Studio v2.0 software (LI-COR Biosciences).

### ***Cell proliferation assays***

Cell proliferation was assessed by counting the percentage of surfactant protein positive (SPC+) tumor cells that were also bromodeoxyuridine (BrdU) or Ki67-positive by double label immunofluorescence. In *BRaf<sup>CA</sup>* mice, 9 tumors were analyzed with 9 grids each for a total of 5,900 SPC+ cells evaluated. In *BRaf<sup>CA</sup>; R26<sup>MYC(T58A)/+</sup>* mice, 10 tumors were analyzed with 10 grids each for a total of 5,718 SPC+ cells evaluated. Similar numbers of cells were evaluated for

the presence of SPC/Ki67 double-positive cells in tumors from  $BRaf^{CA}$ ,  $BRaf^{CA}; R26^{MYC(T58A)/+}$ ,  $BRaf^{CA}; Ctnnb1^{ff}$ , and  $BRaf^{CA}; Ctnnb1^{ex3(f)/+}$  mice.

### ***Lung tumor cell isolation, culture and analysis***

Lungs of tumor bearing mice were perfused with dispase (BD) and individual lobes were minced and incubated with 2mg/ml dispase/collagenase (19). Cell suspensions from  $BRAF^{V600E}/CTNNB1^*/TP53^{Null}$ -induced lung cancers were then filtered and plated directly into culture in Hams-F12/Glutamax media supplemented with 10%(v/v) fetal bovine serum. Following the outgrowth of a mixed population of lung cancer derived cells a number of single cell-derived clones were isolated by limiting dilution and then expanded to create  $BRAF^{V600E}/CTNNB1^*/TP53^{Null}$  (BCT) lung tumor derived cells.

Ecotropic virus was produced by transient transfection of pBabePuro-MYC:ER<sup>TM</sup> (gift of Dr. Gerard Evan) into Plat-E cells (49). BCT cells were infected and selected in DMEM containing 2μg/ml puromycin. RNAi-mediated inhibition of β-catenin expression was performed using β-catenin siRNAs 1 (GGTGCTGACTATCCAGTTGAT, si-bcat1) or 2 (CCTCCCAAGTCCTTTATGAAT, si-bcat2). A siRNA targeting GFP (AACCACTACCTGAGCACCCAG) was used as a negative control. BCT cells were transfected with siRNA (5nM) by RNAi-Max (Invitrogen) either alone or in the presence of a MEK inhibitor (PD0325901, 1μM, Hansun Trading Co) (80). BCT cells expressing c-MYC:ER were treated with either ethanol (E) or 4-Hydroxytamoxifen (4-OHT, 100nM) to activate the fusion protein. Cell cycle analysis was performed by incubating cells at 50% confluency with pathway-targeted inhibitors for 24 hours with 10μM BrdU (Becton-Dickinson) added for the



final 3 hours. Floating and adherent cells were collected, fixed in ethanol, and stained with anti-BrdU-FITC (Becton-Dickinson) and propidium iodide (Sigma).

### ***Quantitative RT-PCR***

RNAs were purified from cultured cells using RNeasy (QIAGEN) and reverse-transcribed using the Advantage RT-for-PCR kit (Takara-Clontech). Real-time quantitative PCR was performed using SYBR green Premix EX Taq (Takara) on an Applied Biosystems 7500 real-time PCR system (Applied Biosystems). Sense and antisense primers were b-actin: GTGCTTCTAGGCGGACTGTT and TGCGCAAGTTAGGTTTTGTCA or c-MYC: GCCCAGTGAGGATATCTGGA and ATCGCAGATGAAGCTCTGGT. The following cycle parameters were used: denaturation at 95°C for 10 seconds, and annealing and elongation for 30 seconds at 60°C.

Figure 2-1a

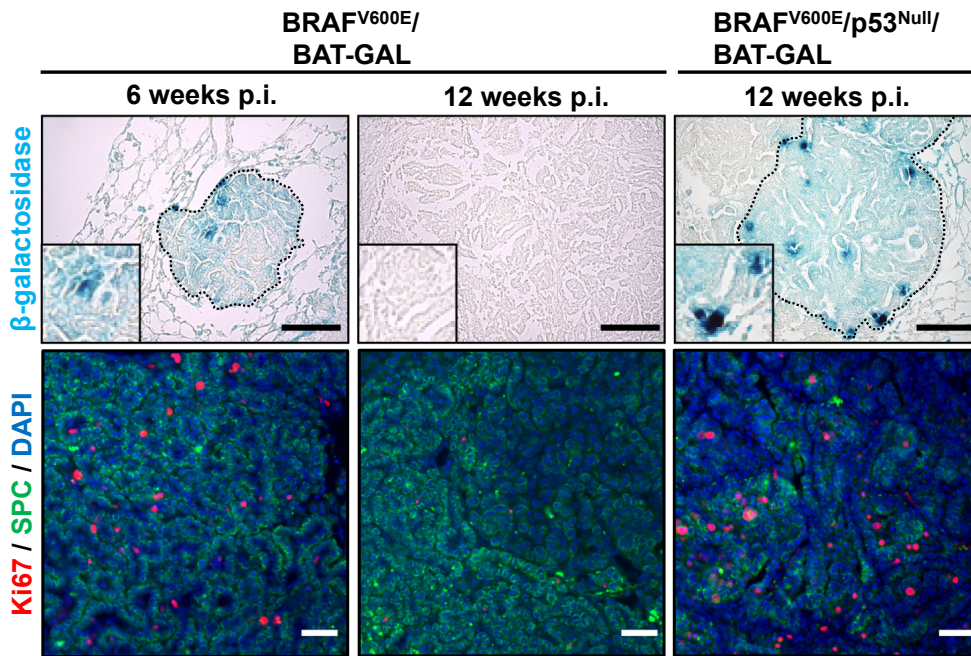


Figure 2-1b

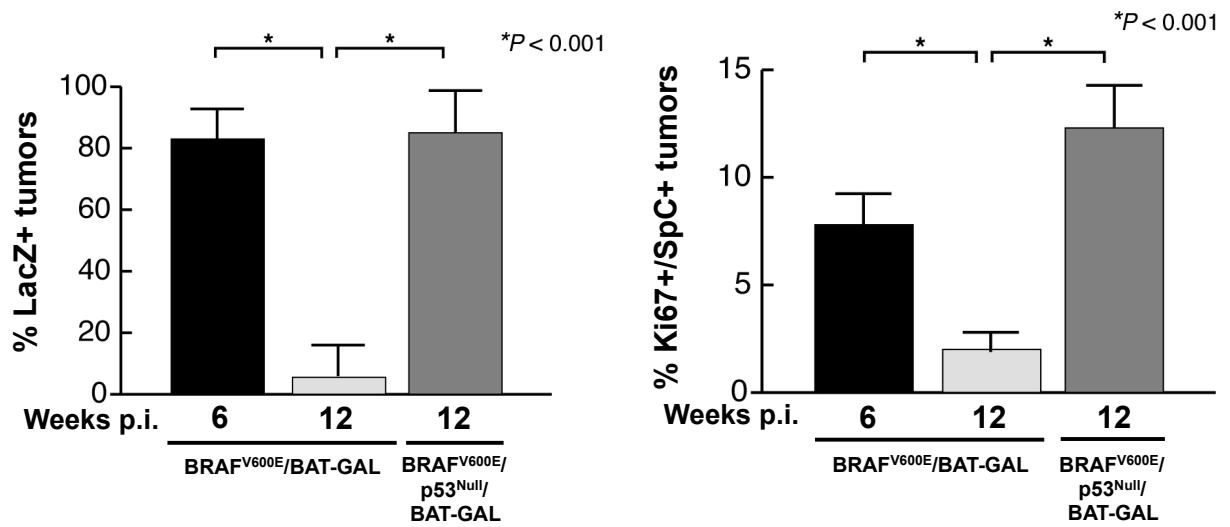
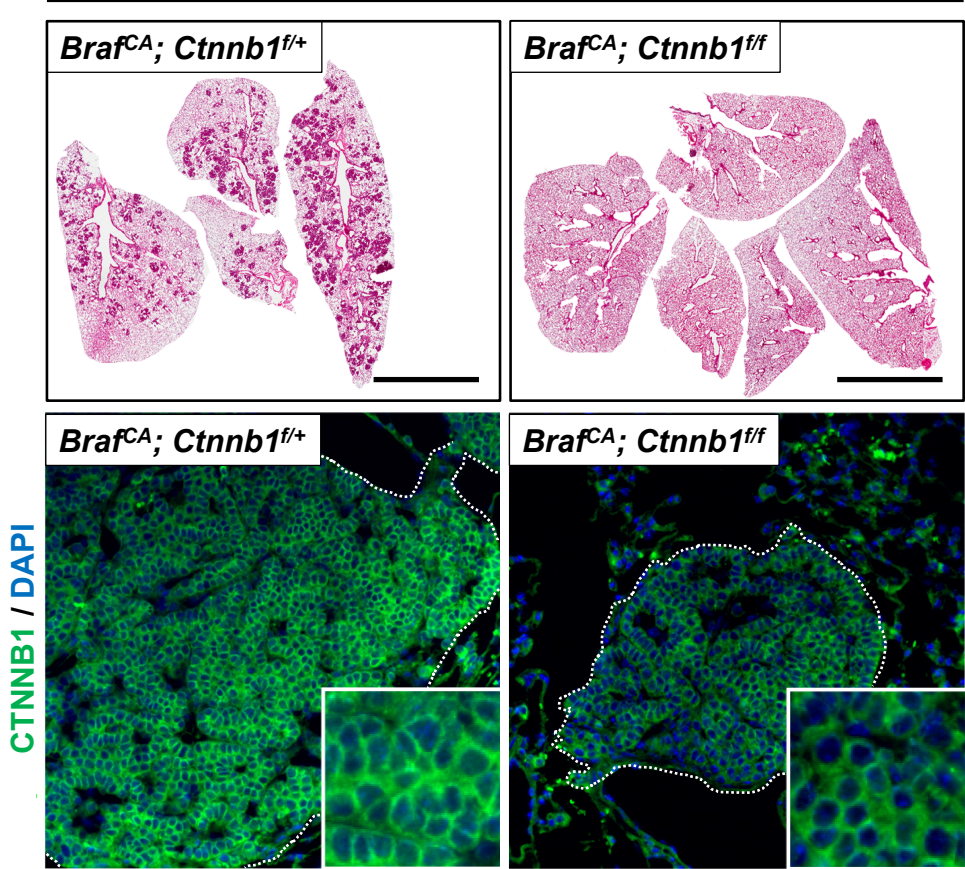
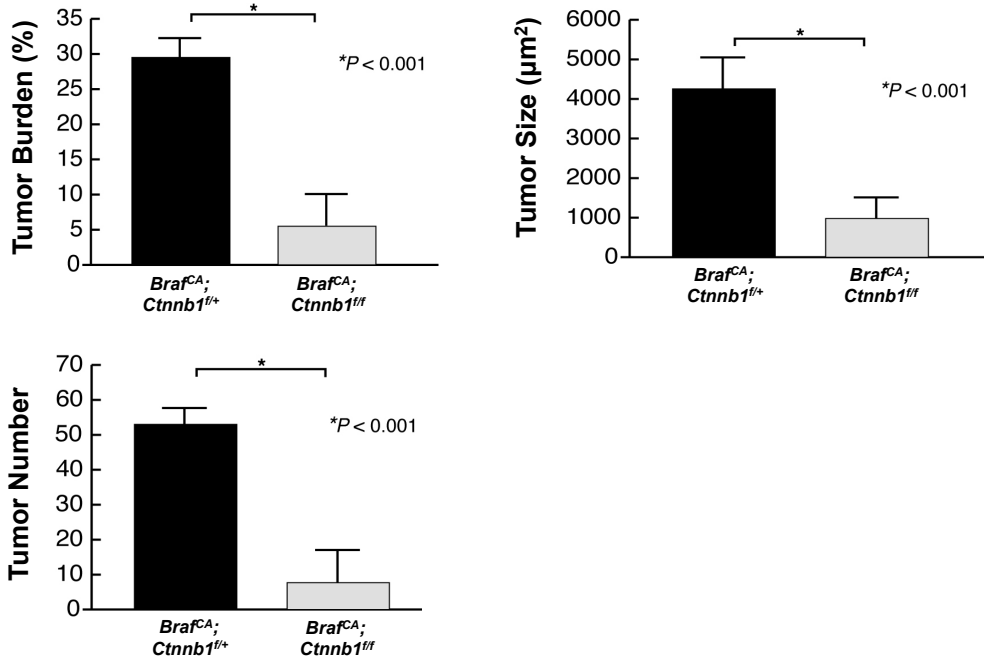


Figure 2-1c

12 weeks p.i.



**Figure 2-1d**



**Figure 2-1.  $\beta$ -catenin is required for BRAF<sup>V600E</sup>-induced lung tumorigenesis.** Lungs of mice of the indicated genotypes were infected with Ad-Cre and monitored for six or 12 weeks as indicated at which time they were euthanized and frozen or FFPE lung sections were processed for Hematoxylin and Eosin (H&E), lacZ activity or immunofluorescence. (a) Representative lacZ-stained tissue sections from *BRAF<sup>CA</sup>; BAT-GAL* mice euthanized at 6 weeks (top left) or 12 weeks (top middle), and from *BRAF<sup>CA</sup>; Trp53<sup>fl/fl</sup>; BAT-GAL* mice euthanized at 12 weeks (top right). Immunofluorescence analysis of histological sections from *BRAF<sup>CA</sup>; BAT-GAL* mice euthanized at 6 weeks (bottom left) or 12 weeks (bottom middle) p.i. and from *BRAF<sup>CA</sup>; Trp53<sup>fl/fl</sup>; BAT-GAL* mice euthanized at 12 weeks (bottom right). DAPI in blue, SP-C in green, and Ki67 in red. All scale bars represent 50 $\mu\text{m}$ . (b) Quantification of % LacZ+ tumors and % Ki67+/SP-C+ cells from *BRAF<sup>CA</sup>; BAT-GAL* mice euthanized at 6 weeks or 12 weeks p.i., and from *BRAF<sup>CA</sup>; Trp53<sup>fl/fl</sup>; BAT-GAL* mice euthanized at 12 weeks. (c) Representative H&E-stained tissue sections

from  $BRaf^{CA}$  (left) or  $BRaf^{CA}; Ctnnb1^{ff}$  (right) mice euthanized 12 weeks p.i. All scale bars represent 4mm. Immunofluorescence analysis of histological sections from  $BRaf^{CA}; Ctnnb1^{ff}$  mice euthanized 12 weeks p.i. DAPI in blue,  $\beta$ -catenin in green. All scale bars represent 50 $\mu$ m.

(d) Quantification of tumor number, tumor size, and tumor burden in  $BRaf^{CA}; Ctnnb1^{ff/+}$  and  $BRaf^{CA}; Ctnnb1^{ff}$  mice euthanized 12 weeks p.i.

Figure 2-2a

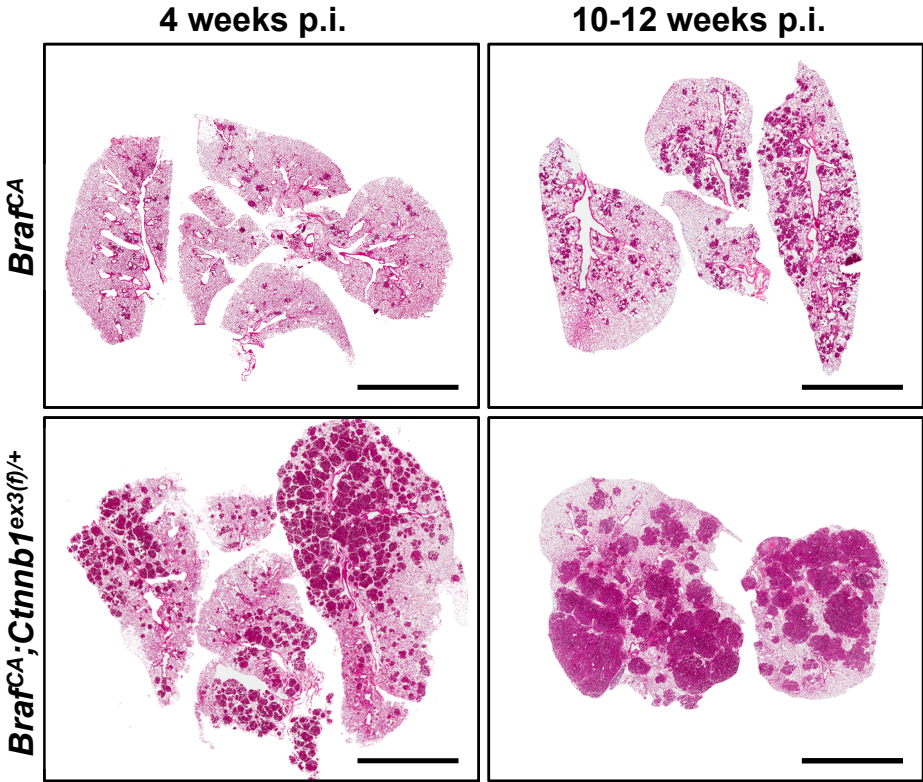


Figure 2-2b

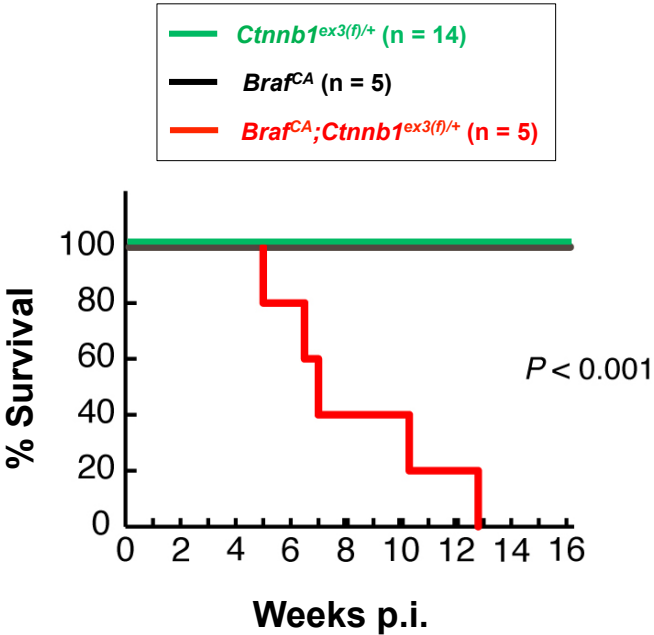


Figure 2-2c

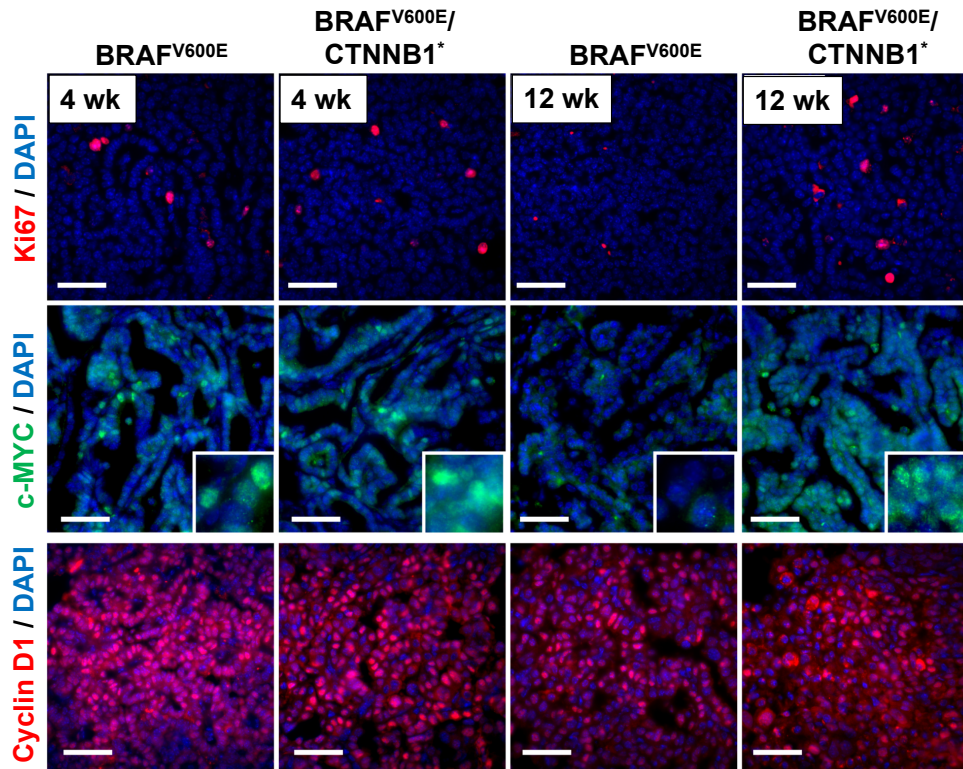
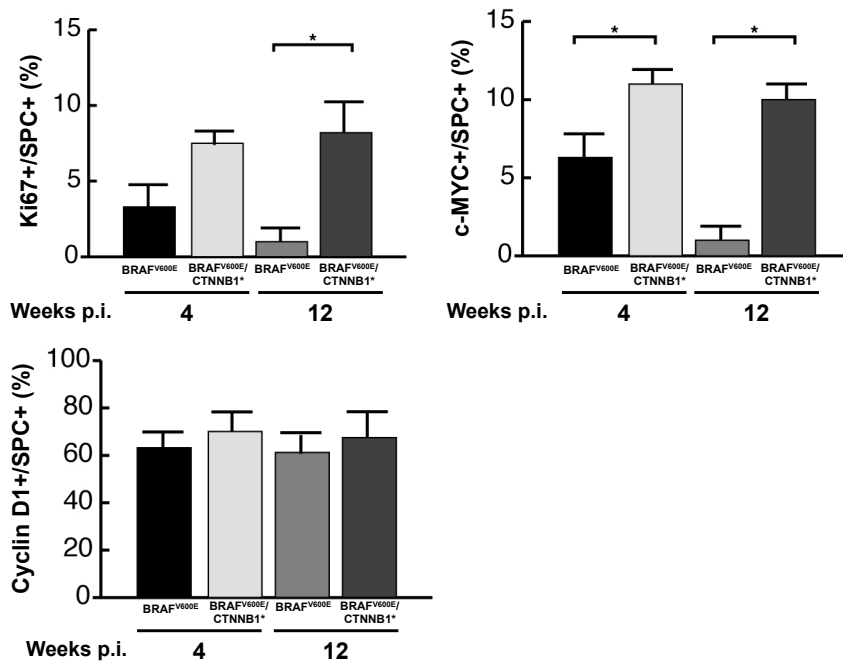


Figure 2-2d





**Figure 2-2. BRAF<sup>V600E</sup> cooperates with gain-of-function CTNNB1\* to promote lung tumorigenesis.** (a) Lungs of mice of the indicated genotypes were infected with Ad-Cre and monitored for four or 10-12 weeks as indicated at which time they were euthanized and their lungs processed for H&E staining. Representative H&E-stained tissue sections of BRAF<sup>V600E</sup> or BRAF<sup>V600E</sup>/CTNNB1\* expressing lung tumors at four weeks or 10-12 weeks are presented. Scale bar is 4mm. (b) *BRaf<sup>CA</sup>;Ctnnb1<sup>ex3(f)/+</sup>* and *BRaf<sup>CA</sup>;Ctnnb1<sup>ex3(f)/+</sup>* mice were infected with Ad-Cre and monitored prospectively over ~120 days. Mice were euthanized on development of end-stage disease per UCSF IACUC regulations and a Kaplan-Meier survival curve was plotted. (c) Immunofluorescence analysis of histological sections from BRAF<sup>V600E</sup> or BRAF<sup>V600E</sup>/CTNNB1\* expressing lung tumors from mice euthanized either four or 12 weeks p.i. with DNA (DAPI) in blue, c-MYC in green, Ki67 and Cyclin D1 in red as indicated. Scale bar is 50µm. (d) Quantification of the percentage of Ki67, Cyclin D1 or c-MYC positive BRAF<sup>V600E</sup> or BRAF<sup>V600E</sup>/CTNNB1\* lung tumor cells (marked by Surfactant protein C, SPC) expression either four or 12 weeks p.i. as indicated.



Figure 2-3a

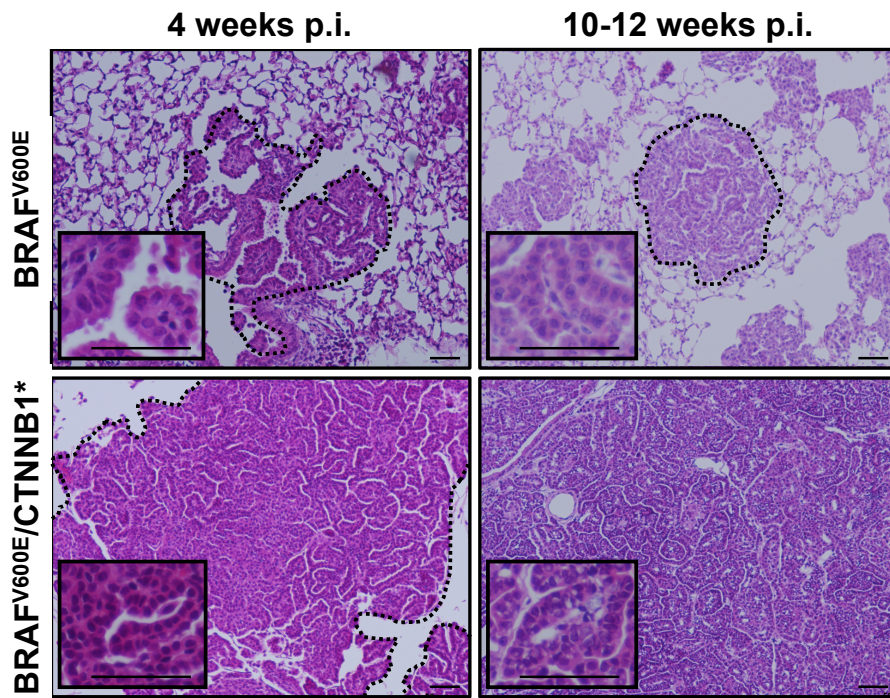


Figure 2-3b

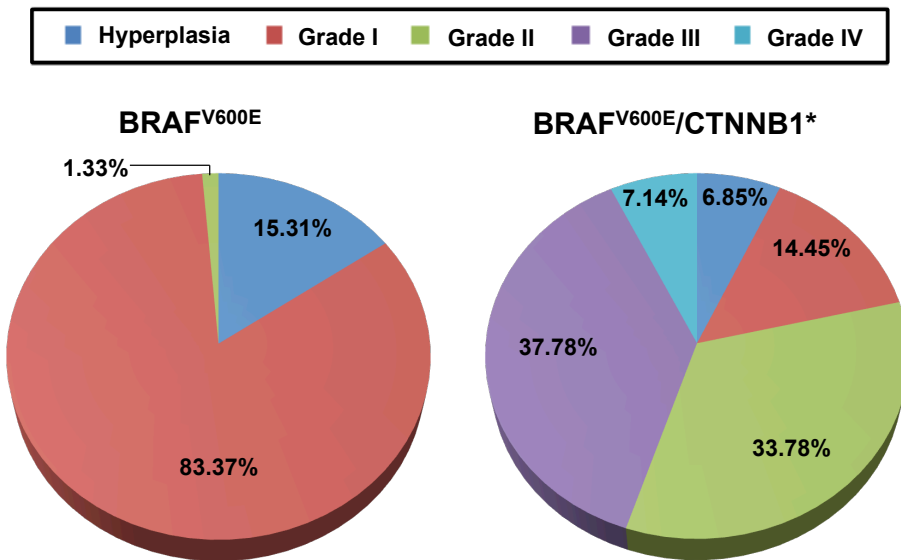


Figure 2-3c

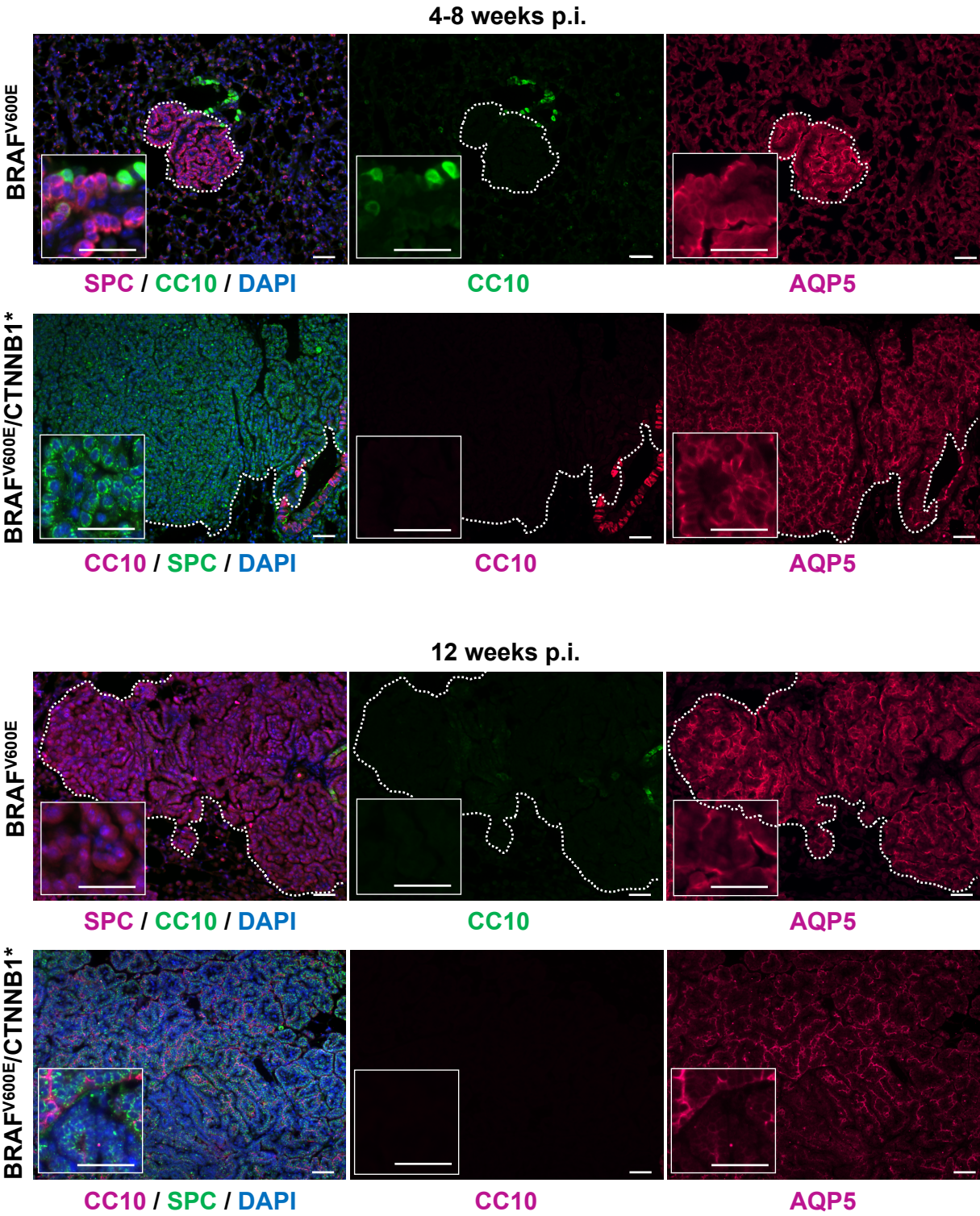




Figure 2-3d

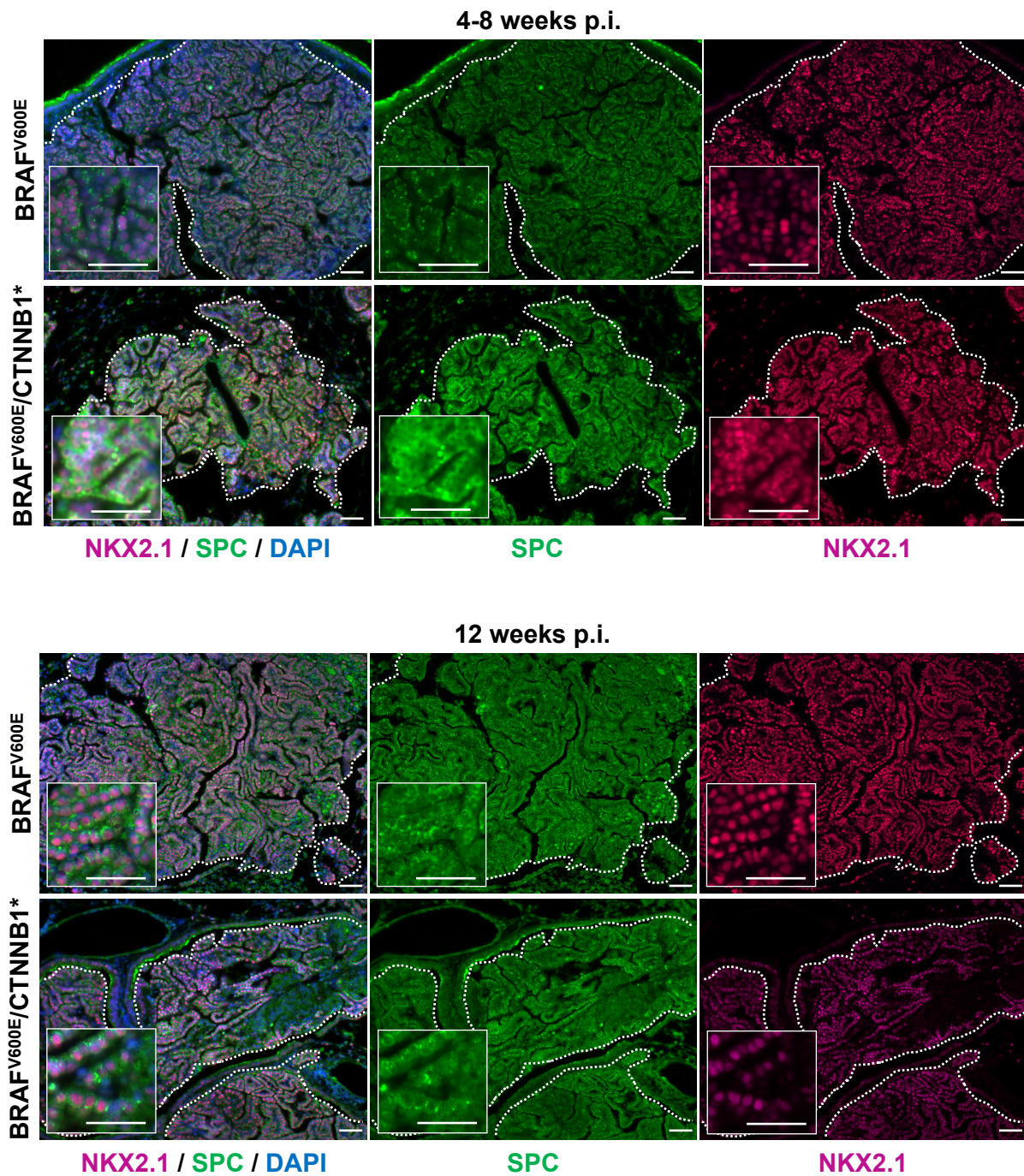


Figure 2-3. BRAF<sup>V600E</sup> and CTNNB1\* cooperate to promote malignant lung carcinogenesis.

(a) BRAF<sup>V600E</sup> or BRAF<sup>V600E</sup>/CTNNB1\* expressing lung tumors were initiated in mice of the appropriate genotype with mice monitored for four weeks (left) or 10-12 weeks (right) at which

time they were euthanized and their lungs processed for H&E staining. Scale bar is 50 $\mu$ m. (b) The grade of BRAF<sup>V600E</sup> or BRAF<sup>V600E</sup>/CTNNB1\* expressing lung tumors was assessed on a 5 point scale based on grading criteria described by Nikitin et al and described in more depth in Figure 10. (c-d) Immunofluorescence analysis of histological sections BRAF<sup>V600E</sup> or BRAF<sup>V600E</sup>/CTNNB1\* expressing lung tumors either 4-8 or 10-12 weeks p.i. as indicated. DNA (DAPI) in blue, SPC in pink (top) and green (bottom), CC10 in green (top) and pink (bottom), AQP5 and NKX2.1 in pink, and NKX2.1.

Figure 2-4a & b

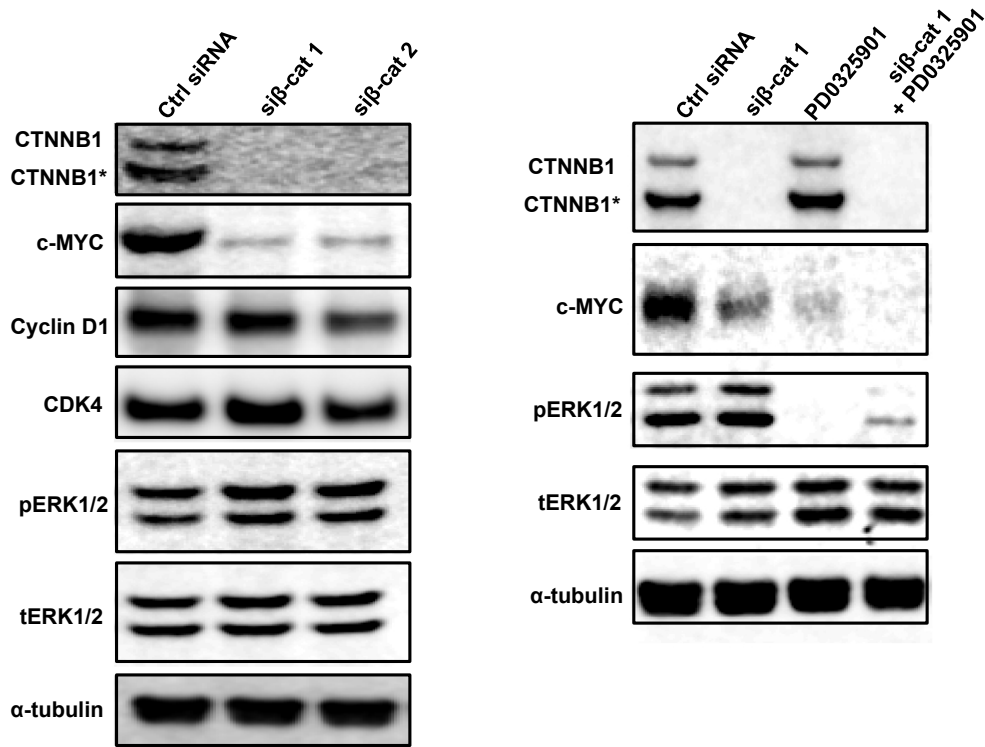
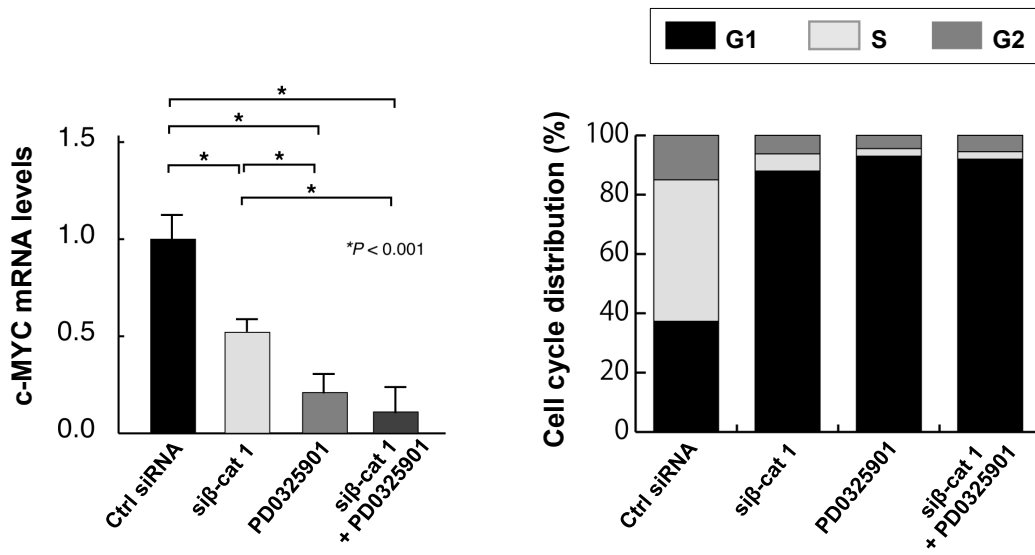
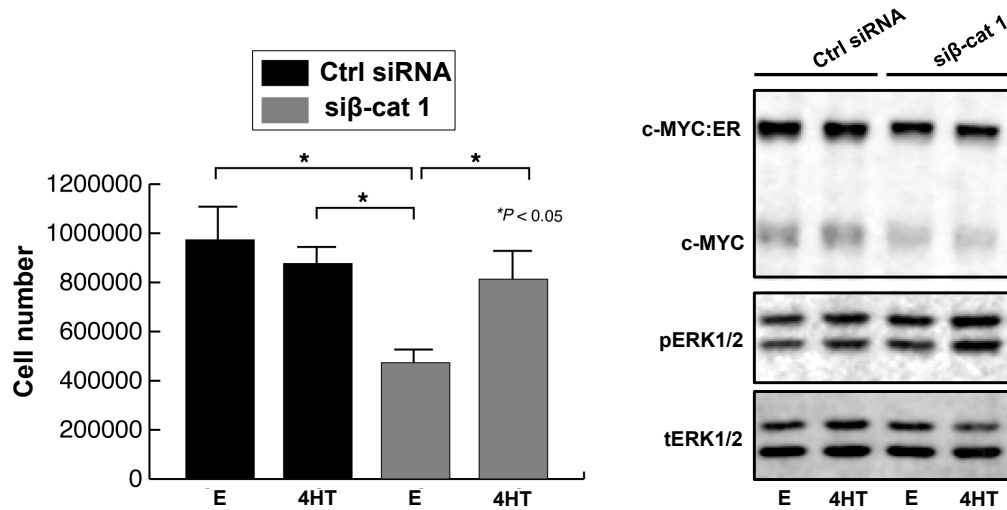


Figure 2-4c & d



**Figure 2-4e & f**



**Figure 2-4. Dual regulation of c-MYC expression by CTNNB1\* and BRAF<sup>V600E</sup>.** (a-d) BCT lung cancer derived cells were transfected with siRNAs against β-catenin (siβ-cat 1 or siβ-cat 2), MEK inhibitor (1mM PD325901) or a combination of siβ-cat 1 and MEK inhibitor as described in Experimental Procedures. Cell extracts were analyzed by immunoblotting as indicated (a-b). RT-PCR was employed to measure c-MYC mRNA levels in BCT cells treated as indicated (c). Cell cycle status of BCT cells treated as indicated was assessed by staining with propidium iodide (d). (e-f) BCT cell proliferation was assessed over 7 days with viable cell number quantified using by trypan blue staining in conjunction with a Countess® Automated Cell Counter as indicated in Materials & Methods (e). Extracts of BCT cells were analyzed by immunoblotting as indicated (f).

Figure 2-5a & b

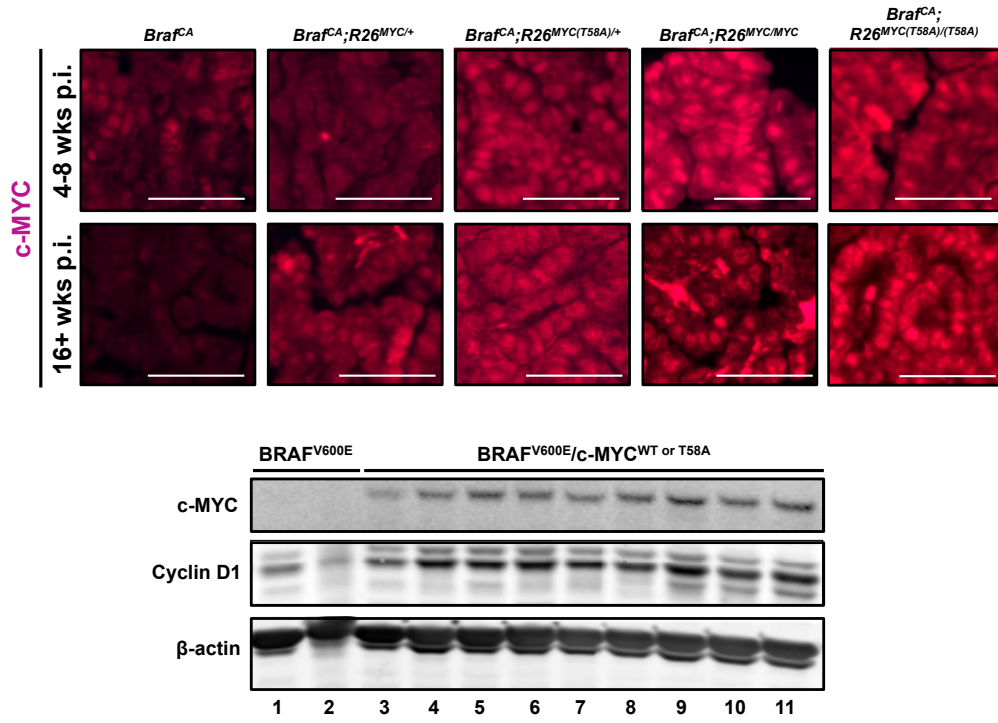


Figure 2-5c

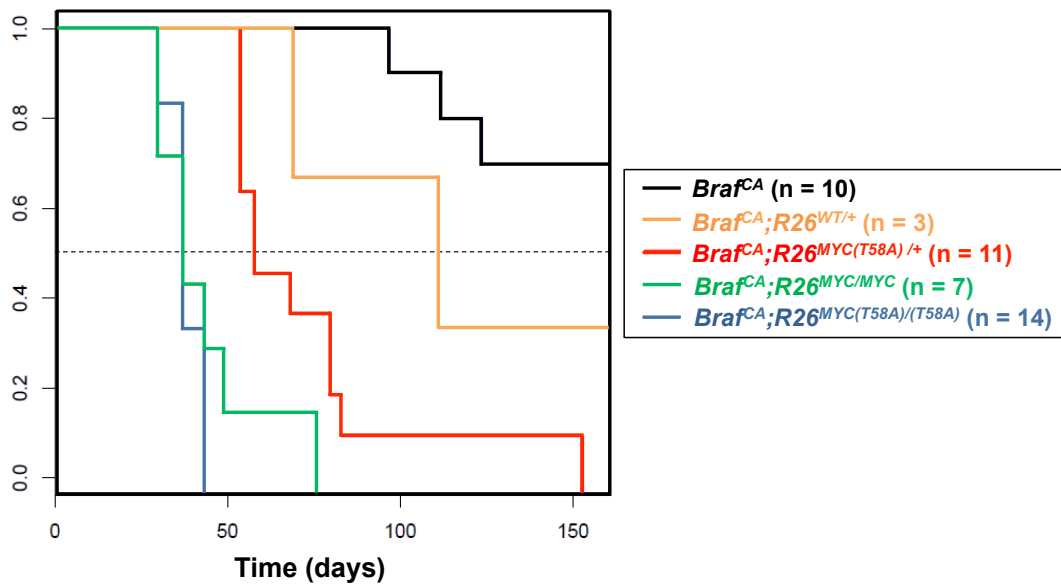


Figure 2-5d

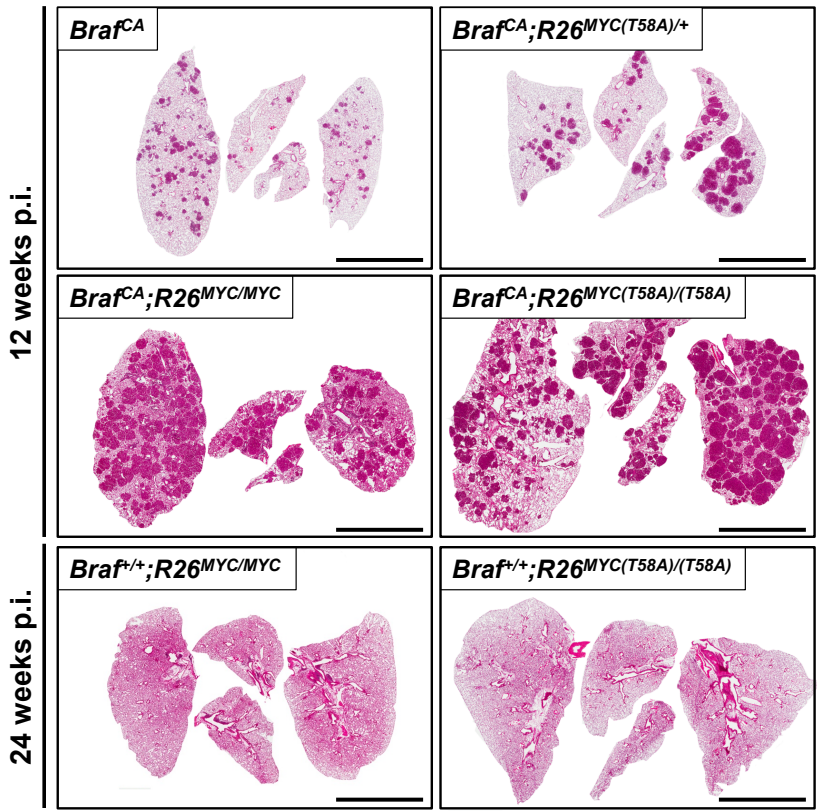


Figure 2-5e

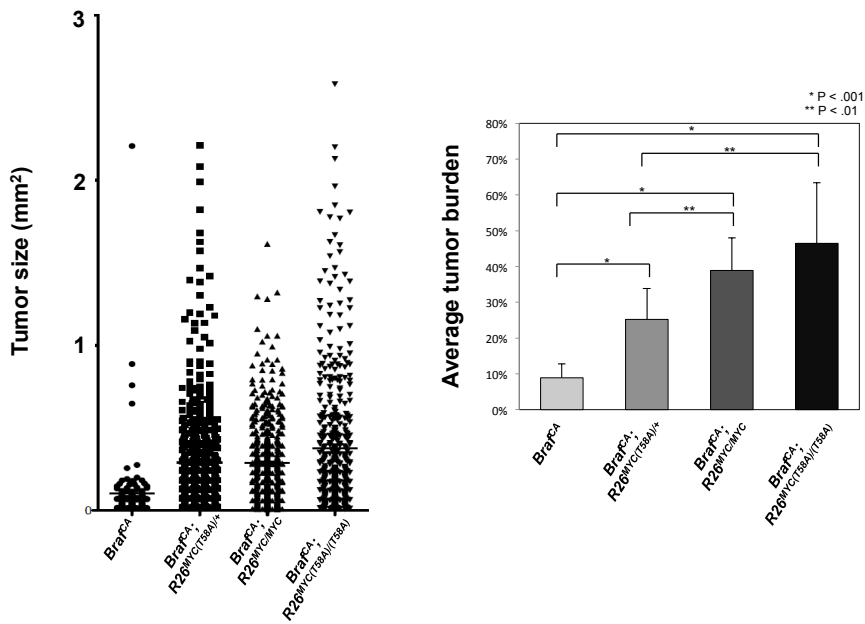




Figure 2-5f

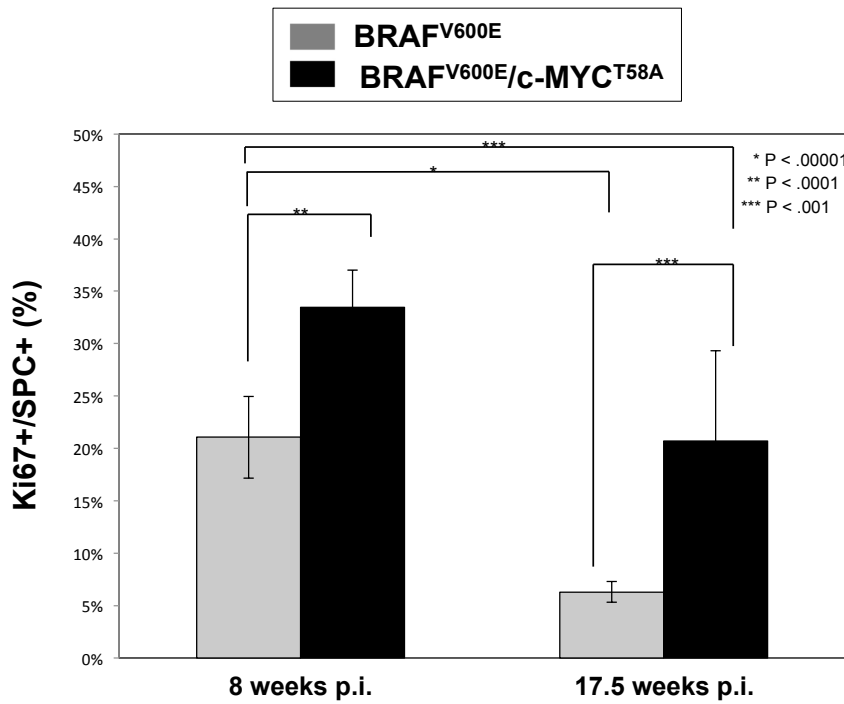
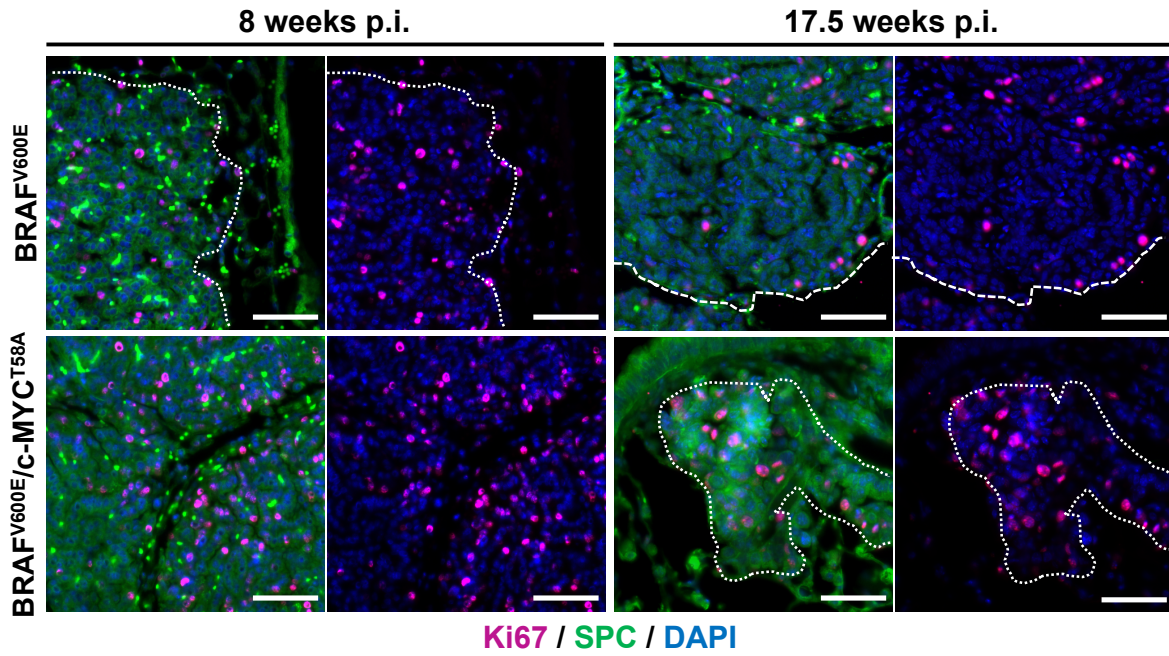
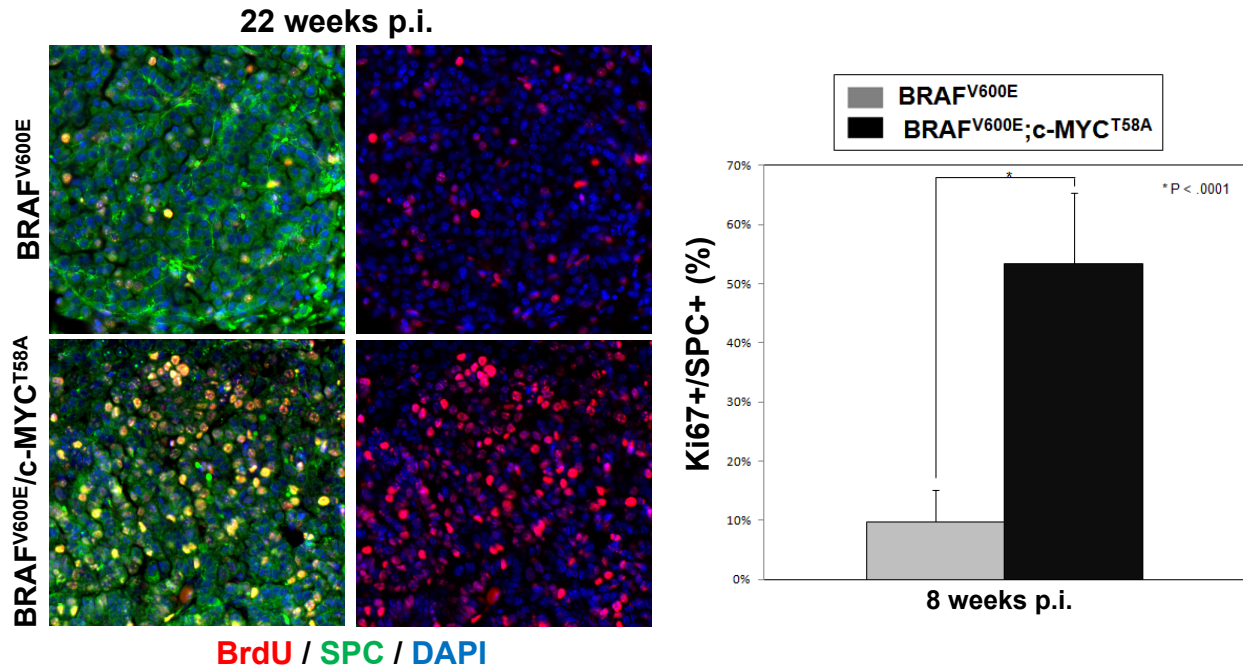


Figure 2-5g



**Figure 2-5. Sustained c-MYC expression promotes BRAF<sup>V600E</sup>-induced lung tumorigenesis but fails to promote malignant lung cancer progression.** (a) Immunofluorescence analysis of

histological sections from: 1. *BRaf<sup>CA</sup>*; 2. *BRaf<sup>CA</sup>; RFS<sup>MYC(WT)/+</sup>*; 3. *BRaf<sup>CA</sup>; RFS<sup>MYC(WT)/(WT)</sup>*; 4. *BRaf<sup>CA</sup>; RFS<sup>MYC(T58A)/+</sup>* and; 5. *BRaf<sup>CA</sup>; RFS<sup>MYC(T58A)/(T58A)</sup>* mice euthanized 4-8 or 16+ weeks p.i. as

indicated with c-MYC expression in red. Scale bar is 50µm. (b) Expression of c-MYC was

assessed by immunoblot analysis of lysates of BRAF<sup>V600E</sup> or BRAF<sup>V600E</sup>/c-MYC expressing lung

tumors isolated directly from mice 6-9 weeks p.i. Lanes 1-2: *BRaf<sup>CA</sup>*, Lanes 3-6: *BRaf<sup>CA</sup>; RFS<sup>MYC(WT)/+</sup>* or *BRaf<sup>CA</sup>; RFS<sup>MYC(T58A)/+</sup>*, Lanes 7-11: *BRaf<sup>CA</sup>; RFS<sup>MYC(WT)/(WT)</sup>* or *BRaf<sup>CA</sup>; RFS<sup>MYC(T58A)/(T58A)</sup>* mice.

(c) Lung tumorigenesis was initiated in mice of the various indicated

*BRaf<sup>CA</sup>* and *RFS<sup>MYC</sup>* genotypes were infected with Ad-Cre and monitored prospectively over ~180

days. Mice were euthanized upon development of end-stage disease per UCSF IACUC

regulations and a Kaplan-Meier survival curve was plotted. (d) Lung tumorigenesis was initiated

in mice of the various indicated *BRaf<sup>CA</sup>* and *RFS<sup>MYC</sup>* genotypes with mice monitored for 12 or 24

weeks as indicated at which time they were euthanized and their lungs processed for H&E staining. Representative H&E-stained lung sections from various indicated  $BRaf^{CA}$  and  $RFS^{MYC}$  genotypes were stained with H&E. (e) Quantification of lung tumor number, tumor size, and tumor burden in mice of the various indicated  $BRaf^{CA}$  and  $RFS^{MYC}$  genotypes at 12 weeks p.i. (f-g) Immunofluorescence analysis of histological sections from  $BRaf^{CA}$  and  $BRaf^{CA}; R26^{MYC(T58A)/+}$  mice euthanized 8, 17.5 or 22 weeks p.i. as indicated with DNA (DAPI) in blue, SPC in green, Ki67 in pink, and BrdU in red as indicated. Scale bar is 50 $\mu$ m. Quantification of % Ki67+/SP-C+ and % BrdU+/SP-C+ cells in BRAF<sup>V600E</sup> or BRAF<sup>V600E</sup>/c-MYC<sup>T58A</sup> tumors.

Figure 2-6a

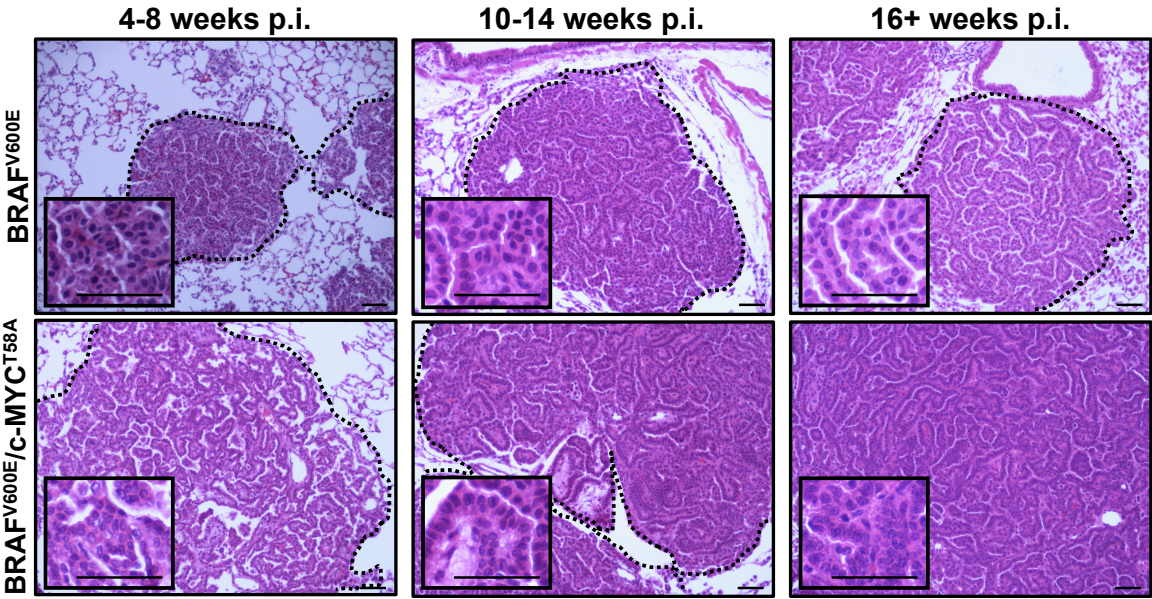


Figure 2-6b

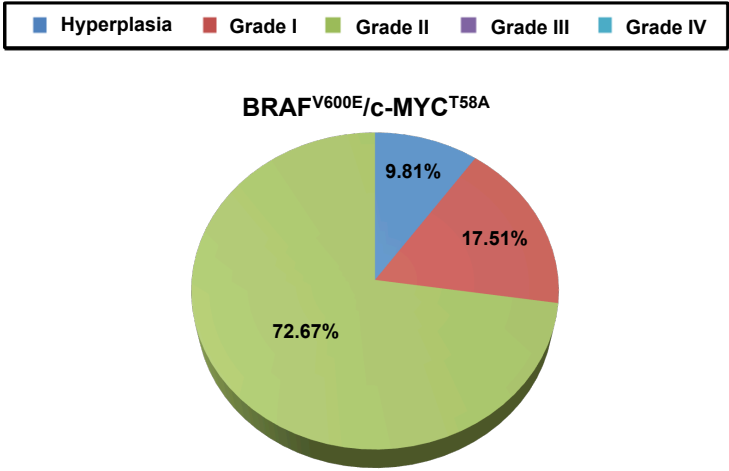




Figure 2-6c

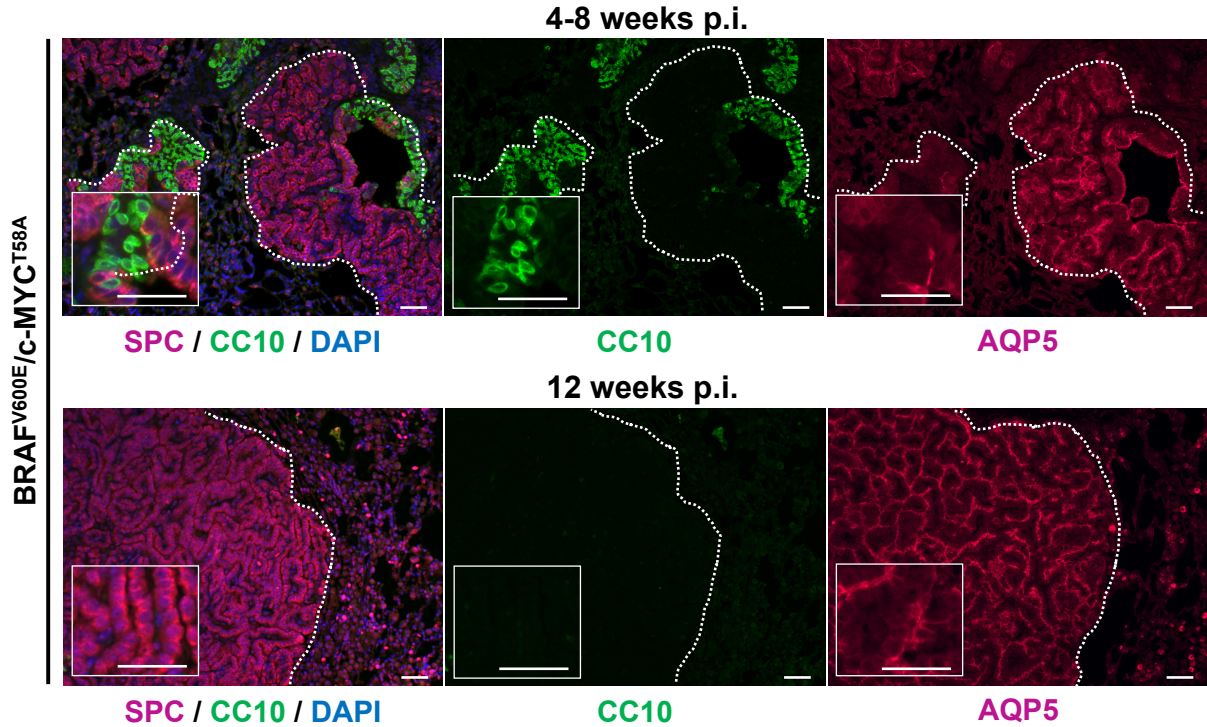


Figure 2-6d

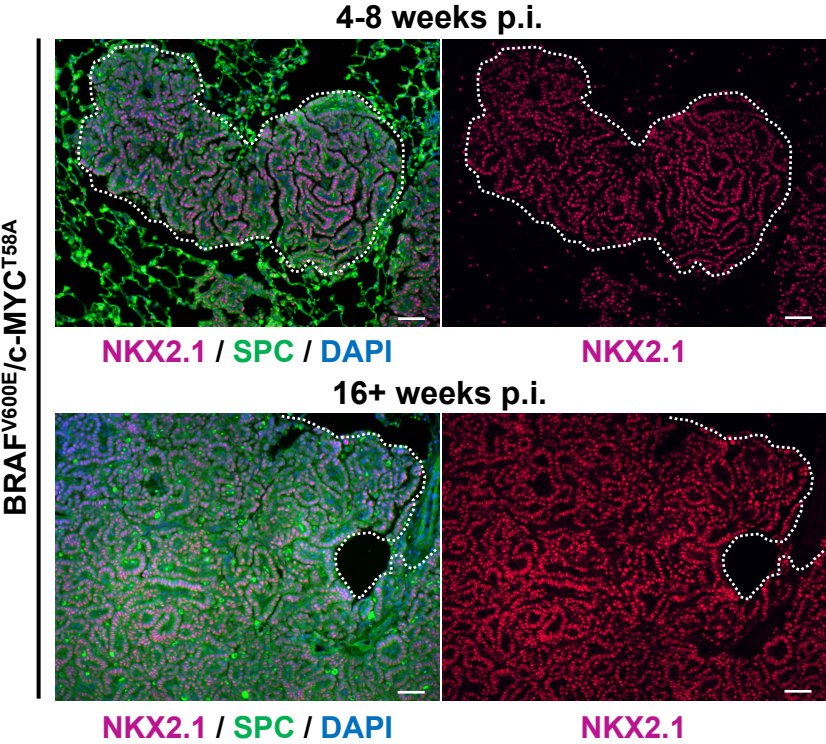


Figure 2-6e

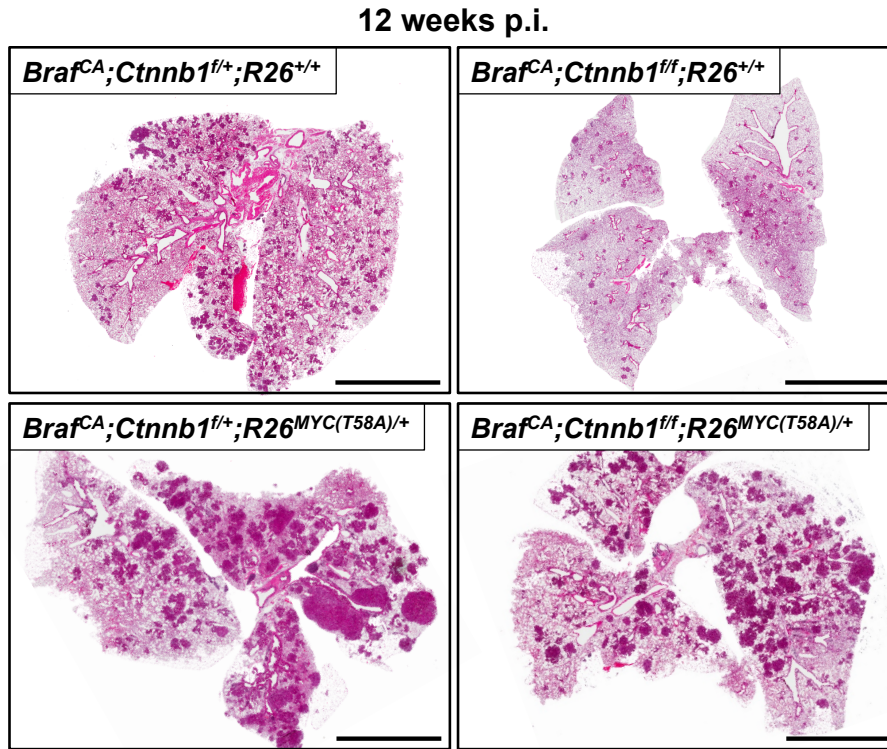


Figure 2-6f

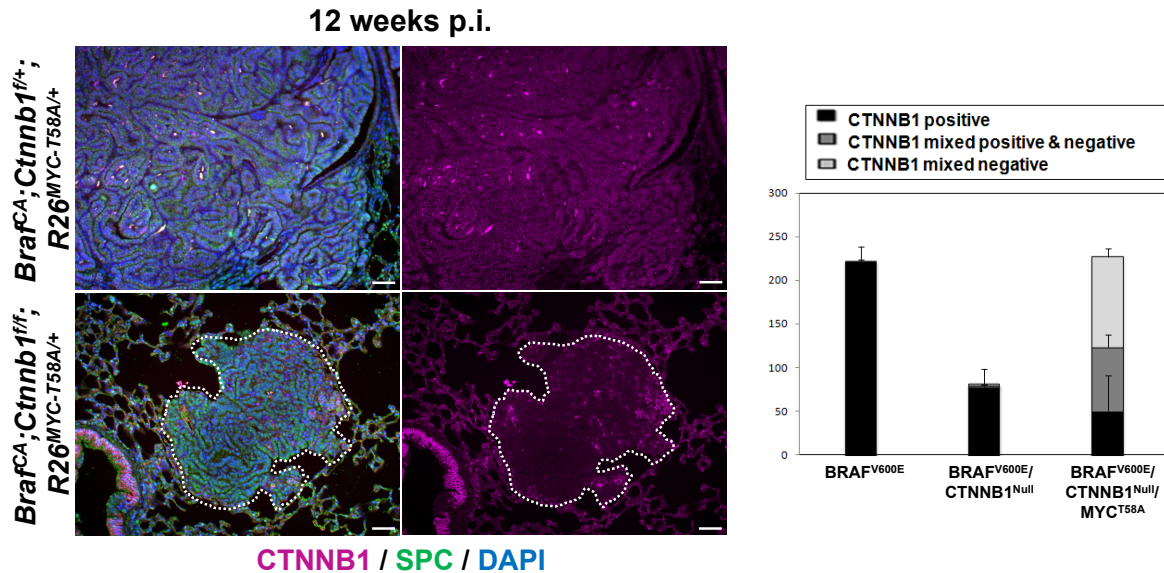
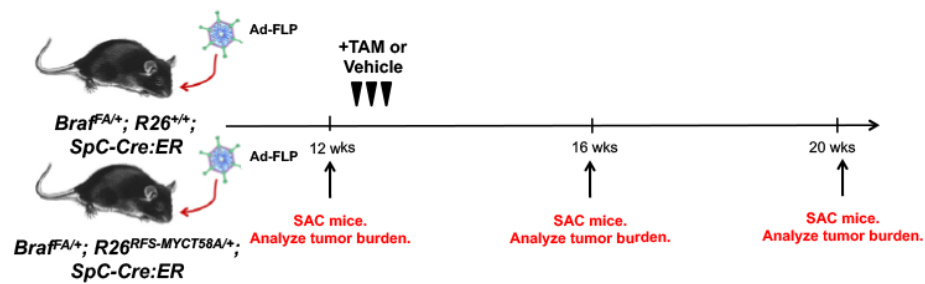


Figure 2-6. c-MYC fails to promote malignant cancer progression of BRAF<sup>V600E</sup>-initiated lung tumors. (a) BRAF<sup>V600E</sup>, BRAF<sup>V600E</sup>/c-MYC<sup>WT</sup>, and BRAF<sup>V600E</sup>/c-MYC<sup>T58A</sup> expressing lung

tumors were initiated in mice of the appropriate genotype with mice monitored for 4-8 weeks (left panels), 10-14 weeks (middle panels) or 16+ weeks (right panels) at which time they were euthanized and their lungs processed for H&E staining. Scale bar is 50 $\mu$ m. (b) The grade of BRAF<sup>V600E</sup>/c-MYC<sup>T58A</sup> expressing lung tumors was assessed as described in Fig. 3A and in Supplemental Figure 1 based on criteria established for the classification of proliferative pulmonary lesions of the mouse (43). (c-d) Immunofluorescence analysis of histological sections BRAF<sup>V600E</sup>/c-MYC<sup>T58A</sup> expressing lung tumors either 4-8 or 10-12 weeks p.i. as indicated. DNA (DAPI) in blue, SPC in pink (top) and green (bottom), CC10 in green (top) and pink (bottom), AQP5 and NKX2.1 in pink, and NKX2.1. Scale bar is 50 $\mu$ m. (e) Lung tumorigenesis was initiated in mice of the indicated genotypes with mice monitored for 12 weeks at which time they were euthanized and their lungs processed for H&E staining. Representative H&E-stained tissue sections from *BRaf<sup>CA</sup>; Ctnnb1<sup>fl/+</sup>; R26<sup>+/+</sup>*, *BRaf<sup>CA</sup>; Ctnnb1<sup>fl/fl</sup>R26<sup>+/+</sup>*, *BRaf<sup>CA</sup>; Ctnnb1<sup>fl/+</sup>; R26<sup>MYC(T58A)/+</sup>*, and *BRaf<sup>CA</sup>; Ctnnb1<sup>fl/fl</sup>;R26<sup>MYC(T58A)/+</sup>* mice euthanized at 12 weeks. Scale bar is 50 $\mu$ m. (f) Immunofluorescence analysis of histological sections of lung tumors from *BRaf<sup>CA</sup>; Ctnnb1<sup>fl/+</sup>; R26<sup>MYC(T58A)/+</sup>* and *BRaf<sup>CA</sup>; Ctnnb1<sup>fl/fl</sup>; R26<sup>MYC(T58A)/+</sup>* mice euthanized 12 weeks after Ad-Cre infection as indicated. DNA (DAPI) in blue, SPC in green, and  $\beta$ -catenin in pink as indicated. Scale bar is 50 $\mu$ m. Quantification of  $\beta$ -catenin-positive, mixed  $\beta$ -catenin-negative/positive and  $\beta$ -catenin-negative lung tumors in *BRaf<sup>CA</sup>*, *BRaf<sup>CA</sup>;Ctnnb1<sup>fl/fl</sup>*, and *BRaf<sup>CA</sup>;Ctnnb1<sup>fl/fl</sup>;R26<sup>MYC(T58A)/+</sup>* mice euthanized 12 weeks post Ad-Cre infection.

**Figure 2-7a**



**Figure 2-7b**

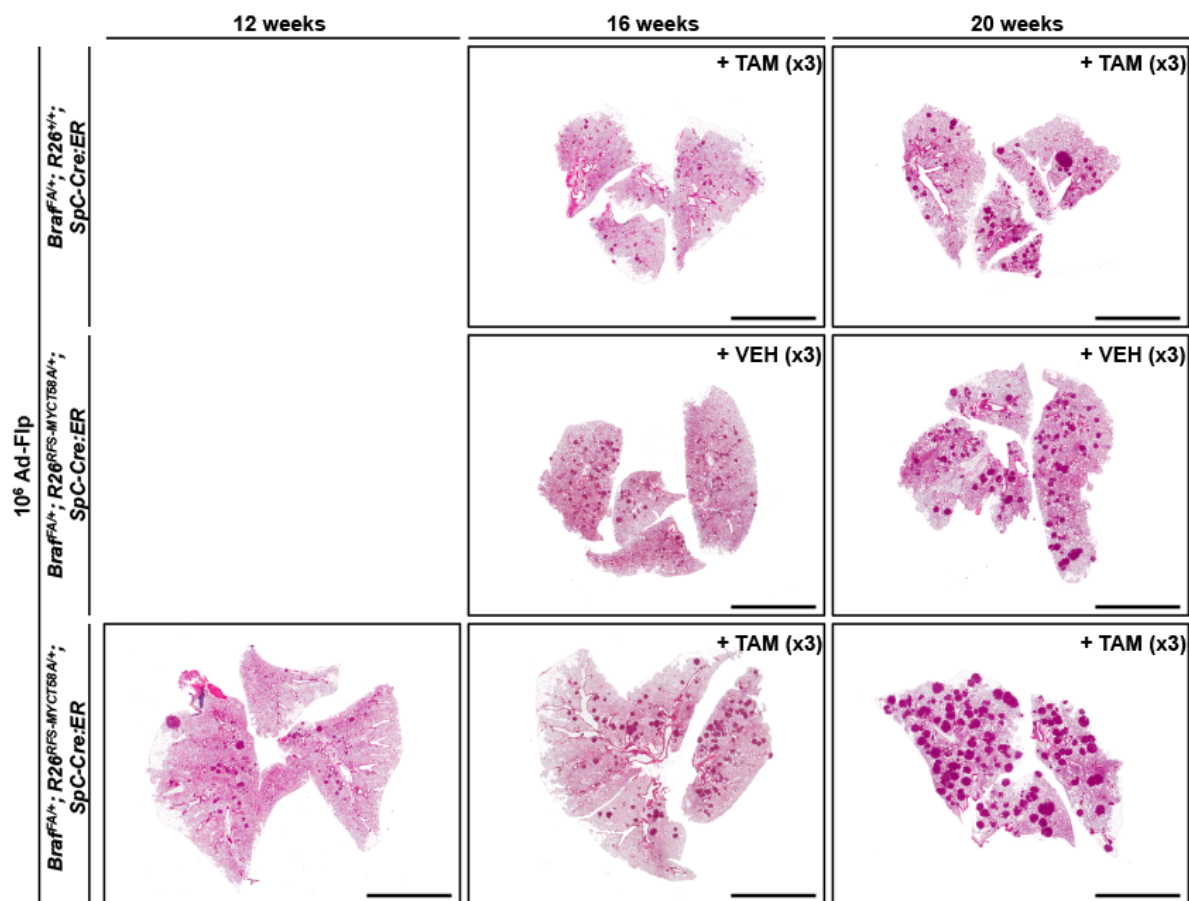




Figure 2-7c

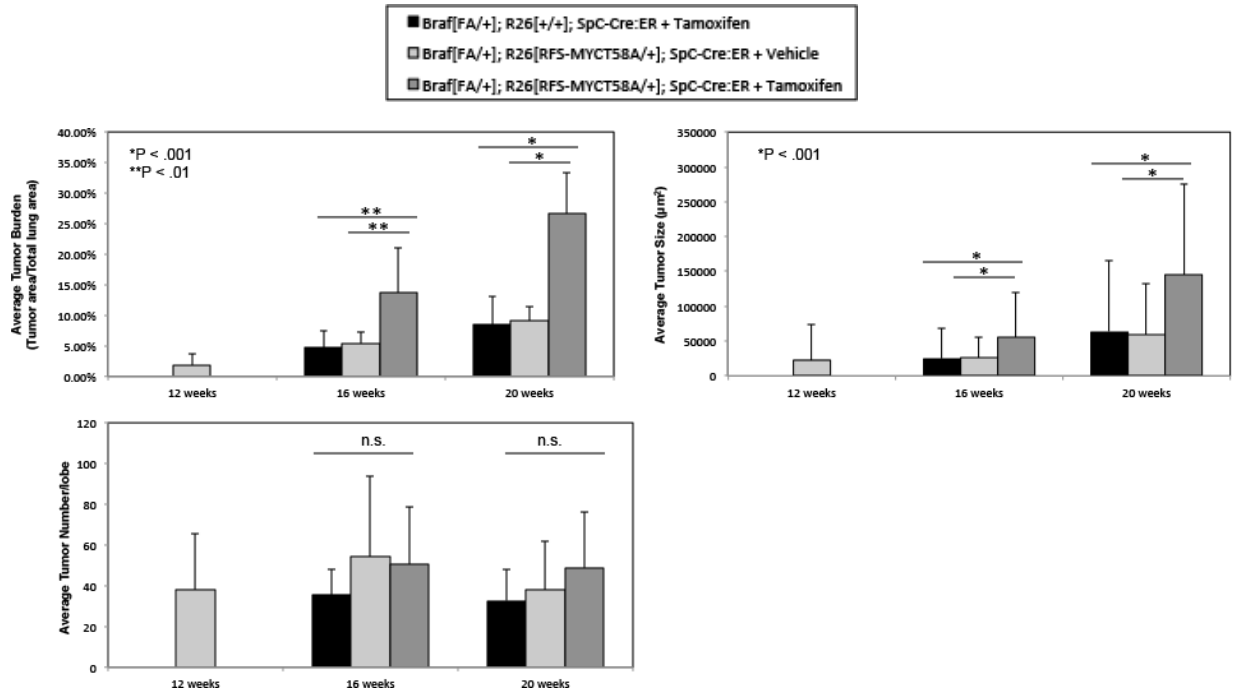


Figure 2-7d

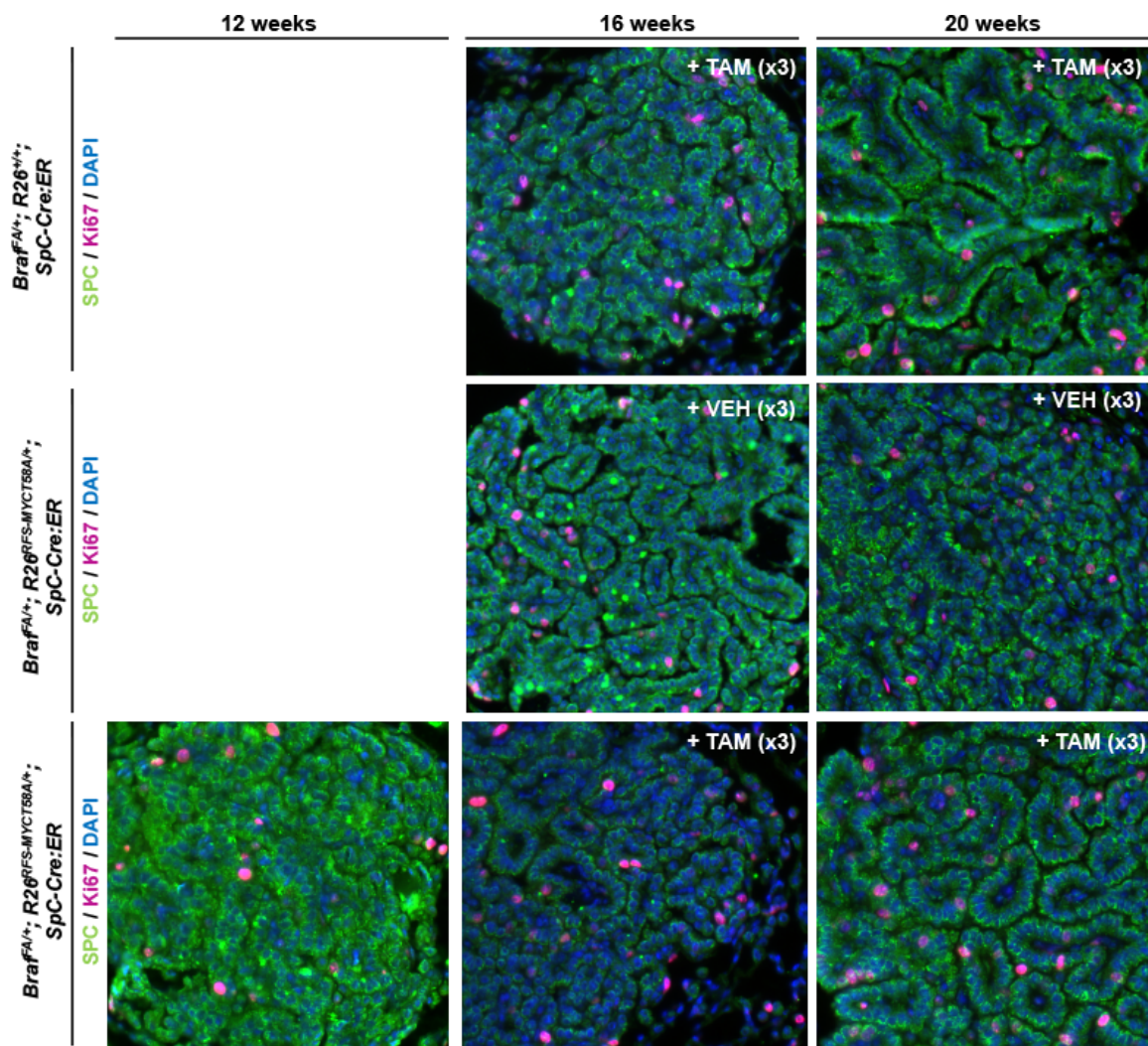
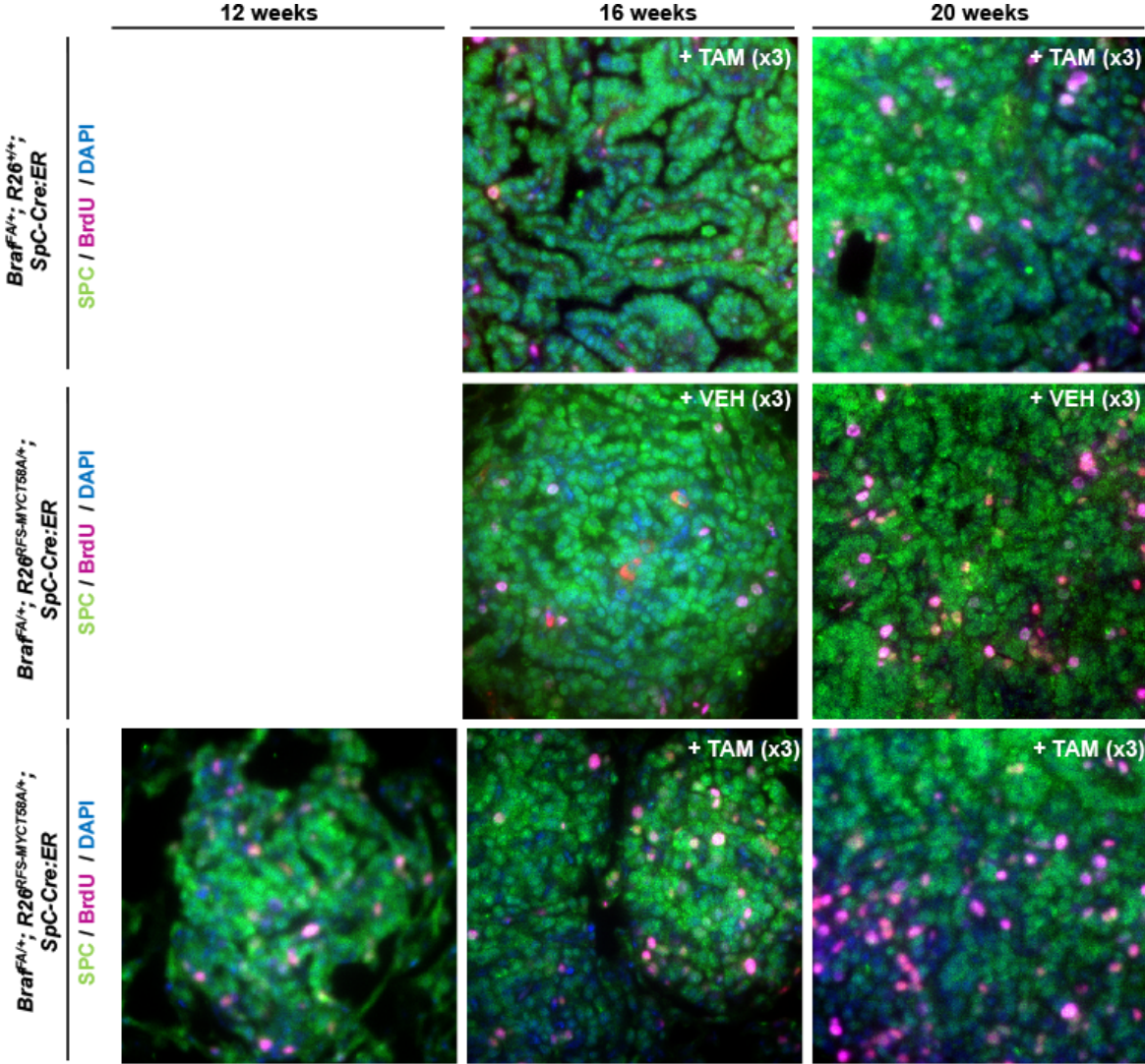
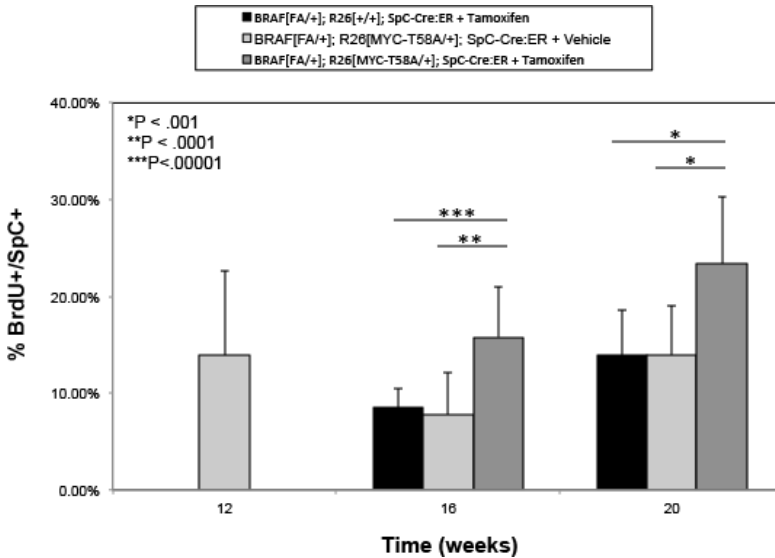


Figure 2-7e



**Figure 2-7f**



**Figure 2-7. Overexpression of c-MYC bypasses growth arrest of BRAF<sup>V600E</sup>-induced lung adenomas, in a two switch model of lung tumorigenesis.** (a) Lungs of mice of the indicated genotypes were infected with Ad-Cre and monitored 12 weeks as indicated at which time they were given intraperitoneal injections of either vehicle or tamoxifen. Mice were then euthanized at 12, 16, or 20 weeks p.i. to assess tumor size, burden, and grade. (b) Representative FFPE lung sections processed for Hematoxylin and Eosin (H&E). (c) Quantification of tumor number, tumor size, and tumor burden in mice of the aforementioned genotypes injected with either vehicle or tamoxifen and euthanized 12, 16, or 20 weeks p.i. (d-e) Immunofluorescence analysis of histological sections from mice of the indicated genotypes euthanized 12, 16 or 20 weeks p.i. as indicated with DNA (DAPI) in blue, SPC in green, Ki67 in pink, and BrdU in red as indicated. (f) Quantification of % BrdU+/SP-C+ cells from BRAF<sup>V600E</sup>-induced tumors with (+ tamoxifen) or without (+ vehicle) c-MYC overexpression, euthanized at either 12, 16, or 20 weeks p.i.

Figure 2-8a

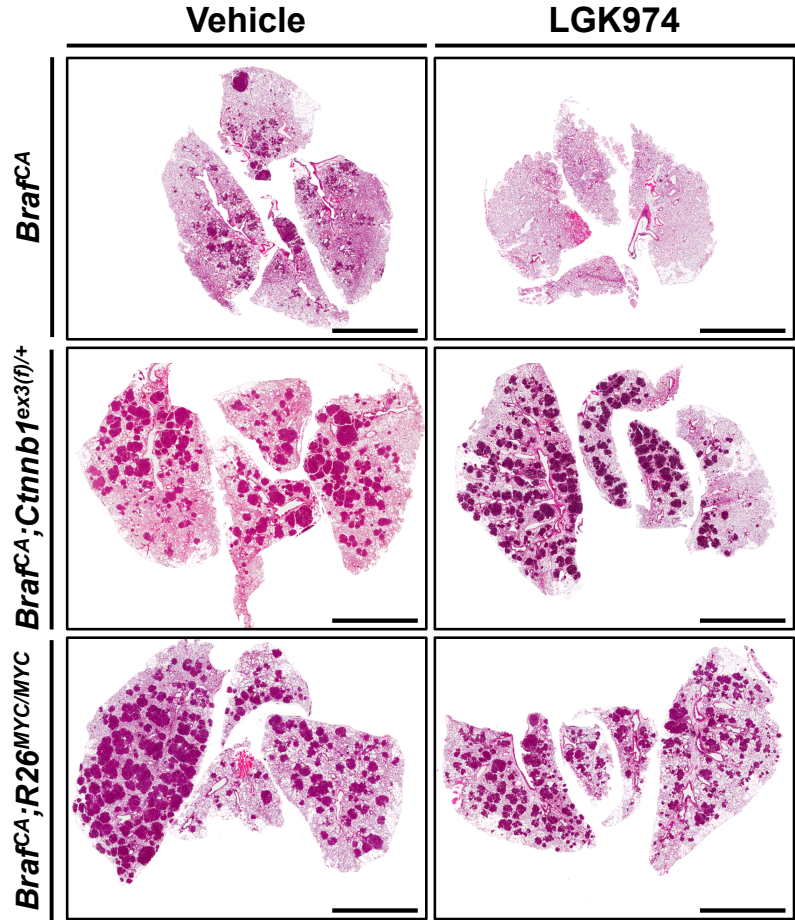


Figure 2-8b

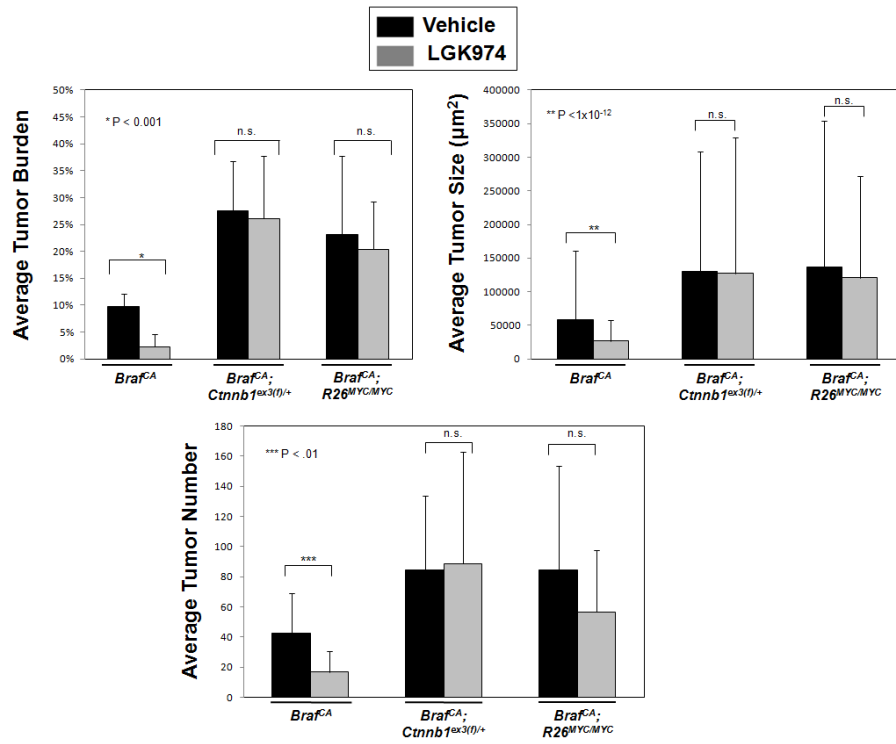
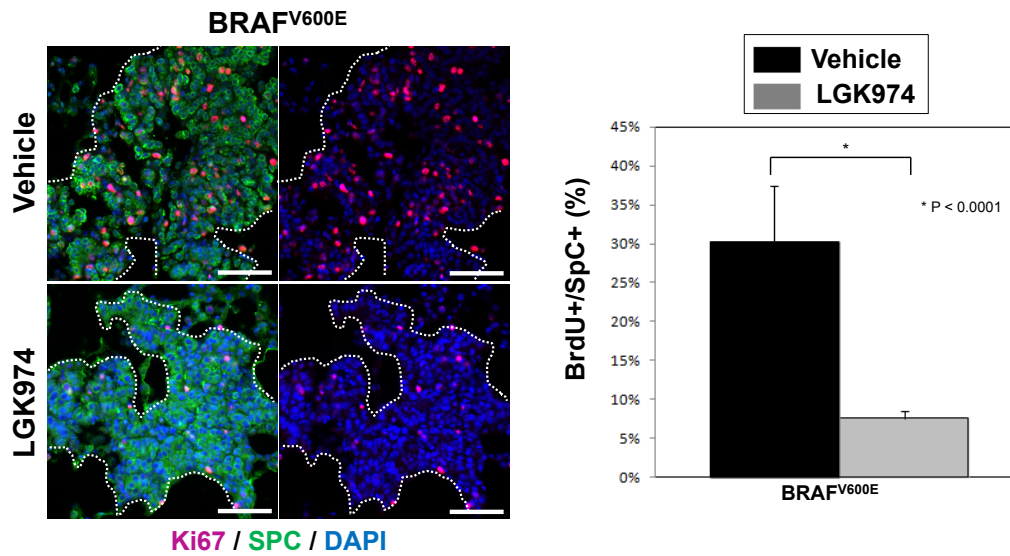
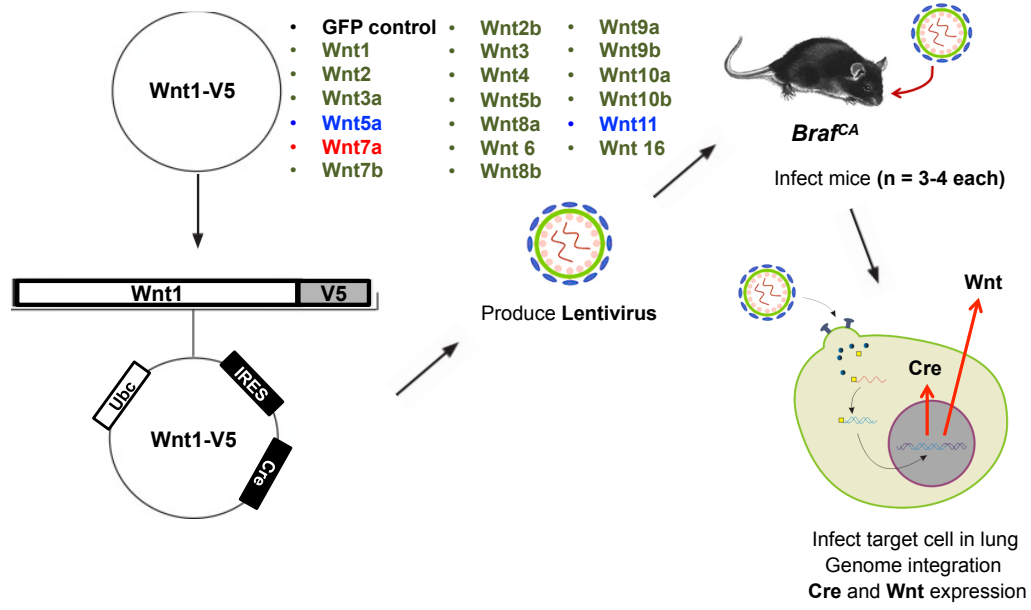


Figure 2-8c





**Figure 2-8d**



**Figure 2-8e**

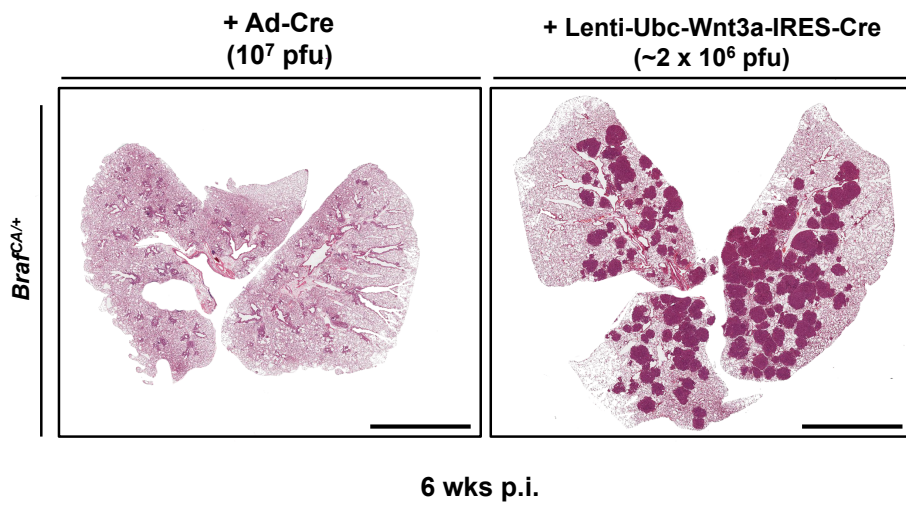


**Figure 2-8f**

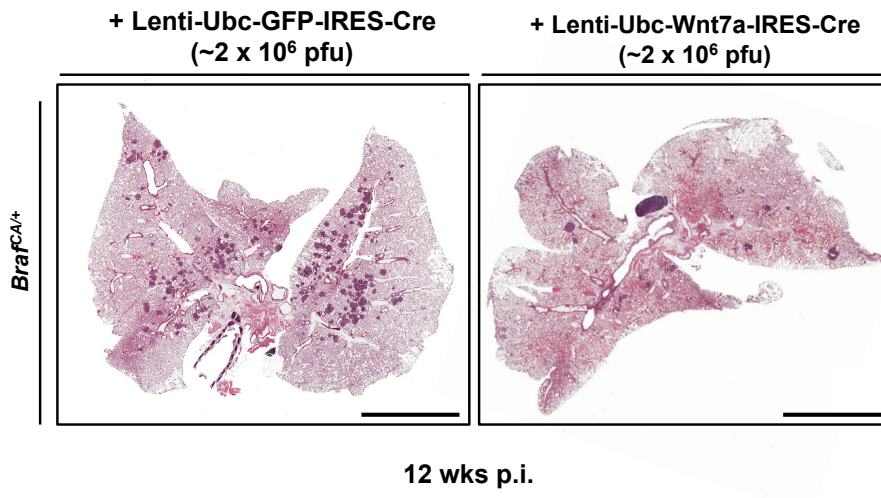


**Figure 2-8g**

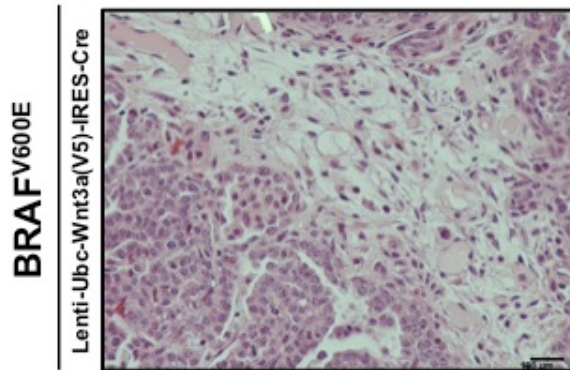
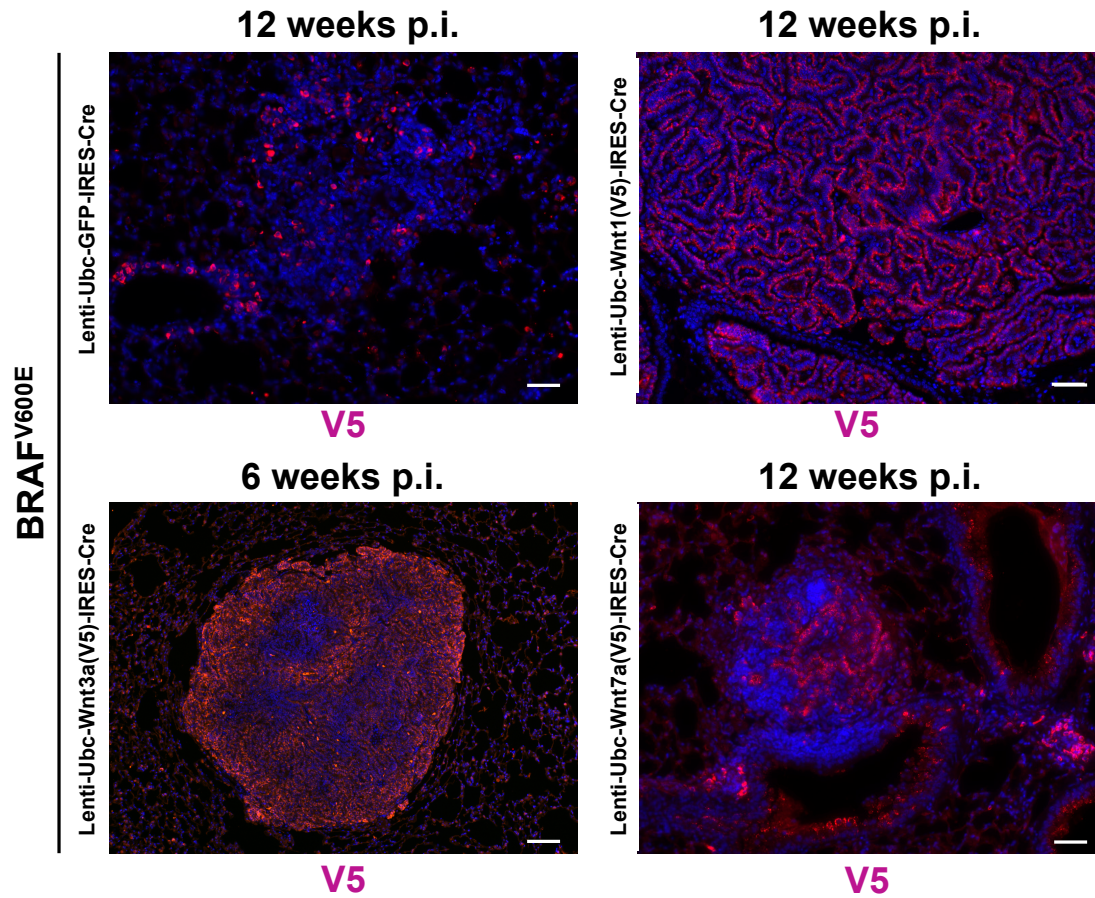




Figure 2-8h



**Figure 2-8. BRAF<sup>V600E</sup>-induced lung tumorigenesis is WNT ligand dependent.** (a) BRAF<sup>V600E</sup>, BRAF<sup>V600E</sup>/CTNNB1\* or BRAF<sup>V600E</sup>/c-MYC<sup>T58A</sup> expressing lung tumors were initiated in mice of the appropriate genotype. One week later mice were dosed for five weeks with vehicle control or LGK974 as described in Experimental Procedures at which time mice were euthanized and lungs prepared for H&E staining. All scale bars represent 4mm. (b) Quantification of the effects of LGK974 on lung tumor number, size and overall burden in mice bearing BRAF<sup>V600E</sup>, BRAF<sup>V600E</sup>/CTNNB1\* or BRAF<sup>V600E</sup>/c-MYC<sup>T58A</sup> expressing lung tumors as described in Experimental Procedures. (c) Immunofluorescence analysis of BRAF<sup>V600E</sup> tumors dosed for five weeks with vehicle control or LGK974 and euthanized 6 weeks p.i. as indicated.

DNA (DAPI) in blue, SPC in pink and CC10 in green. Quantification of % Ki67+/SP-C+ cells from BRAF<sup>V600E</sup>-induced tumors dosed for five weeks with vehicle control or LGK974 and euthanized at 6 weeks post Ad-Cre infection. (d) *Braf*<sup>CA/+</sup> mice were infected with lentiviruses expressing both Cre recombinase and a single V5-tagged WNT ligand. All 19 WNT ligands were tested. (e, g) Representative H&E-stained lung sections from *Braf*<sup>CA/+</sup> mice infected with either GFP-expressing lentivirus-Cre or Wnt3a. (f) Representative H&E-stained lung sections from *Braf*<sup>CA/+</sup> mice infected with either GFP-expressing lentivirus-Cre or Wnt7a. (h) Immunofluorescence analysis of histological sections from *Braf*<sup>CA</sup> mice overexpressing either GFP, Wnt1-V5, Wnt3a-V5, or Wnt7a-V5 euthanized at 6 weeks (bottom left) or 12 weeks (top left, top right, and bottom right) p.i. DAPI in blue, and V5 in red. Scale bar is 50µm.

**Figure 2-9a-d**

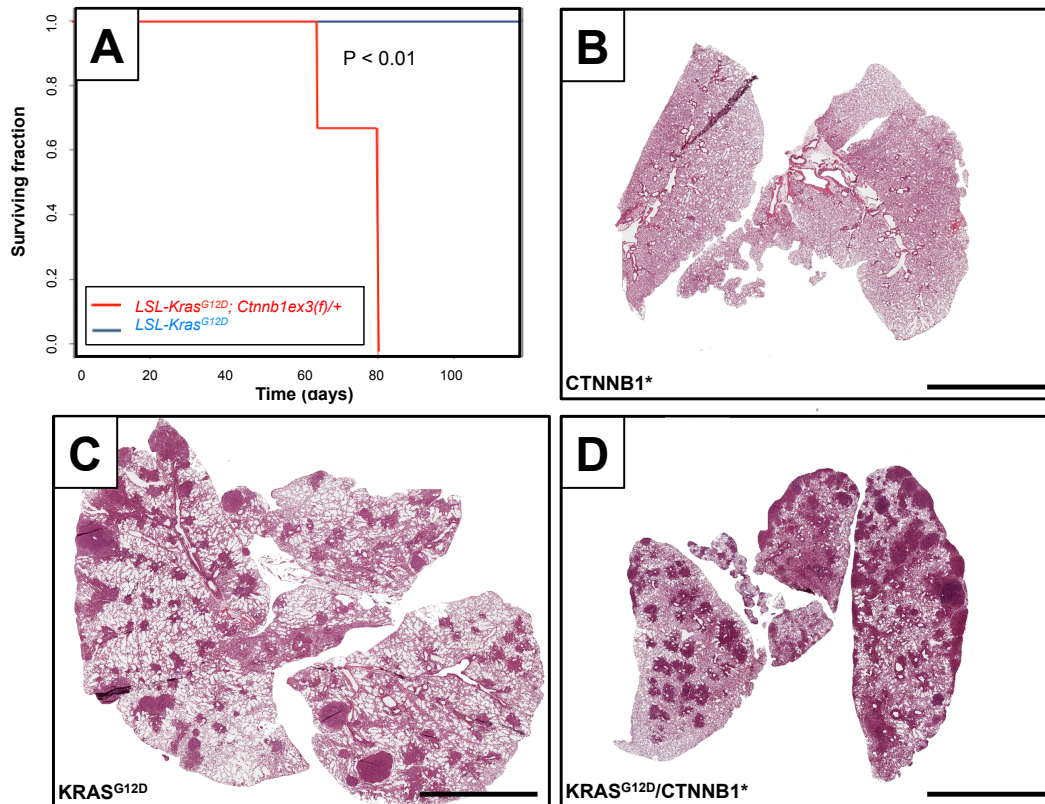


**Figure 2-9. KRAS<sup>G12D</sup> cooperates with CTNNB1\* to promote lethal lung tumorigenesis.** (a) Oncogene expression was initiated in *LSL-Kras<sup>G12D</sup>*, *Ctnnb1<sup>ex3(f)/+</sup>* or compound *LSL-Kras<sup>G12D</sup>; Ctnnb1<sup>ex3(f)/+</sup>* mice using Ad-Cre with mice monitored prospectively over 160 days. Mice were euthanized upon development of end-stage disease per IACUC regulations and a Kaplan-Meier survival curve was plotted (a). Representative H&E-stained lung sections from *Ctnnb1<sup>ex3(f)/+</sup>* mice (b), *LSL-Kras<sup>G12D</sup>* mice (c) euthanized at 160 days p.i. or *LSL-Kras<sup>G12D</sup>; Ctnnb1<sup>ex3(f)/+</sup>* mice (d) euthanized at 80 days p.i are presented. All scale bars represent 4mm.

**Figure 2-10a-e**

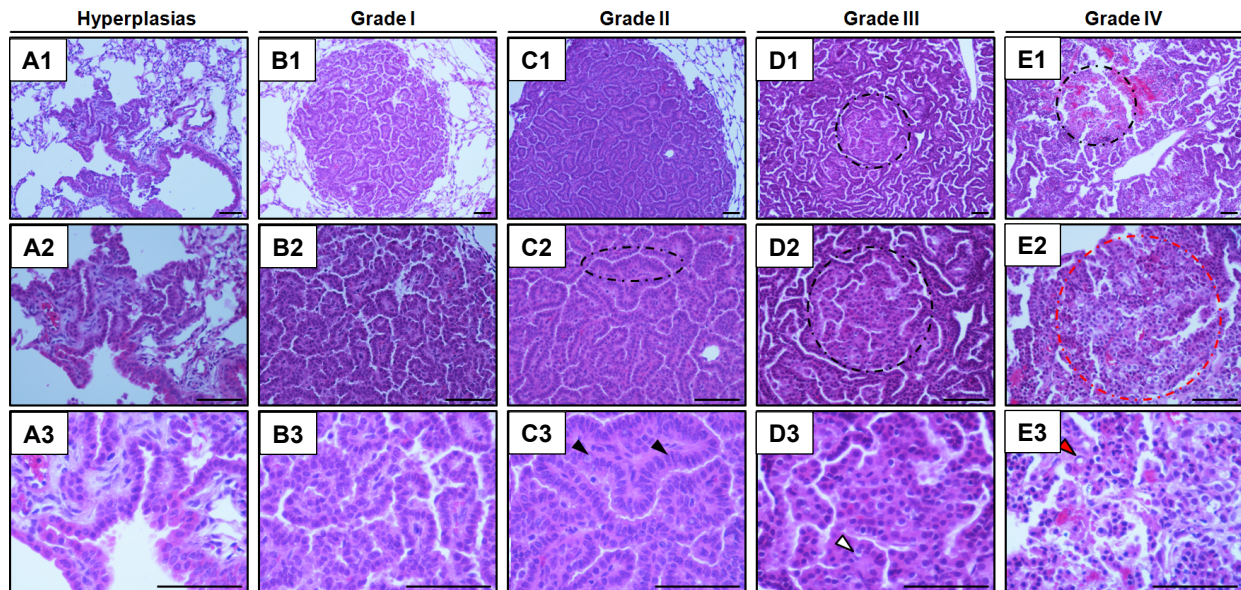


**Figure 2-10. Grading scheme used to classify BRAF<sup>V600E</sup>-initiated lung lesions. (a-a2)**

Hyperplasias: Thickening of the alveoli or airway walls, nuclei and cells display normal cytology (images were taken from a *BRaf<sup>CA/+</sup>* mouse 12 weeks post Ad-Cre infection). (b-b2) Grade I: Low grade adenoma – Well-differentiated tumors with normal cytology. Tumor is well circumscribed and nuclei are uniform in size. Papillary growth pattern commonly observed. Images were taken from a *BRaf<sup>CA</sup>* mouse 12 weeks post Ad-Cre infection. (c-c2) Grade II: Higher grade, large benign adenoma – Tumors exhibit cells with increased nuclear:cytoplasmic ratios (black dotted circle) and increased hyperchromatism. Signs of nuclear atypia including enlargement and elongation of nuclei and presence of cytoplasmic inclusions (black arrowheads). Papillary growth pattern prevalent in these tumors. Images were taken from a *BRaf<sup>CA</sup>; R26<sup>MYC(WT)/(WT)</sup>* mouse 12 weeks p.i. (d-d2) Grade III: Advanced adenoma – Increased nuclear:cytoplasmic ratio and nuclear atypia similar to Grade II tumors. Tumors display increased pleomorphism (black dotted circle). Tumor cells are vacuolated. Solid alveolar growth pattern emerges in these tumors. Images were taken from a *BRaf<sup>CA</sup>; Ctnnb1<sup>ex3(f)/+</sup>* mouse

10 weeks post Ad-Cre infection. (e-e2) Grade IV: Adenocarcinoma – Tumors possessing all the features of Grade III tumors including nuclear atypia, solid alveolar growth pattern, and increased pleomorphism (red dotted circle), along with signs of coagulated tumor necrosis (red dotted circle) and scalloping of nuclear membranes (red arrowhead). Images were taken from a *BRaf<sup>CA</sup>; Ctnnb1<sup>ex3(f)/+</sup>* mouse 10 weeks p.i.. Scale bar in all images is 80µm. Scheme is based on the classification of proliferative pulmonary lesions of the mouse by Nikitin et al. (43).



Figure 2-11a-f

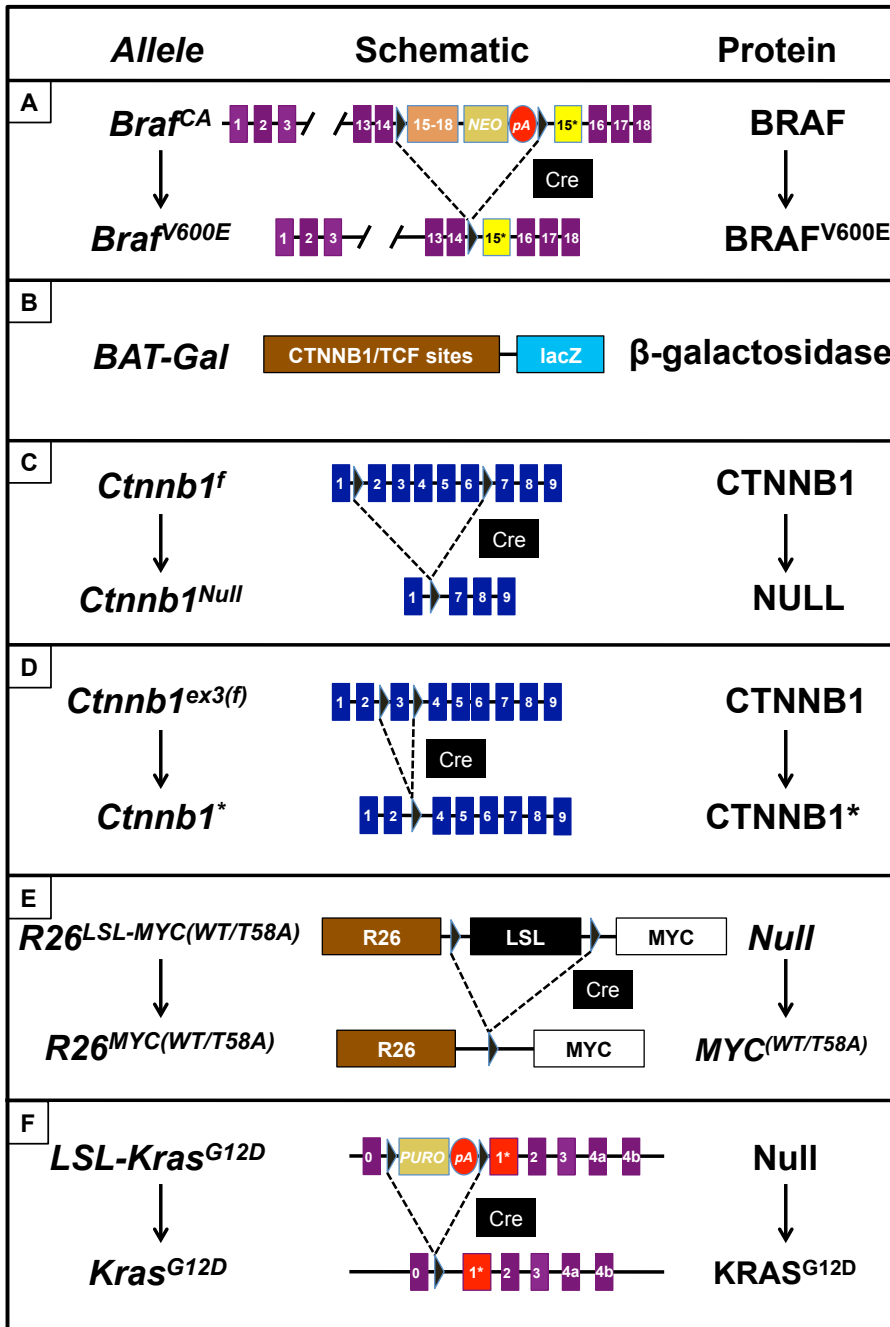
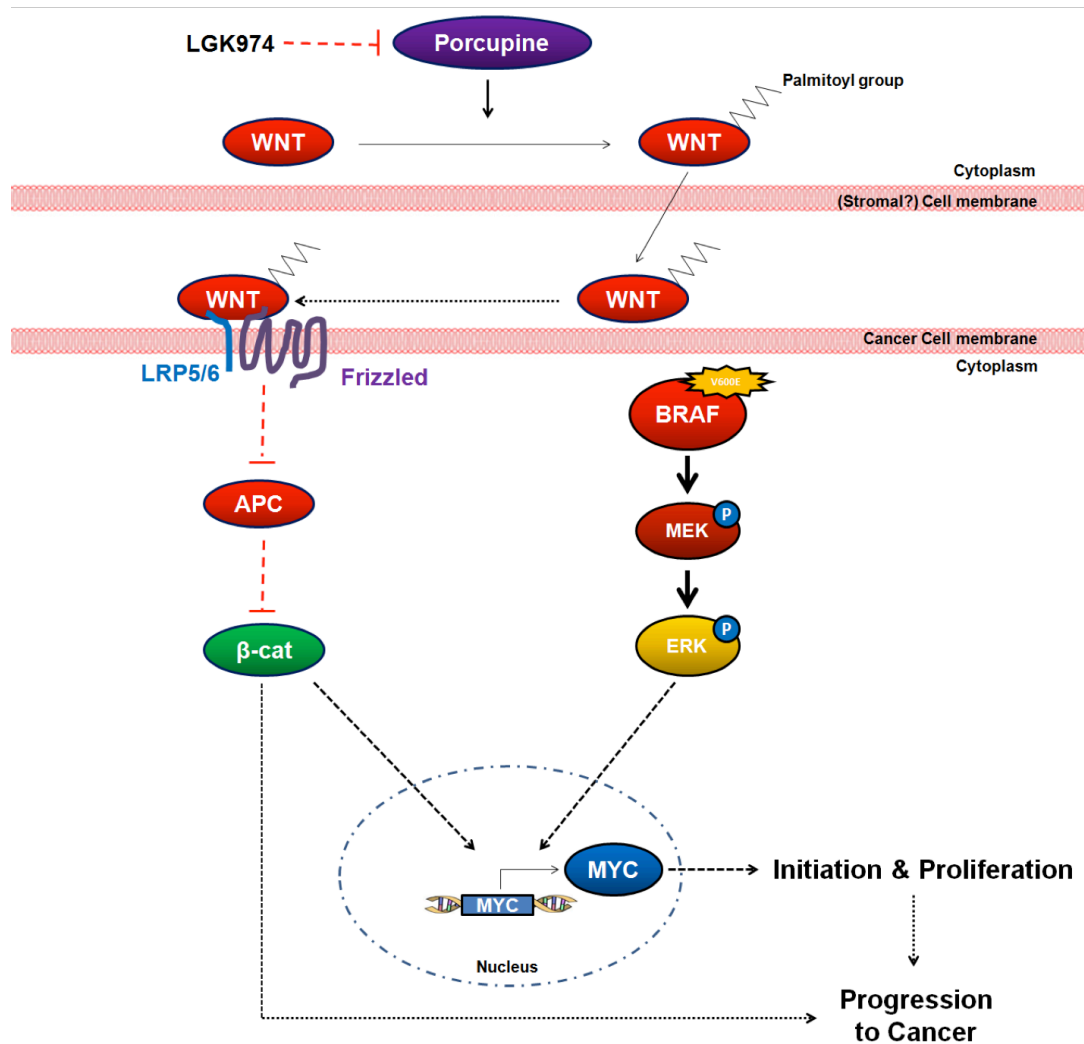


Figure 2-11. Schematic of the *Braf*<sup>CA</sup>, *BAT-GAL*, *Ctnnb1*, *R26*<sup>MYC</sup> and *Kras* alleles. (a) *Braf*<sup>CA</sup> encodes normal BRAF until recombined by Cre recombinase to express BRAF<sup>V600E</sup> (4). (b) The *BAT-GAL* transgene encodes β-galactosidase under the control of a promoter containing multiple TCF/CTNNB1 (β-catenin) binding sites (10). (c) *Ctnnb1*<sup>f</sup> encodes normal CTNNB1

until recombined by Cre recombinase to generate a *Ctnnb1* null allele (38). (d) *Ctnnb1<sup>ex3(f)</sup>* encodes CTNNB1 until recombined by Cre recombinase to express CTNNB1\*, a constitutively active form of  $\beta$ -catenin (39) (e) *RFS<sup>LSL-MYC(WT or T58A)</sup>* is a null allele of *Rosa26* that when recombined by Cre recombinase elicits sustained expression of either c-MYC<sup>WT</sup> or c-MYC<sup>T58A</sup> from the *Rosa26* promoter. This allele was used in either a heterozygous or homozygous configuration as indicated (50). (f) *LSL-Kras<sup>G12D</sup>* is a null allele of *Kras* that, when recombined by Cre recombinase, expresses mutationally activated KRAS<sup>G12D</sup> (Jackson et al., 2001).

Figure 2-12



**Figure 2-12. Cooperation of BRAF<sup>V600E</sup> and Wnt/β-catenin signaling bypasses the growth arrest of BRAF<sup>V600E</sup>-induced lung adenomas and drives progression to lung adenocarcinoma.** Mechanisms of cooperation between oncogenic MAPK signaling and Wnt/β-catenin signaling. Both pathways converge on c-MYC expression to drive tumor proliferation. Targets downstream of Wnt/β-catenin, but independent of c-MYC, likely facilitate the progression to lung adenocarcinoma.





## CHAPTER 3

### ***IN VIVO* SLEEPING BEAUTY SCREEN TO IDENTIFY POTENTIAL TUMOR SUPPRESSOR GENES AND ONCOGENES IMPORTANT FOR LUNG CANCER PROGRESSION**

#### **ABSTRACT**

To gain a global understanding of the selective pressures influencing the progression of BRAF<sup>V600E</sup>-initiated lung adenomas to adenocarcinoma and identify novel oncogenes, tumor suppressor genes, and cancer-related pathways capable of cooperating with the BRAF<sup>V600E</sup> oncogene to drive lung adenocarcinoma formation, we performed Sleeping Beauty (SB) mutagenesis in mice carrying the *Braf*<sup>CA/+</sup> mutation. This approach allowed us to identify genes and pathways critical for the progression of MAPK pathway-driven lesions to malignant lung cancer, including eight trunk driver genes: *Cux1*, *Wapal*, *Top1*, *Cmip*, *Gnaq*, *Snd1*, *Foxp1*, and *Rbms3*.

#### **INTRODUCTION**

To gain a more comprehensive view of the molecular mechanisms responsible for NSCLC formation and progression, we undertook an unbiased approach to identify novel oncogenes, tumor suppressor genes, and oncogenic pathways capable of cooperating with BRAF<sup>V600E</sup> expression in the lung epithelium to drive progression to adenocarcinoma.

We performed an SB transposon mutagenesis screen in conjunction with BRAF<sup>V600E</sup> activation in the lung epithelium by introducing the conditional *Rosa26-CAGGS-loxP-STOP-*

*loxP-(64)-SB11 transposase* allele and high copy *T2/Onc2* (TG.6070) allele into our *Braf<sup>CA</sup>* GEMM. Expression of BRAF<sup>V600E</sup> and the SB11 transposase were restricted to the lung epithelium through intranasal instillation of Adeno-Cre.

This system allowed us to identify both known and novel candidate cancer genes and pathways capable of inducing adenocarcinoma formation in an oncogenic BRAF<sup>V600E</sup> background. This study has given us not only a wealth of genes that warrant further validation for their prognostic and predictive value in NSCLC, but also a global overview of the evolutionary forces and pressures influencing the formation and progression to lung adenocarcinoma.

## RESULTS

### *Transposon Screen*

To identify genes capable of cooperating with oncogenic BRAF<sup>V600E</sup> expression to drive progression to lung adenocarcinoma, we performed SB transposon mutagenesis screens in mouse lines carrying the *Braf<sup>CA/+</sup>* sensitizing mutations. Activation of BRAF<sup>V600E</sup> and the SB11 transposase specifically in the lung epithelium was performed via intranasal instillation of virus-Cre at low titer (Ad-Cre, 10<sup>6</sup> pfu).

SB mutagenesis shortened the lifespans of *Braf<sup>CA/+</sup>* mice containing the *Rosa26-CAGGS-loxP-STOP-loxP-(64)-SB11 transposase* and *T2/Onc2* alleles (TG.6070) (n = 34), but not that of *Braf<sup>CA/+</sup>* mice containing only the *RCL::SB* allele (n = 19), or wild-type mice (n = 3). Median survival for *Braf<sup>CA/+</sup>; RCL::SB; T2/Onc2* mice were 205 days versus 338 days for *Braf<sup>CA/+</sup>; RCL::SB* mice.

Tumors were assessed for evidence of malignant progression using previously established grading criteria described in the previous chapter (43). Only *Braf*<sup>CA/+</sup>; *RCL::SB*; *T2/Onc2* mice had lesions progress to adenocarcinoma, whereas *Braf*<sup>CA/+</sup>; *RCL::SB* harbored benign adenomas and *RCL::SB*; *T2/Onc2* mice failed to form tumors. Despite the ability of SB mutagenesis to drive progression to lung adenocarcinoma, tumors did not metastasize.

### ***Identification of candidate cancer genes***

To identify genes mutated by SB that may potentially contribute to malignant tumor progression when combined with oncogenic BRAF<sup>V600E</sup> expression, we sequenced the transposon insertion sites from 28 *Braf*<sup>CA/+</sup>; *RCL::SB*; *T2/Onc2* tumors (Fig. 3-1). Tumors were chosen based on histology and tumor grade, size, and detection of the SB transposase (Fig. 3-2, Fig. 3-3a-c, Fig. 2-10a-e).

Common transposon insertion sites (CISs) were then identified using two statistical methods: the locus-centric Gaussian kernel convolution (GKC) method and a gene-centric statistical method called gCIS (Table 1 and Table 2). Both methods identify genomic regions containing a higher density of insertions than predicted by chance either within a specific kernel width (GKC) or within a gene (gene centric CIS, or gCIS), suggesting these regions likely contain a cancer driver gene. Adjusted p-values were determined using the Bonferroni correction method to counteract the problem of multiple comparisons and were ranked according to these values. Candidate cancer genes from these CISs were defined as genes whose corrected p-values < 0.05. Merging these two lists led to the generation of a non-redundant list of 884 CIS genes, of which 852 had human orthologs. Pathway annotations for these candidate cancer genes were then determined using the Kyoto Encyclopedia of Genes and Genomes (KEGG).

The SB screen identified CIS genes involved in pathways known to be important to lung cancer progression including components of the RAS/RAF/MEK/ERK MAPK pathway such as *Braf*, *Map3k1*, and *Mapk1*. Previous work has suggested that high levels of signaling from the RAS/RAF/MEK/ERK MAPK pathway facilitates lung cancer progression (81). In agreement with the previous chapter, CIS genes involved in Wnt/ $\beta$ -catenin signaling such as *Lrp6*, and *Cttna1* were also identified. Work in other labs have demonstrated the importance of insulin-like growth factor receptor signaling in KRAS-mutant NSCLC, and not surprisingly, *Igf2r* was also identified as a highly statistically significant CIS (82). Finally, recently identified molecules with roles in oncogenic MAPK-driven cancer such as *Iqgap1* were also identified by the screen (83).

A number of CIS genes also enrich for processes whose exact molecular roles (if any) in NSCLC have yet to be elucidated. These include members of the SWI/SNF remodeling complex such as *Arid2* and *Pbrm1*. Other epigenetic modifiers including *Kdm6a* and *Kmt2e* were similarly identified. Genes highly mutated in human cancers including *Fat1*, *Cux1*, and *Stag2* were also found to be highly significant CIS genes (84-86).

Beyond the lists of top 50 genes from the GKC and gCIS analyses, genes involved in axon guidance such as *Ephb1* and *Gli1*, and in particular genes involved in ROBO receptor signaling such as *Srgap1*, *Srgap2*, *Robo1*, and *Robo2* were also significantly enriched for by our SB screen. Interestingly, SB screens in other tissues have independently identified axonal guidance molecules as having key roles in tumorigenesis, most recently in pancreatic cancer, suggesting this pathway may be a central mediator of tumorigenesis in multiple contexts (19).

### ***Identification of trunk driver genes***

To identify CIS genes that were potential trunk driver genes, we looked for the CIS genes

that contained 5 or more sequence read counts per tumor from 3 or more tumors and have corrected  $P < 0.05$  by gCIS analysis (Table 3).

Eight genes were found to be putative trunk drivers: *Cux1* (17/28 tumors), *Wapal* (7/28), *Top1* (12/28 tumors), *Cmip* (12/28 tumors), *Gnaq* (12/28 tumors), *Snd1* (13/28 tumors), *Foxp1* (18/28 tumors), and *Rbms3* (14/28 tumors). In total, 26 out of 28 tumors contained one or more SB insertions into at least 1 trunk driver gene. 21 out of 28 tumors had one or more SB insertions into 3 or more trunk driver genes, and 9 out of 28 tumors had one or more SB insertions into 5 or more trunk driver genes.

## DISCUSSION

Our studies have identified a number of genes and pathways with previously uncharacterized roles in NSCLC including *Cux1*, *Stag2*, *Arid2*, *Kdm6a*, *Fat1*, and *Srgap2*. While beyond the scope of this dissertation, work is currently underway to validate whether disruption of these genes can indeed cooperate with BRAF<sup>V600E</sup> signaling to drive progression to adenocarcinoma. This includes the intranasal delivery of a lentivirus containing the recently described pSECC vector (expressing a sgRNA of interest, Cas9, and Cre), which allows us to both activate BRAF<sup>V600E</sup> expression while simultaneously using the CRISPR/Cas9 system to delete our candidate cancer genes in the lung epithelium of our *Braf*<sup>CA</sup> GEMM of lung cancer (87). Tumors will then be assessed for deletion of the target gene of interest and the effects of this deletion on overall survival, tumor size, and tumor grade. Validation in a human NSCLC line harboring the BRAF<sup>V600E</sup> mutation, HCC364, is also underway. Again, using the CRISPR/Cas9/sgRNA-mediated target gene modification system, we will delete putative tumor suppressor genes from

this cell line, introduce these cells into the lungs of NOD scid gamma (NSG) mice by tail vein injection, and assess the effects of this gene modification on tumor growth.

The genes identified in this SB transposon screen provide major insights into the molecular mechanisms underlying NSCLC. Genes that overlap with the list of genes frequently mutated in human lung adenocarcinoma are also likely to have an active, rather than passive/bystander role in lung tumorigenesis. Because of the high rate of mutation in NSCLC, cross-species analysis allows us to filter out passenger mutations from driver mutations that may then serve as prognostic and predictive biomarkers, and the pathways they regulate may be attractive therapeutic targets for this disease.

## **MATERIALS AND METHODS**

### ***Mice and Adenovirus delivery***

As described in the previous chapter, all animal experiments were conducted in accordance with protocols approved by the UCSF Institutional Animal Care and Use Committee (IACUC). *BRaf<sup>CA</sup> (BRaf<sup>tm1Mmcm</sup>)*, *Rosa26-CAGGS-loxP-STOP-loxP (64)::SB*, and *T2/Onc2* (Strain 6070 [B6;C3- TgTn(sb-T2/Onc2)6070Njen]) mice were bred and genotyped as previously described (4, 10, 38, 39, 50, 78). Stocks of Adenovirus encoding Cre recombinase (Ad-CMV-Cre) were purchased from Viraquest (North Liberty, IA) and instilled into the lungs of adult mice as previously described (4, 79).

### ***Histology and quantification of lung tumor burden***

Lungs were processed for analysis as described previously (33). Hematoxylin and Eosin (H&E) stained slides were scanned with an Aperio ScanScope scanner with quantification performed using Aperio Spectrum ImageScope software.

### ***Immunostaining of mouse lung tissue, LacZ detection and immunoblotting***

Mouse lungs were fixed in zinc-buffered formalin, processed and embedded in paraffin, cut into 5µm sections and mounted on glass slides. Citrate-mediated antigen retrieval was performed and then the following antibodies were used for detection: Sleeping Beauty Transposase (R&D Systems).

### ***Illumina sequencing and subsequent analysis***

Tumor DNA was extracted from FFPE tissues using the Gentra PureGene cell kit (Qiagen, 158767), and transposon insertion sites were amplified using linker-mediated PCR (LM-PCR). The lab of David Adams at the Wellcome Trust Sanger Institute performed Illumina sequencing.

### ***Raw Sequence Processing***

Twenty-eight tumours from 10 mice (2310 (n=1), 2343 (n=6), 2347 (n=1), 2425 (n=3), 2426 (n=3), 2438 (n=1), 2469 (n=2), 2480 (n=6), 2485 (n=1) and 2519 (n=4)) were pair-end sequenced using a set of customised baits and aligned to the mouse genome reference assembly GRCm38 using BWA (version 1.16) (88).

To improve SNP and indel calling, the GATK (89) 'IndelRealigner' was used to realign reads near indels from the Mouse Genome Programme (90). The BAM files were re-sorted and quality



scores were recalibrated using GATK 'TableRecalibration'. SAMtools 'calmd' was then used to recalculate MD/NM tags in the BAM files (91). All lanes from the same library were then merged into a single BAM file using Picard tools using version 1.72 and PCR duplicates were marked using Picard 'MarkDuplicates'.

### ***Merging and Filtering***

The BAM files were processed using RetroSeq version 1.41 to identify pair reads where one read aligned to the reference mouse genome and the other read to the Sleeping Beauty (SB) transposon sequence. (Retroseq was run in "Discovery" mode using the default parameters: Min anchor quality: 20; Min percent identity: 80; Min length for hit: 36). This generated a total of 72,981 individual putative transposon insertion regions (7) across all 28 tumour samples. The sequence and analysis methodologies do not allow the exact SB insertion sites to be identified to the resolution of genomic basepairs hence the location of transposons are referred to as regions as opposed to sites.

Overlapping, individual IRs within each sample were merged using bedtools (92) to generate a set of 41,152 IRs. Chromosome four is the donor chromosome for the 6070 transposon line. To reduce the effects of local-hopping that can skew the downstream statistical analysis, all IRs that were located on chromosome four (4,609) were thereby excluded from the analysis. Insertions on other secondary scaffolds e.g *GL456393*, were also excluded. This left a total of total of 36,510 IRs.

Further filtering of the IRs was performed by removing IRs within the regions of two known genes into which the SB concatemer preferentially inserts (on *GRCm38:En2*; chr5:28165696-28173612 and *Foxf2*; chr13:31625816-31631403.). Nineteen genomic regions reported in (93)

into which the SB transposon inserts under no selection pressure were also used to exclude IRs that are likely not to be cancer-driving. Following these filtering steps a final set of 36,426 IRs remained.

### ***Identification of common insertion sites***

Common insertion sites were as described previously in the work by Takeda et al. (94). Briefly, to detect CISs, a GKC method was employed using 15,000, 30,000, 50,000, 75,000, 120,000, and 240,000 kernel widths. When CISs were detected over several kernel widths, the CISs were merged and the smallest window size is reported. Gene centric CISs (gCISs) were analyzed using the methods published in the work by Mann et al. (95)

### ***Trunk driver analysis***

A gene-centric statistical method was used to identify CIS genes, and genes that had 5 or more read counts and had insertions in three or more tumors were selected as trunk driver genes.

**Figure 3-1**

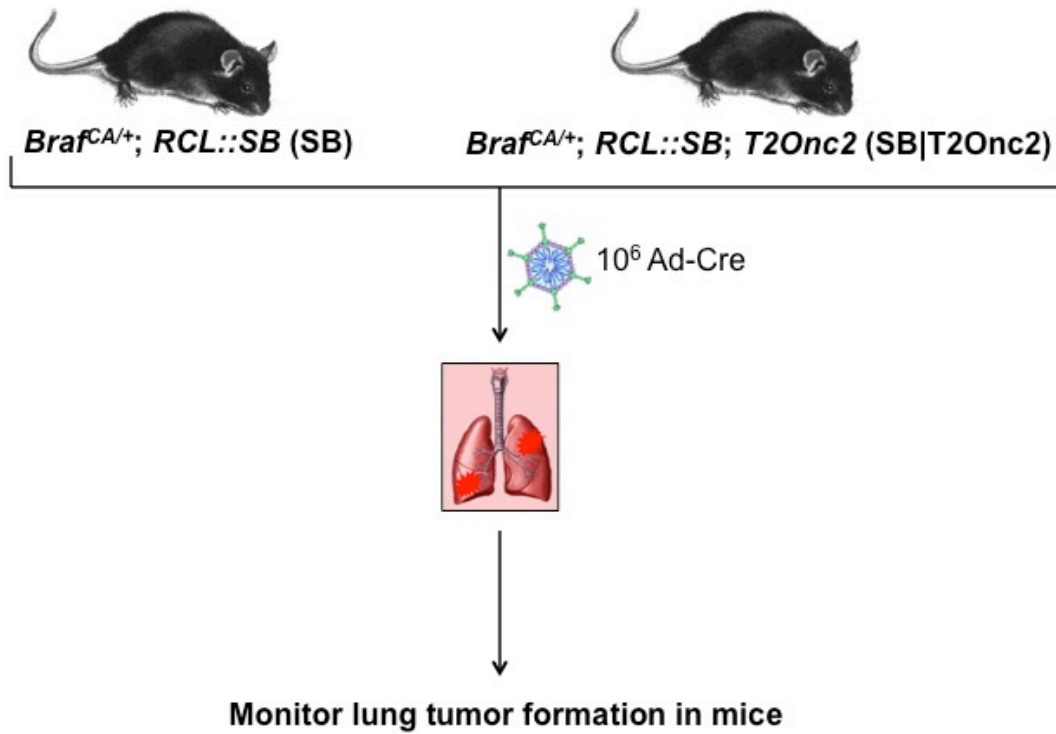


**Figure 3-1. Experimental set-up for SB screen in BRAF<sup>V600E</sup>-initiated lung tumors.** BRAF<sup>V600E</sup> expression was initiated in the lungs of mice with (SB|T2Onc2) or without (SB) the full Sleeping Beauty transposon system using low titer Adenovirus-Cre ( $10^6$  p.f.u.)

Figure 3-2

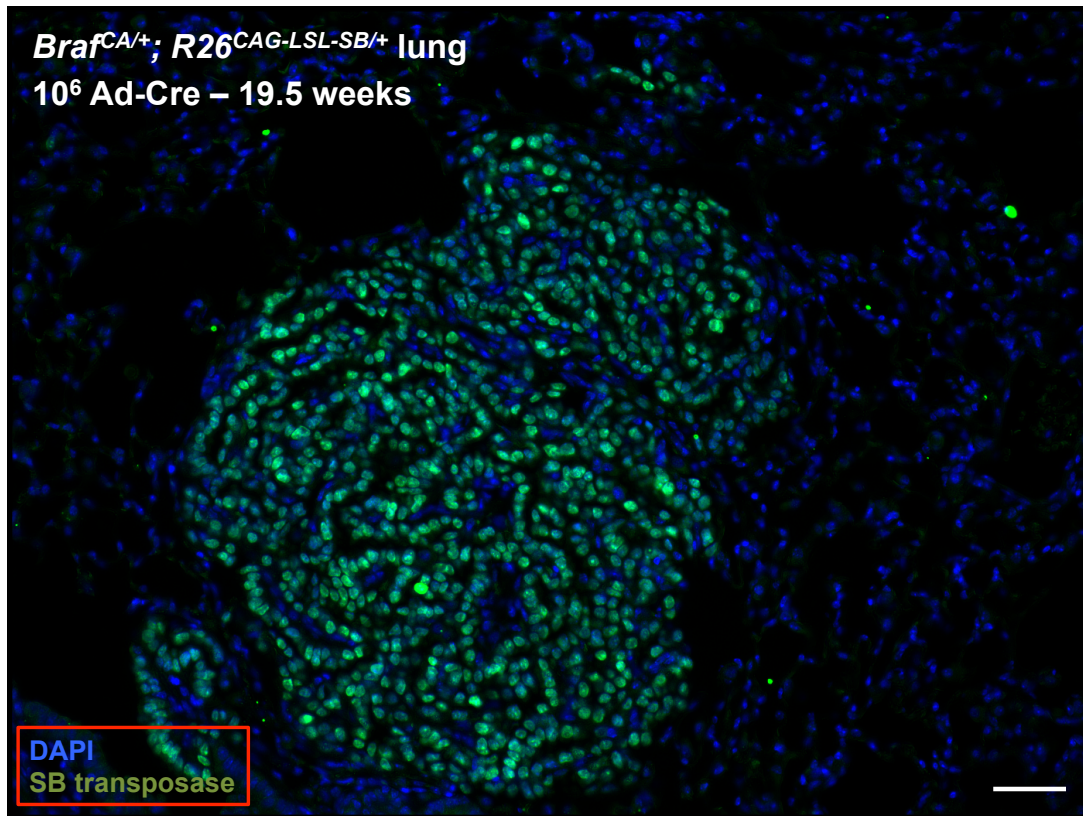


**Figure 3-2. Detection of SB transposase expression.** Immunofluorescence analysis of histological sections of BRAF<sup>V600E</sup>/SB transposase expressing lung tumors 19.5 p.i. DNA (DAPI) in blue, SB transposase in green.

Figure 3-3a

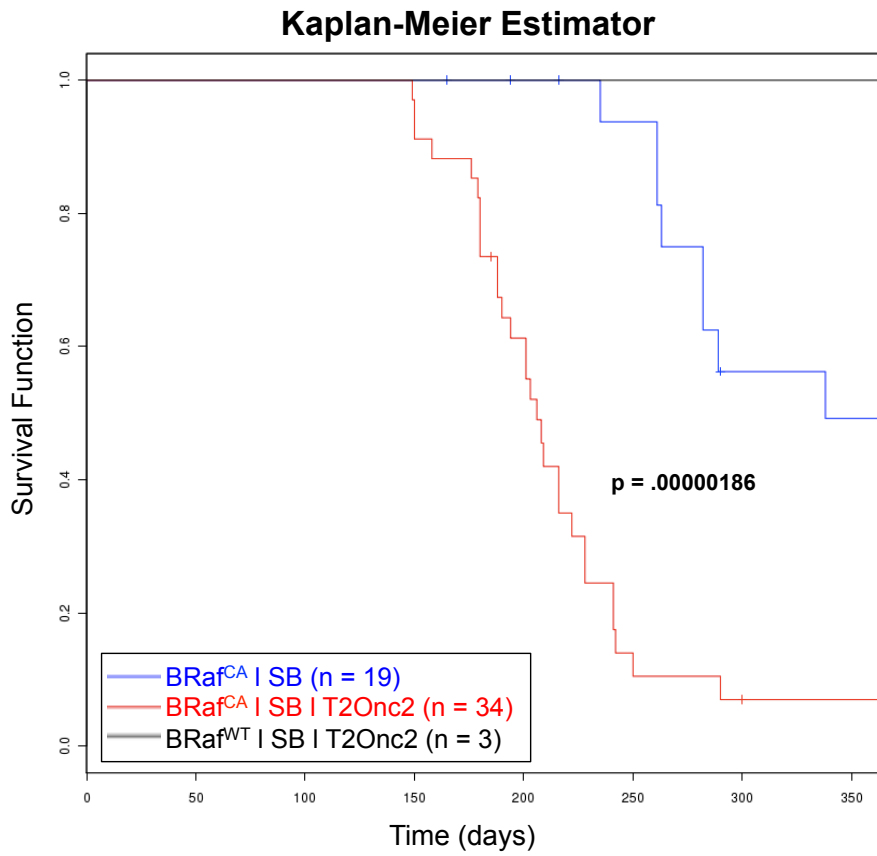


Figure 3-3b

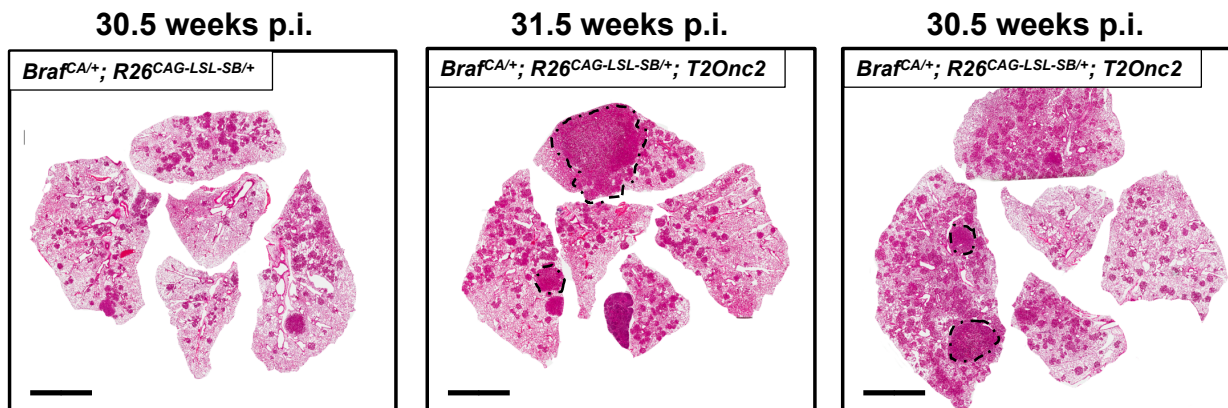
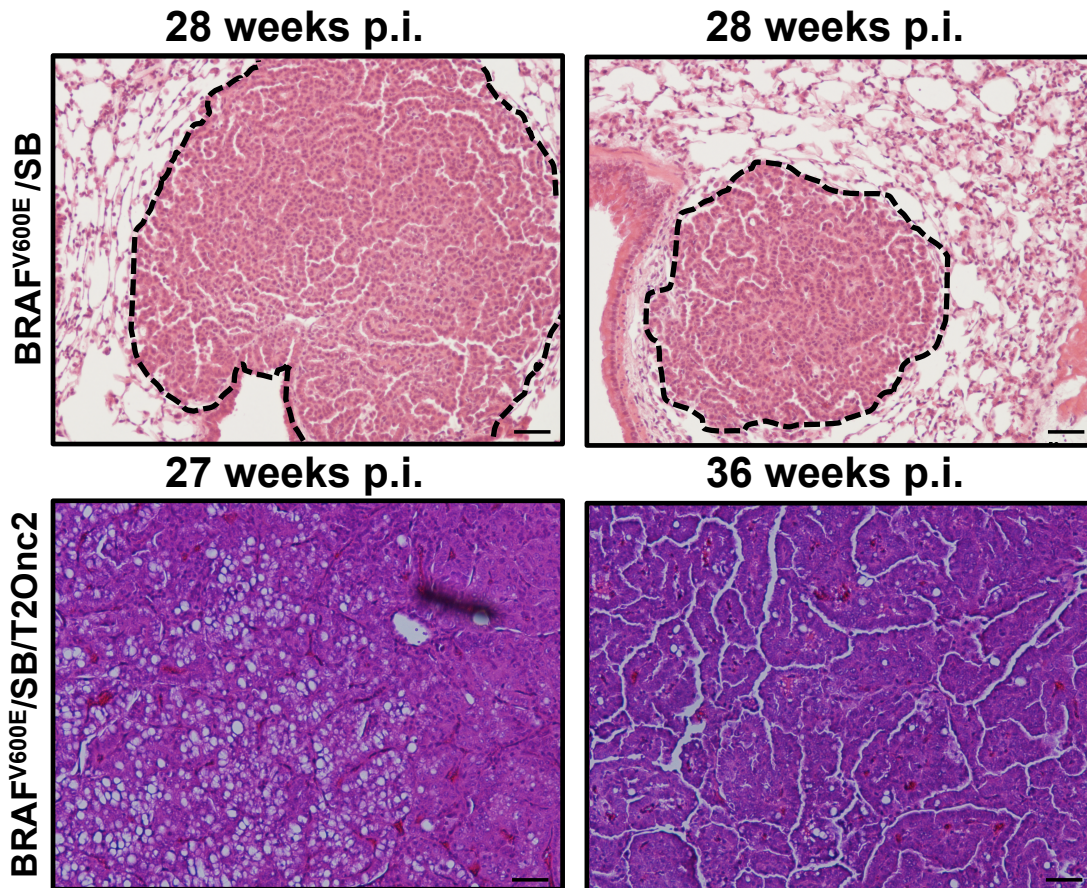


Figure 3-3c



**Figure 3-3. Mouse survival times were shortened and tumor progression was induced by SB-mediated mutagenesis.** (a) Mice were monitored for 365 days at which time mice with BRAF<sup>V600E</sup> expression and SB transposition required euthanasia due to lung cancer progression. (b-c) At euthanasia mice with BRAF<sup>V600E</sup> expression and SB transposition displayed clear evidence of lung cancer progression compared to the relevant controls.

**Table 1. Genes involved in lung adenocarcinoma progression of BRAF<sup>V600E</sup>-initiated tumors (GKC).**

CIS gene	P value (adj)	GKC Scale	CIS gene	P value (adj)	GKC Scale
<b>Setd5</b>	0	15000	<b>Nfat5</b>	0	15000
Diap3	0	15000	<b>Gbp1</b>	0	15000
CIS12:20229491_15k	0	15000	<b>Slc26a9</b>	0	15000
Cat	0	15000	<b>Fat1</b>	0	15000
<b>Top1</b>	0	15000	<b>Lrp6</b>	0	15000
<b>Clec16a</b>	0	15000	<b>Fam117b</b>	0	15000
<b>Api5</b>	0	15000	<b>Ncoa3</b>	0	15000
<b>Braf</b>	0	15000	<b>Adam10</b>	0	15000
Abhd2	0	15000	<b>Cnot2</b>	0	15000
Fabp6	0	15000	<b>Mapk1</b>	0	30000
<b>Cux1</b>	0	15000	<b>Ap1m1</b>	0	15000
<b>Kdr</b>	0	15000	<b>Bmpr1a</b>	0	30000
<b>Adrbk2</b>	0	15000	<b>Ano6</b>	0	15000
<b>Braf</b>	0	15000	<b>Snx7</b>	0	15000
Wapal	0	15000	<b>Dock4</b>	0	15000
Suv420h1	0	240000	<b>Pbrm1</b>	0	30000
<b>Atp6v0a4</b>	0	15000	<b>Dyrk1a</b>	0	15000
<b>Arid2</b>	0	15000	<b>Ctnna1</b>	0	50000
Qrich1	0	15000	<b>Ppp1r3e</b>	0	15000
<b>Ube2g1</b>	0	15000	<b>Matr3</b>	0	15000
<b>Kmt2e</b>	0	15000	<b>Setd5</b>	0	15000
<b>Kdm6a</b>	0	15000	<b>Psenen</b>	0	15000
Gnaq	0	15000	<b>Wdr26</b>	0	15000
<b>Pip5k1b</b>	0	50000	<b>Tead1</b>	0	15000
<b>Lsm14a</b>	0	15000	<b>Dennd4b</b>	0	15000

**Table 1.** CIS genes as identified by the locus-centric Gaussian kernel convolution (GKC) method and ranked by p-value. Genes appearing on the list of top 50 CISs as ranked by corrected p-value, determined by both GKC and gCIS analyses are denoted in red.



**Table 2. Genes involved in lung adenocarcinoma progression of BRAF<sup>V600E</sup>-initiated tumors (gCIS).**

CIS gene	<i>P</i> value (adj)	CIS gene	<i>P</i> value (adj)
Foxp1	0.029147246	Tmem163	4.37E-05
<b>Cux1</b>	1.21E-07	<b>Stag2</b>	0.001040256
<b>Braf</b>	1.21E-14	<b>Tead1</b>	0.006559496
Map3k5	3.23E-10	<b>Kmt2e</b>	2.12E-10
<b>Api5</b>	1.36E-97	<b>Kdm2b</b>	7.93E-10
<b>Ncoa3</b>	1.58E-31	<b>Fat1</b>	9.33E-09
<b>Dock9</b>	7.55E-06	<b>Ube2g1</b>	1.71E-08
<b>Fndc3b</b>	0.001102976	<b>Smarcc1</b>	1.22E-06
<b>Cnot2</b>	2.76E-13	<b>Arid2</b>	2.33E-05
<b>Sipa1l3</b>	1.62E-12	<b>Ppp2r5e</b>	0.005483574
<b>Kdm6a</b>	1.34E-07	<b>Map3k1</b>	2.40E-15
<b>Tanc1</b>	2.94E-05	<b>Fancd2</b>	5.25E-14
<b>Top1</b>	1.53E-15	<b>Igf2r</b>	1.14E-11
<b>Cmip</b>	3.74E-09	<b>Mapk1</b>	2.19E-11
<b>Nrp1</b>	1.07E-07	<b>Iqgap1</b>	1.58E-09
<b>Zfp704</b>	2.10E-06	<b>Adrbk2</b>	1.63E-09
<b>Ctnna1</b>	2.16E-06	<b>Wac</b>	1.98E-08
<b>Lmo7</b>	0.002170831	<b>Gpbp1</b>	3.78E-08
<b>Atp8a1</b>	0.017676792	<b>Snx25</b>	4.00E-07
<b>Kdr</b>	8.94E-38	<b>Celsr1</b>	4.57E-07
<b>Sept9</b>	1.41E-12	<b>Setd5</b>	2.99E-06
<b>Tcf7l1</b>	6.37E-08	<b>Elf1</b>	2.67E-05
<b>Dyrk1a</b>	4.15E-07	<b>Bmpr1a</b>	3.99E-05
<b>Lrp6</b>	1.36E-06	<b>Tshr</b>	6.66E-05
<b>Map4k3</b>	3.04E-05	<b>Nfat5</b>	6.76E-05

**Table 2.** CIS genes as identified by a gene-centric statistical method (gCIS) method and ranked by p-value. Genes appearing on the list of top 50 CISs as ranked by corrected p-value, determined by both GKC and gCIS analyses are denoted in red.



**Table 3. Trunk driver genes involved in lung adenocarcinoma progression of BRAF<sup>V600E</sup>-initiated tumors.**

<b>CIS gene</b>	<b>P value (adj)</b>
<b>Cux1</b>	3.25E-99
<b>Wapal</b>	1.24E-79
<b>Top1</b>	1.50E-71
<b>Cmip</b>	5.90E-50
<b>Gnaq</b>	5.74E-23
<b>Snd1</b>	3.75E-14
<b>Foxp1</b>	1.73E-11
<b>Rbms3</b>	0.004987717

**Table 3.** CIS genes containing 5 or more sequence read counts per tumor from 3 or more tumors and have corrected  $P < 0.05$  by gCIS analysis.

## CHAPTER 4

### CONCLUSIONS AND FUTURE PERSPECTIVES

Each year about 4,000 patients die every year in the United States from *BRAF* mutated lung cancer. Previous work in our lab has demonstrated that despite its essential role in lung tumorigenesis, oncogenic MAPK signaling via expression of the *BRAF*<sup>V600E</sup> oncogene is insufficient to form lung adenocarcinoma (29). Rather, progression from benign adenomas to lung cancer depends upon the cooperation of oncogenic MAPK activity coupled with the deregulation of additional cooperating genes and pathways (33). Therefore, the primary goal of this dissertation was to identify novel mechanisms of cooperation between the *BRAF*<sup>V600E</sup> oncogene with additional known and putative oncogenes and TSGs to gain a better understanding of the molecular basis for the initiation, progression, and pathway-targeted therapy of NSCLC. To achieve this goal, two methods were utilized: a candidate-based approach alongside a more unbiased forward-genetics approach, were both undertaken.

Strong evidence along with careful characterization of adenocarcinomas formed in our *Braf*<sup>CA</sup> GEMM strongly implicated the Wnt/ $\beta$ -catenin pathway in lung cancer progression. In addition, various studies have demonstrated a strong link between Wnt/ $\beta$ -catenin pathway activation and NSCLC in human patients, as well as the growth dependency of some human NSCLC lines on Wnt/ $\beta$ -catenin signaling *in vitro* (13, 68, 96-98). My results definitively established that Wnt/ $\beta$ -catenin pathway signaling is both necessary and sufficient for NSCLC formation.

I have shown that enforced Wnt/ $\beta$ -catenin signaling (either through expression of a constitutively active  $\beta$ -catenin mutant or overexpression of specific WNT ligands) in the lung

can drive progression to adenocarcinoma when paired with oncogenic activation of the MAPK signaling pathway (either through expression of the KRAS<sup>G12D</sup> or BRAF<sup>V600E</sup> oncogenes). In addition, I have demonstrated that Wnt/ $\beta$ -catenin signaling is also essential for lung tumorigenesis. Deletion of the *CTNNT1* gene from BRAF<sup>V600E</sup>-initiated cells in the lung epithelium or inhibition of WNT ligand secretion using a Porcupine inhibitor, LGK974, both suppressed lung tumor formation. Finally, I demonstrated that a major downstream effector of Wnt/ $\beta$ -catenin signaling is c-MYC. The results show that both the MAPK and Wnt/ $\beta$ -catenin signaling pathways coordinately regulate c-MYC expression and stability. Overexpression of c-MYC is able to rescue the inhibitory effects of either *CTNNT1* deletion or pharmacological inhibition of WNT ligand secretion during lung tumorigenesis. However, while overexpression of c-MYC is capable of bypassing the proliferative arrest seen in BRAF<sup>V600E</sup>-initiated tumors, it is not sufficient to drive progression to adenocarcinoma. This suggests that while bypass of the proliferative arrest observed in BRAF<sup>V600E</sup>-expressing lung adenomas is a prerequisite for cancer progression, it is not sufficient to drive this process and that additional cellular events are required. Work is currently underway to identify the key components downstream of Wnt/ $\beta$ -catenin signaling responsible for driving adenocarcinoma and the necessity and sufficiency of specific WNT ligands to facilitate this signaling.

We initially hypothesized that the barrier to tumorigenesis in BRAF<sup>V600E</sup>-driven lung tumorigenesis was the triggering of oncogene induced senescence (4). My work in this dissertation provides strong evidence that this is not the case. Instead, I propose that BRAF<sup>V600E</sup>-driven adenomas undergo a senescence-like (but reversible) proliferative arrest, triggered by an insufficiency of critical factors in the tumor microenvironment, including WNT ligands. The strongest evidence for this proposal is that overexpression of c-MYC in BRAF<sup>V600E</sup>-initiated

adenomas after they have already entered a growth-arrested state can drive these cells back into cell cycle to drive tumor growth.

In parallel to these efforts, an unbiased, forward genetics screen was also utilized to identify novel oncogenes and TSGs capable of cooperating with BRAF<sup>V600E</sup> expression to drive cancer progression in the lung. Sleeping Beauty transposon mutagenesis has served as a powerful tool in the discovery of novel candidate cancer genes in multiple tissues (99). Using this mutagenesis system in our *Braf*<sup>CA</sup> GEMM of NSCLC, we were able to identify a large set of novel candidate cancer genes for follow-up studies. Beyond this, the findings of this work has identified pathways both known to be essential for lung tumorigenesis (e.g., RAS/RAF/MEK/ERK MAPK, Wnt/ $\beta$ -catenin, Insulin-like growth factor, and PI3K signaling), as well as pathways and processes whose roles in NSCLC have not yet been characterized (e.g., axonal guidance and cell–cell junctions). This gives us insight not only into oncogenic pathways likely to be active in human NSCLC, but also gives us clues into the insufficiencies and microenvironmental pressures influencing cancer progression.

The efforts of this dissertation have aided in the identification and molecular characterization of pathways capable of cooperating with BRAF<sup>V600E</sup> to drive tumorigenesis. Specifically, the work in this dissertation provides valuable insights into the insufficiencies of oncogenic MAPK (BRAF<sup>V600E</sup>) driven signaling to the process of lung tumorigenesis and the systems properties and evolutionary pressures driving NSCLC development. The cancer-driving genes identified and characterized in this work are therefore aiding in both the prioritization of putative human cancer genes as potential prognostic and predictive biomarkers as well as therapeutic targets.

As mentioned previously, work is currently underway to validate the candidate cancer genes identified in our screen as bona fide oncogenes and tumor suppressors in NSCLC. From a basic science standpoint this work sheds light on some unanswered questions regarding the genes and pathways that are both redundant with and complement oncogenic MAPK kinase signaling during NSCLC formation, and the complex interactions responsible for this disease. From a clinical standpoint, similar to the discovery and characterization of Wnt/ $\beta$ -catenin, IGF1R, and PI3K signaling in this disease and their implications in lung cancer therapies, perhaps this level of molecular understanding will give us additional rationale for the design and implementation of additional combination therapies for NSCLC patients (82, 100, 101).

Lung cancer is a disease characterized by a very high mutational burden, and in result driver mutations are buried amongst a slew of passenger mutations (102). These efforts of this work will aid in separating these bystanders from the true drivers of this disease, and in result will identify new prognostic and predictive biomarkers in lung cancer as well as potentially uncover novel therapeutic targets. Ultimately, the hope is that the insights provided by this dissertation can help translate the genetic characterization and molecular profiling of human NSCLC into clinically actionable results.

## REFERENCES

1. R. S. Herbst, J. V. Heymach, S. M. Lippman, Lung cancer. *N Engl J Med* **359**, 1367-1380 (2008).
2. N. Cancer Genome Atlas Research, Comprehensive molecular profiling of lung adenocarcinoma. *Nature* **511**, 543-550 (2014).
3. S. Khozin *et al.*, U.S. Food and Drug Administration approval summary: Erlotinib for the first-line treatment of metastatic non-small cell lung cancer with epidermal growth factor receptor exon 19 deletions or exon 21 (L858R) substitution mutations. *The oncologist* **19**, 774-779 (2014).
4. D. Dankort *et al.*, A new mouse model to explore the initiation, progression, and therapy of BRAFV600E-induced lung tumors. *Genes Dev* **21**, 379-384 (2007).
5. D. Dankort *et al.*, Braf(V600E) cooperates with Pten loss to induce metastatic melanoma. *Nat Genet* **41**, 544-552 (2009).
6. D. Hanahan, R. A. Weinberg, Hallmarks of cancer: the next generation. *Cell* **144**, 646-674 (2011).
7. F. A. Shepherd *et al.*, Erlotinib in previously treated non-small-cell lung cancer. *N Engl J Med* **353**, 123-132 (2005).
8. K. S. Nguyen, J. W. Neal, First-line treatment of EGFR-mutant non-small-cell lung cancer: the role of erlotinib and other tyrosine kinase inhibitors. *Biologics : targets & therapy* **6**, 337-345 (2012).
9. R. Fodde, R. Smits, H. Clevers, APC, signal transduction and genetic instability in colorectal cancer. *Nature reviews. Cancer* **1**, 55-67 (2001).
10. S. Maretto *et al.*, Mapping Wnt/beta-catenin signaling during mouse development and in colorectal tumors. *Proc Natl Acad Sci U S A* **100**, 3299-3304 (2003).
11. Y. Zhang *et al.*, A Gata6-Wnt pathway required for epithelial stem cell development and airway regeneration. *Nat Genet* **40**, 862-870 (2008).
12. G. Akiri *et al.*, Wnt pathway aberrations including autocrine Wnt activation occur at high frequency in human non-small-cell lung carcinoma. *Oncogene* **28**, 2163-2172 (2009).
13. D. T. Bravo *et al.*, Frizzled-8 receptor is activated by the Wnt-2 ligand in non-small cell lung cancer. *BMC cancer* **13**, 316 (2013).
14. M. Tennis, M. Van Scoyk, R. A. Winn, Role of the wnt signaling pathway and lung cancer. *Journal of thoracic oncology : official publication of the International Association for the Study of Lung Cancer* **2**, 889-892 (2007).
15. A. Rappaport, L. Johnson, Genetically engineered knock-in and conditional knock-in mouse models of cancer. *Cold Spring Harbor protocols* **2014**, 897-911 (2014).
16. R. Sears *et al.*, Multiple Ras-dependent phosphorylation pathways regulate Myc protein stability. *Genes Dev* **14**, 2501-2514 (2000).
17. A. M. Bender *et al.*, Sleeping beauty-mediated somatic mutagenesis implicates CSF1 in the formation of high-grade astrocytomas. *Cancer research* **70**, 3557-3565 (2010).
18. A. J. Dupuy, K. Akagi, D. A. Largaespada, N. G. Copeland, N. A. Jenkins, Mammalian mutagenesis using a highly mobile somatic Sleeping Beauty transposon system. *Nature* **436**, 221-226 (2005).
19. A. V. Biankin *et al.*, Pancreatic cancer genomes reveal aberrations in axon guidance pathway genes. *Nature* **491**, 399-405 (2012).
20. S. Courtois-Cox *et al.*, A negative feedback signaling network underlies oncogene-induced senescence. *Cancer Cell* **10**, 459-472 (2006).
21. R. B. Corcoran *et al.*, Synthetic lethal interaction of combined BCL-XL and MEK inhibition promotes tumor regressions in KRAS mutant cancer models. *Cancer Cell* **23**, 121-128 (2012).
22. J. F. Gainor *et al.*, ALK Rearrangements Are Mutually Exclusive with Mutations in EGFR or KRAS: An Analysis of 1,683 Patients with Non-Small Cell Lung Cancer. *Clin Cancer Res* **19**, 4273-4281 (2013).

23. R. S. Heist, J. A. Engelman, SnapShot: non-small cell lung cancer. *Cancer Cell* **21**, 448 e442 (2012).
24. N. TCGAR, Diversity of lung adenocarcinoma revealed by integrative molecular profiling. Nature Under Review. *Under Review*, (2014).
25. P. B. Chapman *et al.*, Improved survival with vemurafenib in melanoma with BRAF V600E mutation. *N Engl J Med* **364**, 2507-2516 (2011).
26. K. Flaherty *et al.*, Phase I study of PLX4032: Proof of concept for V600E BRAF mutation as a therapeutic target in human cancer. *Journal of Clinical Oncology* **25**, 1 (2009).
27. A. Prahallad *et al.*, Unresponsiveness of colon cancer to BRAF(V600E) inhibition through feedback activation of EGFR. *Nature* **483**, 100-103 (2012).
28. C. Montero-Conde *et al.*, Relief of feedback inhibition of HER3 transcription by RAF and MEK inhibitors attenuates their antitumor effects in BRAF-mutant thyroid carcinomas. *Cancer Discov* **3**, 520-533 (2013).
29. C. L. Trejo, J. Juan, S. Vicent, A. Sweet-Cordero, M. McMahon, MEK1/2 inhibition elicits regression of autochthonous lung tumors induced by KRASG12D or BRAFV600E. *Cancer research* **72**, 3048-3059 (2012).
30. C. A. Pratilas *et al.*, Genetic predictors of MEK dependence in non-small cell lung cancer. *Cancer Res* **68**, 9375-9383 (2008).
31. R. P. Charles, G. Iezza, E. Amendola, D. Dankort, M. McMahon, Mutationally activated BRAF(V600E) elicits papillary thyroid cancer in the adult mouse. *Cancer Res* **71**, 3863-3871 (2011).
32. E. A. Collisson *et al.*, A central role for RAF-->MEK-->ERK signaling in the genesis of pancreatic ductal adenocarcinoma. *Cancer Discov* **2**, 685-693 (2012).
33. C. L. Trejo *et al.*, Mutationally Activated PIK3CAH1047R Cooperates with BRAFV600E to Promote Lung Cancer Progression. *Cancer Res* **73**, 6448-6461 (2013).
34. M. F. Beers, E. E. Morrisey, The three R's of lung health and disease: repair, remodeling, and regeneration. *J Clin Invest* **121**, 2065-2073 (2011).
35. E. E. Morrisey, B. L. Hogan, Preparing for the first breath: genetic and cellular mechanisms in lung development. *Dev Cell* **18**, 8-23 (2010).
36. E. C. Pacheco-Pinedo *et al.*, Wnt/beta-catenin signaling accelerates mouse lung tumorigenesis by imposing an embryonic distal progenitor phenotype on lung epithelium. *J Clin Invest* **121**, 1935-1945 (2011).
37. D. J. Stewart, Wnt signaling pathway in non-small cell lung cancer. *Journal of the National Cancer Institute* **106**, djt356 (2014).
38. V. Brault *et al.*, Inactivation of the beta-catenin gene by Wnt1-Cre-mediated deletion results in dramatic brain malformation and failure of craniofacial development. *Development* **128**, 1253-1264 (2001).
39. N. Harada *et al.*, Intestinal polyposis in mice with a dominant stable mutation of the beta-catenin gene. *EMBO J* **18**, 5931-5942 (1999).
40. T. C. He *et al.*, Identification of c-MYC as a target of the APC pathway. *Science* **281**, 1509-1512 (1998).
41. O. Tetsu, F. McCormick, Beta-catenin regulates expression of cyclin D1 in colon carcinoma cells. *Nature* **398**, 422-426 (1999).
42. O. J. Sansom *et al.*, Cyclin D1 is not an immediate target of beta-catenin following Apc loss in the intestine. *J Biol Chem* **280**, 28463-28467 (2005).
43. A. Y. Nikitin *et al.*, Classification of proliferative pulmonary lesions of the mouse: recommendations of the mouse models of human cancers consortium. *Cancer Res* **64**, 2307-2316 (2004).
44. H. Clevers, R. Nusse, Wnt/beta-catenin signaling and disease. *Cell* **149**, 1192-1205 (2012).
45. J. F. Ohren *et al.*, Structures of human MAP kinase kinase 1 (MEK1) and MEK2 describe novel noncompetitive kinase inhibition. *Nat Struct Mol Biol* **11**, 1192-1197 (2004).

46. N. Aziz, H. Cherwinski, M. McMahon, Complementation of defective colony-stimulating factor 1 receptor signaling and mitogenesis by Raf and v-Src. *Mol Cell Biol* **19**, 1101-1115 (1999).
47. L. Soucek *et al.*, Inhibition of Myc family proteins eradicates KRas-driven lung cancer in mice. *Genes Dev* **27**, 504-513 (2013).
48. M. Eilers, D. Picard, K. R. Yamamoto, J. M. Bishop, Chimaeras of myc oncoprotein and steroid receptors cause hormone-dependent transformation of cells. *Nature* **340**, 66-68 (1989).
49. T. D. Littlewood, D. C. Hancock, P. S. Danielian, M. G. Parker, G. I. Evan, A modified oestrogen receptor ligand-binding domain as an improved switch for the regulation of heterologous proteins. *Nucleic Acids Res* **23**, 1686-1690 (1995).
50. X. Wang *et al.*, Phosphorylation regulates c-Myc's oncogenic activity in the mammary gland. *Cancer Res* **71**, 925-936 (2011).
51. G. H. Ashton *et al.*, Focal adhesion kinase is required for intestinal regeneration and tumorigenesis downstream of Wnt/c-Myc signaling. *Dev Cell* **19**, 259-269 (2010).
52. D. J. Murphy *et al.*, Distinct thresholds govern Myc's biological output in vivo. *Cancer Cell* **14**, 447-457 (2008).
53. A. J. Finch, L. Soucek, M. R. Junttila, L. B. Swigart, G. I. Evan, Acute overexpression of Myc in intestinal epithelium recapitulates some but not all the changes elicited by Wnt/beta-catenin pathway activation. *Mol Cell Biol* **29**, 5306-5315 (2009).
54. V. Tabor, M. Bocci, N. Alikhani, R. Kuiper, L. G. Larsson, MYC Synergizes with Activated BRAF(V600E) in Mouse Lung Tumor Development by Suppressing Senescence. *Cancer Res* **In Press**, (2014).
55. L. Lum, H. Clevers, Cell biology. The unusual case of Porcupine. *Science* **337**, 922-923 (2012).
56. K. Hofmann, A superfamily of membrane-bound O-acyltransferases with implications for wnt signaling. *Trends Biochem Sci* **25**, 111-112 (2000).
57. E. Siegfried, E. L. Wilder, N. Perrimon, Components of wingless signalling in Drosophila. *Nature* **367**, 76-80 (1994).
58. X. Jiang *et al.*, Inactivating mutations of RNF43 confer Wnt dependency in pancreatic ductal adenocarcinoma. *Proc Natl Acad Sci U S A* **110**, 12649-12654 (2013).
59. K. M. Haigis, Wistuba, II, J. M. Kurie, Lung premalignancy induced by mutant B-Raf, what is thy fate? To senesce or not to senesce, that is the question. *Genes Dev* **21**, 361-366 (2007).
60. J. Zhu, D. Woods, M. McMahon, J. M. Bishop, Senescence of human fibroblasts induced by oncogenic Raf. *Genes Dev* **12**, 2997-3007 (1998).
61. D. Woods *et al.*, Raf-induced proliferation or cell cycle arrest is determined by the level of Raf activity with arrest mediated by p21Cip1. *Mol Cell Biol* **17**, 5598-5611 (1997).
62. L. Boulter *et al.*, Macrophage-derived Wnt opposes Notch signaling to specify hepatic progenitor cell fate in chronic liver disease. *Nat Med* **18**, 572-579 (2012).
63. W. E. Damsky *et al.*, beta-catenin signaling controls metastasis in Braf-activated Pten-deficient melanomas. *Cancer Cell* **20**, 741-754 (2011).
64. S. M. Powell *et al.*, APC mutations occur early during colorectal tumorigenesis. *Nature* **359**, 235-237 (1992).
65. L. Soucek *et al.*, Modelling Myc inhibition as a cancer therapy. *Nature* **455**, 679-683 (2008).
66. J. Wang *et al.*, B-Raf activation cooperates with PTEN loss to drive c-Myc expression in advanced prostate cancer. *Cancer Res* **72**, 4765-4776 (2012).
67. U. R. Rapp *et al.*, MYC is a metastasis gene for non-small-cell lung cancer. *PLoS One* **4**, e6029 (2009).
68. J. Mazieres, B. He, L. You, Z. Xu, D. M. Jablons, Wnt signaling in lung cancer. *Cancer letters* **222**, 1-10 (2005).
69. J. Mazieres *et al.*, Wnt inhibitory factor-1 is silenced by promoter hypermethylation in human lung cancer. *Cancer research* **64**, 4717-4720 (2004).
70. L. You *et al.*, Inhibition of Wnt-2-mediated signaling induces programmed cell death in non-small-cell lung cancer cells. *Oncogene* **23**, 6170-6174 (2004).



71. Y. H. Cha *et al.*, MiRNA-34 intrinsically links p53 tumor suppressor and Wnt signaling. *Cell Cycle* **11**, 1273-1281 (2012).
72. E. Meylan *et al.*, Requirement for NF-kappaB signalling in a mouse model of lung adenocarcinoma. *Nature* **462**, 104-107 (2009).
73. J. L. Kissil *et al.*, Requirement for Rac1 in a K-ras induced lung cancer in the mouse. *Cancer Res* **67**, 8089-8094 (2007).
74. M. M. Winslow *et al.*, Suppression of lung adenocarcinoma progression by Nkx2-1. *Nature* **473**, 101-104 (2011).
75. H. Ji *et al.*, Mutations in BRAF and KRAS converge on activation of the mitogen-activated protein kinase pathway in lung cancer mouse models. *Cancer Res* **67**, 4933-4939 (2007).
76. R. Straussman *et al.*, Tumour micro-environment elicits innate resistance to RAF inhibitors through HGF secretion. *Nature* **487**, 500-504 (2012).
77. T. R. Wilson *et al.*, Widespread potential for growth-factor-driven resistance to anticancer kinase inhibitors. *Nature* **487**, 505-509 (2012).
78. E. L. Jackson *et al.*, Analysis of lung tumor initiation and progression using conditional expression of oncogenic K-ras. *Genes Dev* **15**, 3243-3248 (2001).
79. A. Fasbender *et al.*, Incorporation of adenovirus in calcium phosphate precipitates enhances gene transfer to airway epithelia in vitro and in vivo. *J Clin Invest* **102**, 184-193 (1998).
80. J. S. Sebolt-Leopold, MEK inhibitors: a therapeutic approach to targeting the Ras-MAP kinase pathway in tumors. *Curr Pharm Des* **10**, 1907-1914 (2004).
81. D. M. Feldser *et al.*, Stage-specific sensitivity to p53 restoration during lung cancer progression. *Nature* **468**, 572-575 (2010).
82. M. Molina-Arcas, D. C. Hancock, C. Sheridan, M. S. Kumar, J. Downward, Coordinate direct input of both KRAS and IGF1 receptor to activation of PI3 kinase in KRAS-mutant lung cancer. *Cancer discovery* **3**, 548-563 (2013).
83. K. L. Jameson *et al.*, IQGAP1 scaffold-kinase interaction blockade selectively targets RAS-MAP kinase-driven tumors. *Nature medicine* **19**, 626-630 (2013).
84. A. S. Brohl *et al.*, The genomic landscape of the Ewing Sarcoma family of tumors reveals recurrent STAG2 mutation. *PLoS genetics* **10**, e1004475 (2014).
85. C. E. de Bock *et al.*, The Fat1 cadherin is overexpressed and an independent prognostic factor for survival in paired diagnosis-relapse samples of precursor B-cell acute lymphoblastic leukemia. *Leukemia* **26**, 918-926 (2012).
86. S. Ripka *et al.*, CUX1: target of Akt signalling and mediator of resistance to apoptosis in pancreatic cancer. *Gut* **59**, 1101-1110 (2010).
87. F. J. Sanchez-Rivera *et al.*, Rapid modelling of cooperating genetic events in cancer through somatic genome editing. *Nature* **516**, 428-431 (2014).
88. H. Li, R. Durbin, Fast and accurate long-read alignment with Burrows-Wheeler transform. *Bioinformatics* **26**, 589-595 (2010).
89. A. McKenna *et al.*, The Genome Analysis Toolkit: a MapReduce framework for analyzing next-generation DNA sequencing data. *Genome research* **20**, 1297-1303 (2010).
90. T. M. Keane *et al.*, Mouse genomic variation and its effect on phenotypes and gene regulation. *Nature* **477**, 289-294 (2011).
91. H. Li *et al.*, The Sequence Alignment/Map format and SAMtools. *Bioinformatics* **25**, 2078-2079 (2009).
92. A. R. Quinlan, I. M. Hall, BEDTools: a flexible suite of utilities for comparing genomic features. *Bioinformatics* **26**, 841-842 (2010).
93. A. L. Sarver, J. Erdman, T. Starr, D. A. Largaespada, K. A. Silverstein, TAPDANCE: an automated tool to identify and annotate transposon insertion CISs and associations between CISs from next generation sequence data. *BMC bioinformatics* **13**, 154 (2012).
94. H. Takeda *et al.*, Transposon mutagenesis identifies genes and evolutionary forces driving gastrointestinal tract tumor progression. *Nature genetics* **47**, 142-150 (2015).

95. K. M. Mann *et al.*, Sleeping Beauty mutagenesis reveals cooperating mutations and pathways in pancreatic adenocarcinoma. *Proceedings of the National Academy of Sciences of the United States of America* **109**, 5934-5941 (2012).
96. B. He *et al.*, Wnt signaling in stem cells and non-small-cell lung cancer. *Clinical lung cancer* **7**, 54-60 (2005).
97. B. He, D. M. Jablons, Wnt signaling in stem cells and lung cancer. *Ernst Schering Foundation symposium proceedings*, 27-58 (2006).
98. J. Kim *et al.*, Wnt inhibitory factor inhibits lung cancer cell growth. *The Journal of thoracic and cardiovascular surgery* **133**, 733-737 (2007).
99. M. B. Mann, N. A. Jenkins, N. G. Copeland, K. M. Mann, Sleeping Beauty mutagenesis: exploiting forward genetic screens for cancer gene discovery. *Current opinion in genetics & development* **24**, 16-22 (2014).
100. J. Juan, T. Muraguchi, G. Iezza, R. C. Sears, M. McMahon, Diminished WNT -> beta-catenin -> c-MYC signaling is a barrier for malignant progression of BRAFV600E-induced lung tumors. *Genes & development* **28**, 561-575 (2014).
101. C. L. Trejo *et al.*, Mutationally activated PIK3CA(H1047R) cooperates with BRAF(V600E) to promote lung cancer progression. *Cancer research* **73**, 6448-6461 (2013).
102. D. L. Gibbons, L. A. Byers, J. M. Kurie, Smoking, p53 mutation, and lung cancer. *Molecular cancer research : MCR* **12**, 3-13 (2014).

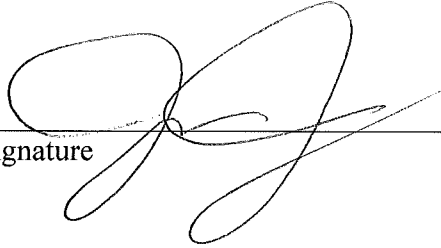
**Publishing Agreement**

*It is the policy of the University to encourage the distribution of all theses, dissertations, and manuscripts. Copies of all UCSF theses, dissertations, and manuscripts will be routed to the library via the Graduate Division. The library will make all theses, dissertations, and manuscripts accessible to the public and will preserve these to the best of their abilities, in perpetuity.*

***Please sign the following statement:***

*I hereby grant permission to the Graduate Division of the University of California, San Francisco to release copies of my thesis, dissertation, or manuscript to the Campus Library to provide access and preservation, in whole or in part, in perpetuity.*

\_\_\_\_\_  
Author Signature

A handwritten signature in black ink, consisting of several loops and a long horizontal stroke extending to the right.

\_\_\_\_\_  
Date

3.29.2015